Intranasal Administration of Simvastatin for Neuroprotection

Development of Micro and Nanoemulsions for Intranasal Delivery of Simvastatin in Ischemic Stroke

Versão final após defesa

Francisco Gama Sousa

Dissertação para obtenção do Grau de Mestre em
Ciências Biomédicas
(2º ciclo de estudos)

Orientadora: Prof. Doutora Adriana Oliveira dos Santos
Co-orientador: Prof. Doutora Patrícia Sofia Cabral Pires
Mestre Sara Alexandra Meirinho

agosto de 2022

Acknowledgments

The research work was carried out at the Health Sciences Research Center (CICS-UBI), at the University of Beira Interior, within the Biomedicinal Chemistry and Drug Research (BCDR) group. The work, including the formation in animal experimentation of Francisco Gama Sousa, was supported by national funds from the base financing (reference UIDB/00709/2020) and programmatic financing through CICS-UBI (reference UIDP/00709/2020). Francisco Gama Sousa also benefited from a grant through the Project MERCI ("Programa Verão com Ciência") through "Fundação para a Ciência e a Tecnologia".

I would like to thank BASF Pharma and Gattefossé for kindly donating some of the excipients used throughout the research work, and also to Hospital Universitário Cova da Beira for supplying the human blood samples, and Dr. Isabel Torrão for her solicitude.

FCT
Fundação para a Ciência e a Tecnologia
MINISTÉRIO DA CIÊNCIA, TECNOLOGIA E ENSINO SUPERIOR

CICSUBI
Health Sciences Research Centre

In order to thank everyone that contributed for the success of this work I will now address to them writing in Portuguese.

Queria agradecer à Professora Adriana por toda a ajuda, pela simpatia e por tudo o que me ensinou ao longo deste último ano. À Sara por toda a disponibilidade, paciência e esforço para que este trabalho conseguisse sempre avançar. E também à Patrícia por todo o auxílio que a distância permitiu.

Queria também agradecer a todos os que de uma forma direta ou indireta participaram neste projeto, especialmente a todos os colegas com os quais me cruzei durante este meu percurso no CICS.

A todos os meus amigos com um especial obrigado aos que há muitos anos me acompanham e aos que embora mais recentes parecem de velhos se tratar.

À minha família o maior dos obrigados e um ainda maior para a minha mãe por todos os sacrifícios para que eu pudesse estar onde estou.

Por fim a ti Margarida por tudo o que sabes que és.

Abstract

Ischemic stroke is one of the most impactful chronic diseases in the world and a leading cause of disability and death. Due to the lack of therapeutic options, and the limitations of those currently available, it is crucial to find new approaches to prevent and treat ischemic stroke events.

This study aimed to exploit simvastatin neuroprotective effects by developing a formulation capable of delivering it to the brain through nasal administration. For that, different formulation strategies of micro and nanoemulsions were pursued, to finally select the most promising to be compared in *in vivo* studies.

To achieve this, an initial screening was conducted to optimize formulation composition, maximizing drug loading capacity while maintaining target nanometric and homogeneous droplet size and neutral to positive zeta potential. Evaluation of short-term physical stability (drug precipitation upon storage at 4 °C up to 30 days) was combined with the initial screening in order to determine the formulations with the best potential to be further studied. The safety of the selected formulations was tested by hemolysis assays using human blood. An assay for simvastatin quantification was validated using liquid chromatography coupled with UV detection, and long-term physical and chemical stability tests were conducted at three different storage temperatures, 4 °C, 25 °C and 40 °C for 4 months. Preliminary *in vitro* drug release profiles were characterized using horizontal Ussing Chambers. The nano and microemulsions with the highest potential were also characterized in terms of their osmolality and viscosity, and nanoemulsion's viscosity was further optimized. Two lead formulations (a microemulsion and a nanoemulsion) were intranasally administered to Wistar rats and compared at 3 time points (30, 120, and 360 min) regarding brain concentrations of both prodrug (simvastatin) and active form (tenivastatin). A second *in vivo* test was conducted at 4 time points (15, 30, 60, and 360 min) to obtain more data regarding the previously tested micro and nanoemulsions, to determine the impact of nanoemulsion's viscosity and surface charge on simvastatin's brain concentrations, and to compare these formulations to a tenivastatin solution.

After the different optimizations and tests, a promising nanoemulsion strategy with cetalkonium chloride at 0.5% (w/w) was attained, exhibiting great potential in the *in vivo* studies. With drug strengths of 5.66% or 7.41% (w/w), this nanoemulsion under refrigeration had extremely low polydispersity index (0.069 and 0.074, respectively),

small droplet sizes (117.6 nm and 116.4 nm, respectively) and a zeta potential of +25 mV for the lower drug strength. In terms of short-term physical stability, the nanoemulsion with higher simvastatin concentration only achieved stability for 3 days, but drug precipitation was not observed with the lowest concentration. Assuming the more frequently used simvastatin dose applied in ischemic stroke animal models (20 mg/Kg), and the respective two-fold dose (40 mg/Kg), the formulation proved to be safe regarding its hemolytic potential. The lower drug strength nanoemulsion (5.66%) achieved physical stability for a period of 4 months while stored at 4 °C. Simvastatin's chemical stability when using the nanoemulsion was also prolonged when stored at 4 °C. After osmolality characterization, the nanoemulsion obtained hyperosmotic values, which were considered safer than hypoosmotic values for nasal mucosa. However, to be within the safety range of 300 and 700 mOsm/Kg, the nanoemulsion would need to suffer a dilution between 1.59 and 2.66-fold. In a preliminary drug release test, the nanoemulsion displayed a Higuchi Model release profile. The baseline viscosity of the nanoemulsion at 25 °C was 24.6 mPa·s and increased to 186.2 mPa·s using PVP at 0.25% (w/w). *In vivo*, the nanoemulsion with cetalkonium chloride at 0.5% achieved the highest simvastatin brain concentration after 30 minutes in both the first (153 ng/mL) and second test (131 ng/mL). The obtained simvastatin brain concentrations might demonstrate some potential to be neuroprotective but, surprisingly, no tenivastatin was detected during the *in vivo* assays.

In conclusion, a promising nanoemulsion with cetalkonium chloride 0.5% was obtained, enabling the possible use of simvastatin’s neuroprotective features in ischemic stroke using intranasal delivery. Further investigation needs to be done regarding the correlation between pharmacokinetic studies and functional studies using ischemic stroke models, to fully elucidate the role of simvastatin/tenivastatin and to improve drug applicability in cerebrovascular disease.

Keywords

Microemulsions; nanoemulsions; intranasal delivery; simvastatin; ischemic stroke.

Resumo

O acidente vascular cerebral isquémico é uma das doenças crónicas com maior impacto mundial e uma das principais causas de morte e incapacidade. Devido ao escasso número de opções terapêuticas e algumas das suas limitações, é necessário encontrar alternativas para prevenir e tratar casos de acidente vascular isquémico.

Este trabalho teve como objetivo desenvolver uma formulação capaz de entregar sinvastatina ao cérebro através da administração nasal, de forma a explorar os efeitos de neuroprotecção da sinvastatina. Diferentes estratégias de formulação em micro e nanoemulsões foram avaliadas de modo a selecionar um grupo promissor a ser comparado em estudos *in vivo*.

Para tal, foi realizado um *screening* inicial para otimizar a composição das formulações de modo a maximizar a capacidade de incorporação de fármaco, mantendo propriedades como o tamanho de nanométrico e homogéneo de gotícula e potencial zeta neutro a positivo. Fez-se também a avaliação da estabilidade física a curto prazo (análise da precipitação de fármaco durante um armazenamento de 30 dias a 4 °C) para determinar as formulações com maior potencial, e assim serem mais detalhadamente estudadas. A segurança das formulações selecionadas foi testada por ensaios de hemólise usando sangue humano. Foi desenvolvido e validado um ensaio de cromatografia líquida acoplado a deteção UV, para quantificação de sinvastatina usado na avaliação da estabilidade física e química a longo prazo, a três temperaturas de armazenamento diferentes (4 °C, 25 °C e 40 °C durante 4 meses). Os perfis *in vitro* de libertação do fármaco foram caracterizados com recurso a câmaras de Ussing horizontais. As micro e nanoemulsões com maior potencial foram também caracterizadas quando à sua osmolalidade e viscosidade, tendo a viscosidade sido otimizada nas nanoemulsões. Duas estratégias de formulação (uma microemulsão e uma nanoemulsão) foram administradas por via intranasal em ratos Wistar e comparadas tendo em conta as concentrações cerebrais atingidas, tanto do pró-fármaco (sinvastatina) como da forma ativa (tenivastatina), em três tempos distintos (30, 120 e 360 minutos). Um segundo ensaio *in vivo* foi realizado de modo a obter resultados mais robustas das duas formulações anteriormente usadas, e também avaliar o papel da viscosidade e carga da nanoemulsão nas concentrações cerebrais de fármaco. As formulações foram também comparadas com uma solução de tenivastatina.

Após diferentes estudos e processos de otimização, foi obtida uma nanoemulsão com cloreto de cetalcónio a 0.5% (m/m) que demonstrou enorme potencial nos estudos *in vivo*. Dependendo da concentração de fármaco encapsulada, 5.66% ou 7.41% (m/m) obteve-se uma nanoemulsão extremamente homogénea (PDI igual a 0.069 e 0.074, respetivamente), com pequenos tamanhos de gotícula (117.6 nm e 116.4 nm, respetivamente), após refrigeração da mesma (4 °C). A nanoemulsão apresentou caracter catiónico, com potenciais zeta de aproximadamente + 25 mV. Considerando a estabilidade física a curto prazo, a nanoemulsão com menor quantidade de fármaco obteve estabilidade por um período superior a 30 dias. Já a formulação com maior quantidade de fármaco, apenas obteve estabilidade por 3 dias. A nanoemulsão mostrou segurança considerando a dose de sinvastatina mais usada em modelos animais de acidente vascular isquémico (20 mg/Kg), bem como para a dose duas vezes superior (40 mg/Kg). A formulação mostrou ser fisicamente estável quando armazenada a 4 °C por um período de quatro meses. A estabilidade química da sinvastatina foi também prolongada quando a formulação foi armazenada a 4 °C. Quanto à osmolalidade, a formulação mostrou ser hiperosmótica, sendo mais segura face a soluções hiposmóticas. No entanto a formulação precisaria de uma diluição de 1.59 a 2.66 vezes de modo a obter valores de osmolalidade dentro do intervalo descrito como seguro para aplicação na cavidade nasal (300 a 700 mOsm/Kg). Durante os ensaios de libertação *in vitro,* verificou-se uma libertação incompleta, potencialmente devida a adsorção de sinvastatina, que poderá ter comprometido os resultados obtidos. É assim necessário avaliar otimizar este modelo *in vitro* para que melhor caracterizar o perfil de libertação da sinvastatina usando as diferentes formulações. Apesar disso os resultados poderão ser informativos, tendo a nanoemulsão obtido um perfil de libertação segundo o modelo de Higuchi. A 25 °C a nanoemulsão apresentou uma viscosidade de 24.62 mPa·s, que pode ser aumentada para 186.2 mPa·s utilizando PVP a 0.25% (m/m). Nos ensaios farmacocinéticos *in vivo*, a nanoemulsão com cloreto de cetalcónio a 0.5% originou as maiores concentrações cerebrais de sinvastatina após 30 minutos da administração por via intranasal, tanto no primeiro (153 ng/mL) como no segundo teste (131 ng/mL). Ambas as concentrações obtidas poderão ter o potencial de ser neuroprotetores embora, surpreendentemente, não se tenham detetado concentrações cerebrais de tenivastatina durante os ensaios *in vivo*.

Concluindo, foi conseguida uma nanoemulsão com cloreto de cetalcónio a 0.5% (m/m) promissora para ser administrada pela via intranasal, de modo a explorar as propriedades neuroprotetoras da sinvastatina no acidente vascular isquémico. Existe ainda a necessidade de desenvolver estudos futuros que consigam correlacionar os resultados obtidos em ensaios farmacocinéticos e em ensaios funcionais usando modelos

animais de acidente vascular cerebral isquémico já descritos na literatura, para melhor compreender o papel tanto da sinvastatina como da tenivastatin no acidente vascular isquémico e assim poder melhorar a sua utilização terapêutica nesta doença cerebrovascular.

Palavras-chave

Microemulsões; nanoemulsões; entrega intranasal; sinvastatina; acidente vascular cerebral isquémico;

Resumo Alargado

O acidente vascular cerebral (AVC) isquémico é uma doença cerebrovascular, caracterizada por uma alteração do aporte sanguíneo a uma determinada área cerebral, devido a uma obstrução num vaso sanguíneo. A alteração do fluxo sanguíneo leva à diminuição da quantidade de energia e oxigénio que consegue chegar às células, e consequentemente induz danos cerebrais diretamente proporcionais à duração da obstrução sanguínea. Estima-se que o AVC seja a segunda maior causa de mortalidade e de incapacidade a nível mundial, tendo também um enorme impacto a nível económico.

Atualmente, o principal tratamento do AVC isquémico é um agente fibrinolítico (ativador do plasminogénio tecidular), que tem como função remover a obstrução sanguínea devolvendo o normal fluxo sanguíneo ao cérebro. Este tratamento apresenta como desvantagem uma estreita janela de utilização de 4-5 horas após o início dos sintomas e também a limitada aplicabilidade do tratamento, não sendo aconselhado por exemplo a pessoas com historial de AVC, grávidas, pacientes hipertensos ou sob medicação que envolva anticoagulantes, entre outros.

Vários fármacos com ação neuroprotetora têm sido propostos como possível tratamento adicional para facilitar e recuperação após AVC. O grupo farmacológico das estatinas, onde se inclui a sinvastatina, apresenta enorme potencial, havendo alguma evidência em estudos observacionais do seu efeito neuroprotetor, de redução dos danos provocados pelo AVC e também melhoria da recuperação por parte dos pacientes após um AVC. Apesar do seu efeito primário ser focado na hipercolesterolemia devido à inibição da via metabólica responsável por produzir colesterol, a sinvastatina tem também outros efeitos (efeitos pleiotrópicos) devido à supressão da produção de isoprenoides que consequentemente afetam diversas outras vias celulares.

Contudo, a sinvastatina é um fármaco lipofílico e apresenta baixa biodisponibilidade oral causada pelo elevado metabolismo hepático. A baixa solubilidade aquosa da sinvastatina também dificulta a obtenção de dosagens elevadas, de modo a produzir efeitos a nível cerebral. Na entrega de fármacos ao cérebro esta questão é especialmente importante, uma vez que o cérebro é considerado um dos órgãos mais difíceis de alcançar sobretudo devido à barreira-hematoencefálica, que limita a passagem dos fármacos do sangue para o cérebro.

A via intranasal poderá ser uma boa alternativa para solucionar este problema uma vez que consegue evitar o efeito de primeira passagem hepático, aumentando assim a biodisponibilidade do fármaco ao mesmo tempo que possibilita o transporte direto para o cérebro através dos nervos olfativo e trigémeo que enervam a cavidade nasal. Consequentemente a via intranasal pode aumentar a eficácia do fármaco e diminuir as doses necessárias para atingir concentrações terapêuticas no cérebro e assim diminuir potenciais efeitos secundários sistémicos, como miopatias já descritas para o uso de elevadas doses de sinvastatina. Para além disso, esta via é não invasiva podendo ser aplicada por autoadministração, facilitando a sua utilização quando em comparação com a via intravenosa.

Para solucionar a baixa solubilidade aquosa da sinvastatina, a formulação em micro e nanoemulsões óleo em água pode ser usada. Este tipo de emulsões caracteriza-se por ter gotículas oleosas rodeadas por um meio aquoso e estabilizadas através do uso de tensioativos e de co-solventes. Assim, fármacos lipofílicos podem ser encapsulados dentro das gotículas oleosas (melhorando a sua solubilidade) mas mantendo um ambiente aquoso que proporcione a sua absorção. Outros fatores como o tamanho nanométrico, homogeneidade e carga das partículas podem também ser importantes na conjugação deste tipo de formulações com a via de administração intranasal. Devido ao seu potencial de aumentar a dosagem de sinvastatina e potencialmente a sua absorção, a combinação deste tipo de formulações com a via de administração intranasal pode melhorar ainda mais esta nova estratégia terapêutica.

O objetivo deste trabalho foi assim desenvolver uma formulação para entrega intranasal de sinvastatina para aumentar a biodisponibilidade do fármaco e consequentemente as suas concentrações cerebrais e assim explorar a suas propriedades neuroprotetoras no AVC isquémico.

Para isso numa primeira fase do trabalho tentou-se otimizar a composição de micro e nanoemulsões de modo a aumentar a concentração de fármaco encapsulado, enquanto se tentaram manter as boas propriedades de tamanho, homogeneidade e também de estabilidade física. A albumina foi incorporada na fase aquosa das formulações dado à sua capacidade de transporte direto para o cérebro quando administrada por via intranasal em combinação com a forte ligação da sinvastatina a esta molécula. No caso da nanoemulsão a albumina mostrou ter capacidade de estabilizar as formulações permitindo maiores concentrações de fármaco mantendo boas propriedades após refrigeração. Já nas microemulsões a albumina foi usada apenas com o intuito de promover transporte direto para o cérebro e não de aumentar a concentração de

sinvastatina, tendo mantido as propriedades nanométricas (tamanhos ≈ 30 nm) e também elevada homogeneidade (traduzida por um PDI < 0,1).

Apesar disso foi a incorporação de cloreto de cetalcónio (lípido catiónico) na fase oleosa das nanoemulsões (0,5% m/m) que melhores resultados produziu, uma vez que originou elevada estabilidade física a 4 °C de mais de 30 dias para uma concentração de sinvastatina de 5,66% (m/m) e de 15 dias para uma concentração de 7,41% (m/m), ao mesmo tempo que manteve tamanhos ótimos e PDI extremamente homogéneo. Face ao elevado custo da albumina e também a uma maior dificuldade na aprovação de produtos com proteínas biológicas, nanoemulsões com lípido catiónico foram selecionadas como tendo elevado potencial.

Nas microemulsões a maior incorporação de fármaco passou pela alteração das proporções da fase oleosa, fazendo-se aumentar a quantidade de vitamina E para 20 % (M2) ao mesmo tempo que se incorporou lípido catiónico na sua composição (0,1 – 0,25% m/m), tendo-se conseguido atingir até 10,71% de sinvastatina mantendo propriedades ótimas de tamanho e homogeneidade.

Em termo de segurança do ponto de vista da indução de hemólise, ambas as formulações mostraram ser seguras para concentrações de sinvastatina de 0,02 mg/mL, valor definido como meta a atingir, sendo equivalente a uma dose terapêutica de 20 mg/Kg. No entanto, as microemulsões testadas revelaram-se mais seguras do que as nanoemulsões, tendo sido atingida segurança para uma dose terapêutica de 450 mg/Kg. Isto deve-se em parte a maior capacidade de incorporação de fármaco da microemulsões, resultando em menores concentrações de excipientes que podem ter efeito hemolítico. A incorporação de lípido catiónico e de sinvastatina mostrou também ter um papel na hemólise. Já nas microemulsões o aumento de vitamina E mostrou também ter um efeito na hemólise.

Ambas as formulações apresentaram um caracter hiperosmótico. Através de diluições sucessivas da micro e da nanoemulsão, foram calculadas as diluições para as quais as formulações atingiam o intervalo de osmolalidade considerado seguro para administração intranasal. Devido às diferenças de proporções da fase oleosa e da fase aquosa na micro (90% oleosa e 10% aquosa) e na nanoemulsão (50% oleosa e 50 aquosa), uma maior diluição teria de ser feita na microemulsão, 4,13 a 7,67 vezes, para atingir segurança face à diluição de 1,59 a 2,66 vezes necessária nas nanoemulsões. O facto de ambas as formulações apresentarem tampão malato 30 mM na sua fase aquosa poderá também vir a ser um fator a otimizar de modo a diminuir a osmolalidade total das

formulações, visto apresentar um valor de cerca de 70 mOsm/Kg, permitindo assim atingir segurança com menores diluições.

As micro e nanoemulsões foram também testadas quanto à sua capacidade de libertação de fármaco. Para isso foram utilizadas câmaras de Ussing horizontais com uma membrana sintética. Os perfis de libertação obtidas para a microemulsão e para a nanoemulsão testada foram bastante diferentes. Uma libertação mais rápida no caso da nanoemulsão, mas que rapidamente começava a atingir o *plateu*. Já na microemulsão a libertação era mais lenta, mas sustentada ao longo do tempo, aumentando proporcionalmente a quantidade de fármaco libertado. A forma como o fármaco pode atravessar a membrana pode ajudar a explicar os dois perfis distintos de libertação. No caso das nanoemulsões a hipótese mais plausível parece apontar para que o fármaco seja libertado das gotículas oleosas e só depois atravessar mais rapidamente já em solução. Após o equilíbrio ser atingido as gotículas com maiores tamanhos da nanoemulsão têm maior dificuldade em atravessar a membrana, e dai atingir o *plateu*. No caso da microemulsões a hipótese é que o fármaco passe ainda encapsulado na gotícula oleosa. O maior tamanho da gotícula face ao da sinvastatina em solução explica a menor velocidade de libertação, mas também justifica a libertação sustentada.

A viscosidade é também um fator muito importante a ponderar na entrega intranasal, uma vez que pode aumentar o tempo de retenção das formulações na cavidade nasal e assim melhorar a absorção de fármaco. Após o primeiro estudo *in vivo* foi verificado que as microemulsões apresentavam melhor retenção na cavidade nasal (devido à sua viscosidade) enquanto as nanoemulsões eram mais facilmente expelidas pelos animais. Assim procedeu-se a caracterização da viscosidade tendo como objetivo otimizar a viscosidade da nanoemulsão de modo a obter viscosidades próximas da microemulsão (125 a 200 mPa·s). Para tal foram utilizados dois agentes viscosificantes, PVP e HPMC. Após adição destes na fase aquosa verificou-se uma interação que resultou num aumento da viscosidade maior do que o expectável considerando as viscosidades isoladas. Devido a este efeito sinergético e ao comportamento pseudoplástico das nanoemulsões (apresentam elevada viscosidade em repouso) foi possível atingir uma viscosidade de 186.2 mPa·s com PVP a 0.25% (m/m). Já com HPMC a apenas 0.01% (m/m) as viscosidades em repouso mostraram-se demasiado elevadas (699.8 mPa·s)

Quanto à estabilidade física prolongada, as microemulsões demonstraram a sua estabilidade termodinâmica não exibindo qualquer sinal de separação de fases em nenhuma das diferentes temperaturas testas (4°C, 25 °C e 40 °C) durante o período de 4 meses. No caso das nanoemulsões, a 25 °C e 40 °C houve separação de fases ao longo do

período de 4 meses, tendo a temperatura elevada acelerado este processo. Já a 4 °C não houve separação de fases, mostrando o papel da refrigeração não só na otimização dos tamanhos, mas também no aumento da estabilidade física. A estabilidade química da sinvastatina foi também melhorada quando as várias formulações foram armazenadas a 4 °C, e por oposição houve aceleração da degradação da sinvastatina quando as formulações foram armazenadas a 40 °C. Durante o ensaio foi também testada a hipótese de a remoção da fase aquosa poder aumentar a estabilidade da sinvastatina devido à redução de hidrólise (um dos principais processos responsáveis pela degradação de sinvastatina). Apesar da hipótese inicial obteve-se pior estabilidade não usando fase aquosa, mostrando assim o impacto do controlo do pH na melhor estabilidade da sinvastatina, uma vez que a nanoemulsão sem fase externa não apresentava tampão malato responsável pela manutenção do pH 5, no qual se verifica a maior estabilidade da sinvastatina.

Por fim, três estratégias em nanoemulsões (nanoemulsões com e sem lípido catiónico e uma nanoemulsão com lípido catiónico e PVP), uma microemulsão (M2) com lípido catiónico e uma solução de tenivastatina foram comparadas através da sua administração intranasal em ratos, seguindo-se a concentração de sinvastatina e tenivastatina no cérebro ao longo do tempo. Surpreendentemente não foi possível quantificar tenivastatina no cérebro, mesmo quando administrando uma solução de tenivastatina. Várias hipóteses poderão ajudar a explicar este fenómeno, sendo uma delas a possibilidade da concentração de tenivastatina estar abaixo do limite de quantificação do ensaio. Outra explicação poderá ser um grande transporte de efluxo que rapidamente consegue excretar a tenivastatina do parênquima cerebral. O efeito pode também ser devido à falha na metabolização da sinvastatina em tenivastatina no cérebro, podendo o modelo animal usado estar associado a este défice de conversão. Apesar disso, concentrações possivelmente terapêuticas foram atingidas no cérebro, tendo a nanoemulsão catiónica conseguido a maior concentração de sinvastatina de 153 ng/mL após 30 minutos de administração, e tendo assim obtido melhores resultados comparativamente à microemulsão. As estratégias da nanoemulsão sem lipídico catiónico e com o agente viscosificante não mostraram vantagens relativamente à nanoemulsão catiónica, mas evidenciaram a importância de um equilíbrio entre tempo de retenção, permeação e absorção. Ao aumentar a viscosidade mantendo lípido catiónico, o tempo de retenção pode ter aumentado, mas a difusão do fármaco e a sua permeação pela camada de muco pode ter sido diminuída, e consequentemente produzido menor absorção. Já a remoção do lípido catiónico pode ter melhorado a capacidade de permeação pelo muco (pela redução das interações com o mesmo) mas

também diminuído a mucoadesão levando a uma eliminação mais rápida da cavidade nasal e possivelmente a absorção através das membranas.

Concluindo, este trabalho permitiu demonstrar que o uso de nanoemulsões em conjunto com a administração intranasal pode ser uma estratégia benéfica para explorar as propriedades neuroprotetoras da sinvastatina no AVC isquémico. Além disso todo o conhecimento gerado e todas as otimizações realizadas nas diferentes estratégias em micro e nanoemulsões pode ser no futuro usado para servir de veículo para outros fármacos com características lipofílicas semelhantes à sinvastatina e assim melhorar a sua aplicabilidade em conjunto com a via intranasal.

Table of Content

List of Figures

List of Tables

List of Abbreviations

BBB	Blood-Brain-Barrier
BSA	Bovine Serum Albumin
CL	Cationic Lipid
CV	Coefficient of Variation
CYP	Cytochrome P450
EMA	European Medicines Agency
eNOS	Endothelial Nitric Oxide Synthase
FDA	Food and Drug Administration
HMG-CoA	Hydroxymethylglutaryl-Coenzyme A
HPLC	High-Performance Liquid Chromatography
HPMC	(Hydroxypropyl)methylcellulose Polyvinylpyrrolidone
LDL	Low-density lipoprotein
LLOQ	Lower Limit of Quantification
LOD	Limit of Detection
LOQ	Limit of Quantification
MCAO	Middle Cerebral Artery Occlusion
NO	Nitric Oxide
N2B	Nose-to-Brain
PBS	Phosphate Buffered Saline
PDI	Polydispersity Index
PVP	Polyvinylpyrrolidone
QA	Quality Attributes
QC	Quality control
QTPP	Quality Target Product Profile
RCF	Relative Centrifugal Force
RPM	Rotation Per Minute
RT	Retention Time
SDS	Sodium Dodecyl Sulfate
tPA	Tissue Plasminogen Activator

Chapter 1

Introduction

Stroke is the second leading cause of death worldwide and one of the main reasons for long-term disability. It results in 3 to 4% of the healthcare spending made by Western countries, which is translated to 26.6 billion euros in the year 2010 in Europe (1).

Ischemic stroke is the most common type of stroke and is usually caused by an artery blockage due to blood clots, resulting in impaired blood supply to a certain portion of the brain. As consequence, a lack of oxygen and nutrients reaches that area, resulting in brain tissue damage proportional to the duration of the ischemic event (2). Understandably, the current pharmacologic therapy used in patients diagnosed shortly after the beginning of the ischemic event is a thrombolytic drug that acts as tissue plasminogen activator (tPA), breaking down the clots and re-establishing the normal blood flow. Besides other risks, the major downside of this therapeutic approach is its short window of administration of only 4.5-hours after the onset of the ischemic stroke event (2). Due to tPA's limitations and the absence of alternatives, it is necessary to explore and research new treatments for ischemic stroke

Statins emerge as a possible alternative treatment strategy since reports already described their neuroprotective effects, damage reduction, and recovery improvement in acute ischemic stroke events (3).

A meta-analysis of preclinical studies (with stroke animal models) highlights simvastatin as a superior statin alternative in both pre- and post-event administration schedules. Subcutaneous and gavage administration of simvastatin were reported in the studies reviewed in the meta-analysis (4).

Compared to the two methods stated above, intranasal delivery has several advantages when trying to deliver drugs to the brain. Therefore, this administration route becomes very attractive to treat neurological disorders, since drugs can be partially directly transported to the brain, circumventing the blood-brain barrier (BBB). Drugs administered through the nasal cavity can also reach the brain through blood circulation. This allows systemic drug absorption with no gastrointestinal passage and no hepatic first-pass effect. Adding to that, it is a non-invasive and possible self-administration way to deliver drugs (5).

Simvastatin is a lipophilic drug, limiting the drug strengths that can be achieved and thus its therapeutic application. This problem can be solved by using oil in water micro and nanoemulsions capable of increasing drug strength while maintaining good absorption in the nasal cavity.

This project aims to investigate a viable intranasal delivery system for simvastatin brain targeting in pathological situations of ischemic stroke. In this way, we aim to bring together the beneficial neurological properties of simvastatin and the multiple advantages of intranasal delivery systems, surpassing some key limitations when using lipophilic drugs by using micro and nanoemulsions as a drug delivery vehicle.

1.1. Stroke

Annually affecting 15 million people, from which 5.5 million die and another 5 million are left with permanent disabilities, stroke is the second cause of death worldwide, a feature that did not change much over the years (6,7). Despite the death numbers being worrying enough, stroke also puts a massive burden from an economic point of view. Just in Europe and the United States, 64.1 billion euros and 33 billion dollars are spent each year on stroke patients (8).

Stroke is classified as a cerebrovascular disease caused by an obstruction of the normal cerebral blood flow. This changes the normal blood perfusion to a certain part of the brain, leading to metabolic and cellular changes that, if maintained long enough, can result in cell death (9).

Stroke can be classified as ischemic, when there is an obstruction causing a lack of oxygen and energy supply to the brain, or hemorrhagic when there is a rupture of a blood vessel that results in bleeding (7).

Hemorrhagic stroke comprises between 10-15% of all strokes and is related to high mortality rates (2,7,9,10). Blood vessel rupture can result in two types of hemorrhages: Intracerebral (10%) and subarachnoid (3%) (11). Intracerebral hemorrhage is the most common and happens when there is a vessel rupture that causes an abnormal quantity of blood to internally accumulate in the brain (10). Subarachnoid hemorrhage causes blood to accumulate in the subarachnoid region (10). Comorbidities, such as hypertension and disrupted vasculature, combined with extensive use of anticoagulant and thrombolytic drugs are frequent causes of intracerebral hemorrhage, while a

traumatic head injury or a cerebral aneurysm are the most common causes of subarachnoid hemorrhage (10).

Ischemic stroke is the main cause of stroke, representing around 85%-87% of all stroke events (2,7,9). Ischemic strokes can be further characterized as thrombotic and embolic (7). Normally, in thrombotic strokes, atherosclerosis causes the blood vessel diameter to be shortened by cholesterol build-up in its walls, leading to a clot (thrombus) formation with subsequently vessel restriction (7,12). Embolic stroke is caused by an abnormal mass that travels inside the blood vessel (embolus) but was formed away from the obstruction. An embolus can be an air bubble, a large piece of lipid, or even a blood clot usually produced in the heart (12). There are other subtypes of ischemic stroke related to heart failure, with other different etiologies and even with undetermined etiology (12).

While on the topic of stroke pathophysiology, it is important to mention another cause of stroke besides hemorrhagic and ischemic: transient ischemic attack. The reasons and mechanisms for this kind of event are the same as stated for the two other causes of stroke but, in this case, the blood flow restriction lasts less than 24 hours (6,7). Despite the symptoms only lasting for short amounts of time (< 1 hour), transient ischemic attacks can be a predictor and alert to future more serious strokes (6,7).

After an ischemic stroke, neuronal tissue suffers a reduction of oxygen and glucose supply due to the hypo-perfusion caused by the vessel occlusion (13). This results in a compromise of cell energy-dependent mechanisms causing severe stress to the cells and leading directly to necrosis or apoptosis (7,13). Other mechanisms resulting from the ischemic cascade - inflammation, excitotoxicity, cytotoxicity, loss of homeostasis, free radicals and oxidative stress, activation of the immunity system (complement, glial cells, leukocytes) - are also involved in producing brain injury (2,7,9,12,13). The ischemic cascade events are not only responsible for producing damage right after the ischemic event, but also for several stages after reperfusion, lasting days, weeks, and even months (9). Areas surrounding the occlusion can be classified into two types based on the degree of ischemia: core and penumbra (Figure 1). The core is the area subjected to full ischemia and the one that suffers irreversibly damage within minutes. The penumbra is a region surrounding the core that is not in total ischemia but is hypo-perfused, leading to damage that can be reversed if the blood flow to the area is re-established within the first hours (2,9,13). The penumbra region is the focus of a lot of drugs aiming to reduce/block the ischemic cascade events that result in cell death (9). The capacity of decreasing the brain injury produced by ischemic events, without directly targeting tissue reperfusion is called neuroprotection (9,14). Contrarily to what happens when using agents targeted to re-

establish the blood flow (tPA), neuroprotective agents can be applied before, during and after the ischemic event. This leads to an increase in the administration window and consequently better outcomes after the ischemic stroke (14).

This is where simvastatin might play an important role. Evidence has shown that statins can have important neuroprotective properties. This might result in infarct size reduction, increasing cerebral blood flow, protecting BBB, reducing superoxide radical damage, and also the inflammatory response (14).

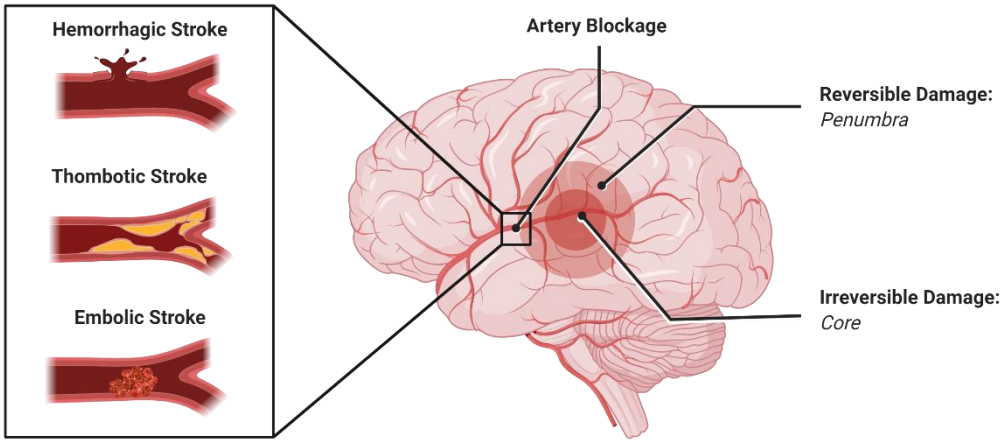

Figure 1. Schematic figure of the different types of strokes and the damaged areas surrounding the artery occlusion. Created with BioRender.com.

1.2. Simvastatin in Stroke

Simvastatin belongs to the statins family, a group of molecules with an inhibitory effect on hydroxymethylglutaryl-Coenzyme A (HMG-CoA) reductase enzyme (15).

Chemically, simvastatin is a derived form of lovastatin, another statin produced by the *Aspergillus terreus* fungus. Structurally simvastatin differs from lovastatin in a methyl group added to its ester side chain (16) (Figure 2). This change increases the affinity to the HMG-CoA reductase enzyme (16).

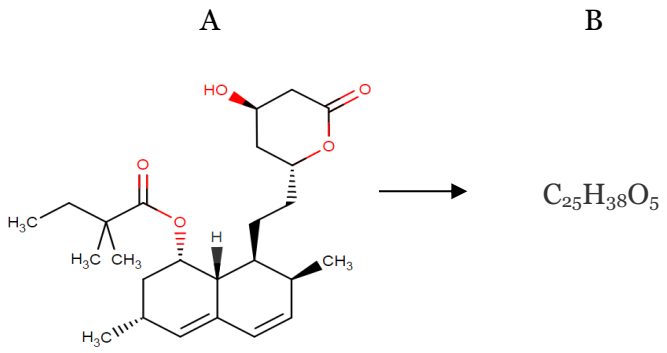

Figure 2. Simvastatin molecular structure (A) and formula (B).

Simvastatin has an affinity to the HMG-CoA reductase enzyme 13000-fold higher than its natural ligand, HMG-CoA (16). By binding to HMG-CoA reductase, simvastatin blocks the conversion of HMG-CoA to mevalonic acid, an important step in cholesterol synthesis(16). The decrease of mevalonate synthesis leads to a downstream reduction of cholesterol and other isoprenoid intermediates in the cholesterol biosynthesis pathway (Figure 3).

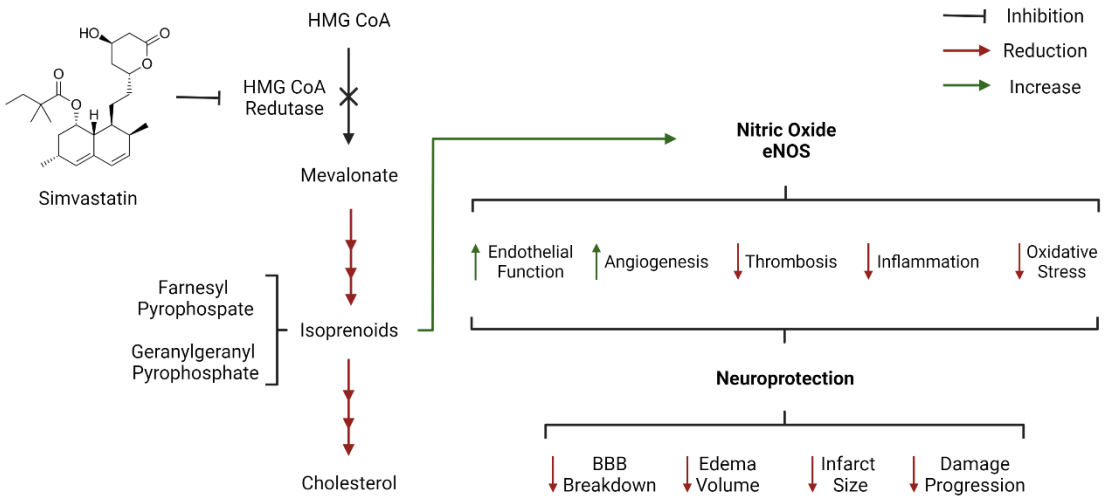

Figure 3. Cholesterol biosynthesis pathway and the possible pleiotropic effects, mediated by nitric oxide and endothelial nitric oxide synthesis (eNOS), following HMG-CoA reductase inhibition by simvastatin. Created with BioRender.com.

The decrease in cholesterol synthesis sparks a chain reaction that increases the low-density lipoprotein (LDL) receptors in hepatocytes leading to a higher LDL uptake, an apolipoprotein rich in cholesterol, by the liver and other tissues (16,17). This increases the extraction of LDL and its precursors from blood circulation, thus reducing cholesterol levels (16–18).

Simvastatin and other statins are linked to a reduction in mortality and risk of cardiovascular disease. Initially, this was mainly attributed to the reduction of LDL-

cholesterol. However, in recent years, retrospective and subgroup analyses of large studies suggested that other non-lipid lowering effects might play a role in it as well (19).

The Heart Protection Study (20) was one of the first studies suggesting that the simvastatin mechanism of reducing the risk of cardiovascular disease, is far more complex than simply reducing cholesterol biosynthesis and is associated with pleiotropic effects. Pleiotropic effects are pharmacological effects that are independent of the impact of simvastatin on lipids and lipoproteins (18). In Heart Protection Study, a reduction in mortality and morbidity was observed in patients with a risk of cardiovascular disease but with normal LDL-cholesterol receiving simvastatin. This highlighted simvastatin's LDL-independent mechanism for ischemic stroke reduction (20). Some of the possible described mechanisms include inflammation reduction, antithrombotic effects, endothelial function enhancements, and atheroma reduction/retardation (19,21).

Other large studies [e.g. Scandinavian Simvastatin Survival Study (4S)] (22) have also demonstrated the beneficial effects of simvastatin in cardiovascular outcomes. Still, a large debate regarding the topic of pleiotropic effects continues to exist (19). The two previously stated studies also demonstrated that simvastatin might play an important role in stroke (18). This is supported by results in two well-established stroke animal models: neonatal hypoxia-ischemia and adult middle cerebral artery occlusion (MCAO). Simvastatin was applied to both neonatal and adult rodents at 20 mg/Kg, either before or after the ischemic insult. In the neonatal model, the study concluded that simvastatin had prophylactic activity, achieving neuroprotection only when administered before the insult, resulting in a reduction in infarct size (21). On the other hand, in the adult model, a reduction in brain damage and tissue damage progression was achieved when simvastatin was applied before and after the ischemic insult. This suggests that simvastatin might simultaneously have a prophylactic and a protective effect after acute stroke (21). If applied 1 or 3 hours after MCAO, simvastatin had a neuroprotective effect that lasted for 48 hours. If applied after 6 hours, the limiting effect on tissue damage was still observed (21).

A meta-analysis concerning statins administration through different routes and doses to stroke adult animal models also demonstrated their efficacy in the protection against ischemic stroke, improving functional outcome, infarct volume, edema volume, and BBB breakdown (4). In the same meta-analysis, simvastatin and pravastatin exhibited better efficacy when compared to the other statins (atorvastatin, lovastatin, pitavastatin, rosuvastatin) (4). Finally, rather than statin dose or time of administration, the administration route displayed higher importance, with subcutaneous injection being

the most effective method when compared to oral, gavage, intraperitoneal, and intravenous (4).

As previously mentioned, reducing mevalonate synthesis leads to the reduction of isoprenoid intermediates, some of which serve as attachments for post-translation modification of different proteins (23). There are two major isoprenoids involved in prenylation (a protein modification mechanism), farnesyl and geranylgeranyl pyrophosphate (24). A wide range of intracellular proteins suffer prenylation (24). Ras, Rac, and Rho, members of the GTPase superfamily (25), are in that group of proteins (24,26). As they have important cellular signaling roles, in cell differentiation, proliferation, cytoskeleton, and apoptosis, we can suspect that a vast spectrum of possible effects can result from the decrease in the HMG-CoA reductase activity by statins (23–25).

By reducing Rho GTPase activity, statins increase the production of endothelium-derived nitric oxide (NO) and upregulate endothelial nitric oxide synthase (eNOS). The impact of statins on Rho, Ras, Rac, NO, and eNOS (27) are associated with an improvement of endothelial function and angiogenesis, a decrease in thrombogenesis, a reduction in the inflammatory response, a reduction of oxidative stress, and apoptosis prevention (26,27). Regarding neuroprotection, the action of simvastatin in eNOS and NO seems to be the main mechanism responsible for the reduction in infarct size (28). This evidence is consistent with studies showing that the lack of the eNOS gene led to larger infarct sizes, while the increase in eNOS activity and NO production resulted in better blood flood to the ischemic area, leading to neuroprotection a damage reduction (27–30). In MCAO models the upregulation of eNOS was observed when simvastatin was applied before or after the vessel occlusion (28).

There is clinical evidence that simvastatin reduces the risk of stroke and can be used as a neuroprotective or prevention solution for stroke (26,31). Despite it, more robust clinical trials need to be performed to fully describe the impact of simvastatin in ischemic stroke outcomes regarding doses, duration, and application of therapy (26).

On a pharmacological approach, simvastatin is a lactone prodrug that is activated by hydrolysis forming its beta-hydroxy acid metabolite (tenivastatin) (16,32). The switch to the active open acid can be performed through different routes: esterases, paraoxonases, and enzyme independent hydrolysis. The reaction is reversible, and the active form can be converted back to simvastatin in the Coenzyme A-dependent pathway or by glucuronidation (18) (Figure 4).

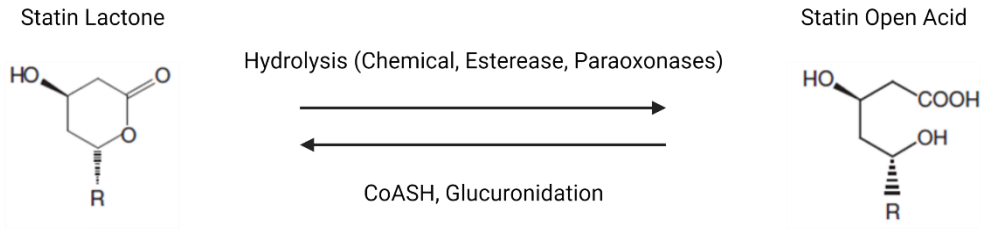

Figure 4. Conversion between the close ring form (prodrug/inactive) and the open ring form (active). Adapted from Pedersen *et. al.* (18).

Statins can be divided into two groups, lipophilic statins, and hydrophilic statins. Simvastatin is a lipophilic statin (17) able to passively cross cell membranes, meaning that it can reach other tissue rather than the liver. Hydrophilic statins need active carrier-mediated transporters to cross the cell membranes. Those transporters are not present in all cells allowing hydrophilic statins to be more liver selective (23).
Oral simvastatin is well absorbed in the gastrointestinal tract (between 60-85%) but has a low bioavailability, less than 5% (17,31), mainly because of the high liver extraction (more than 80%) (15). Simvastatin also has a high protein binding affinity, > 95% (15,31), and a short half-life of 1-2 hours (31,33).

After activation, tenivastatin undergoes extensive first-pass extraction in the liver, suffering oxidative metabolism mainly by the cytochrome P450 (CYP 3A4) pathway, followed by elimination in the feces (58%) and urine (13%) (17,32,33).

The poor oral bioavailability and high liver metabolization can be a hard barrier when trying to use simvastatin in stroke therapy, requiring higher doses in order to reach therapeutic concentrations in the brain. Normally simvastatin is administered in doses between 10 - 40 mg per day. Nevertheless, it can go as high as 80 mg per day, resulting in higher risks of developing side effects (e.g. myopathy) (15,18).

Intranasal delivery is a minimally invasive method that can be overseen as a solution to this problem. This route of administration has the ability to partially deliver drugs directly to the brain, bypassing the BBB, achieving better bioavailability and higher therapeutic concentrations in the brain with lower doses, which results in fewer side effects (34,35).

As stated before, simvastatin is very lipophilic (36) and considered practically insoluble in water (37) [>10000 mL of solvent to dissolve 1 gram of solute (38)]. For simvastatin, water solubility is a major limiting factor to achieve a drug strength capable of producing a pharmacological response (37). Oil-in-water emulsions can be used to obtain better-solubilized simvastatin's strength since they can incorporate lipophilic drugs in lipid

droplets surrounded by an aqueous solution, increasing drug concentration, absorption and bioavailability (39–41).

Simvastatin also has some underlying stability problems because of its chemical structure. It can easily be hydrolyzed depending on the pH [higher degradation at neutral or alkaline pH (42)], and also degraded by oxidation (43,44). Those problems can be solved by using emulsion drug delivery systems since they can protect drugs that undergo hydrolysis, oxidation, and enzymatic degradation (40,41,45,46). By optimizing emulsions' composition (suitable pH and incorporating antioxidants in the excipients) an ideal environment can be created to reduce simvastatin degradation and improve its stability.

Therefore, combining the intranasal route of administration with the micro and nanoemulsions formulation technology can benefit simvastatin's effects on ischemic stroke and overcome some of its disadvantages. Intranasal delivery and oil-in-water emulsions will be covered in more detail in the next topics.

1.3. Intranasal Delivery

The brain is one of the most important organs in our body. It controls and regulates most of the body functions, it is the hub of sensory and emotional perception, enabling us to feel, think and store memories, and embody what makes us human (47). Due to the core role of the brain, neurological disorders [> 600 different types (48)] can have detrimental consequences, not only on the brain itself but also on physical and mental health. Combined with the recent increase in prevalence, mortality, and disability, this makes the study and treatment of neurological disorders, such as stroke, a major global health priority (35,47,49).

Despite several strategies and therapeutic agents being applied to treat neurological disorders, all of them face a major difficulty – crossing the BBB in therapeutic concentrations (35,47,49–51). The BBB acts as a filter, protecting the brain from potentially harmful substances (chemicals, microbes, and endotoxins) passing from the blood to the brain, allowing homeostasis and preventing brain damage (35,47,49–51). During this process, the BBB also restricts the passage of drugs to the brain through different mechanisms - tight endothelial capillary cell junctions, low pinocytic activity combined with degradative enzymes, and high drug efflux by efflux transporters (e.g. P-glycoprotein) (35,47,50,51). This results in about 98% of small neurotherapeutic agents

being blocked to pass by the BBB, and nearly 100% blocked if they are large-molecule drugs (52). So, the BBB can be considered the most difficult membrane to overcome regarding drug delivery (53). Drugs with low molecular weights (< 400 g/mol) and high lipophilicity tend to have better BBB permeation. This is a positive note for simvastatin since it has a lipophilic character with a molecular weight of 418.566 g/mol that, according to some literature evidence, can cross BBB through passive diffusion (54). In order to bypass the BBB, invasive strategies, (e.g., transcranial drug delivery and intrathecal drug administration) and semi-invasive strategies (e.g., BBB disruption) have been employed. However, its limited success and challenges such as cost, suitability to chronic treatments, possible brain exposure to dangerous exogenous agents, invasiveness, and the possible operative and post-operative complications must be carefully considered (47,50,51,55).

For all those reasons, intranasal delivery aiming at brain delivery has attracted a lot of interest in recent years, since it is a simpler, non-invasive method that can avoid bloodstream clearance and bypass the BBB (47,50,51,55). Drug transport through nose-to-brain delivery (N2B) reduces doses necessary to achieve therapeutic concentrations in the brain (2-10 times lower than oral doses) leading to fewer possible drug side effects (51). The human nasal cavity is longitudinally separated by the nasal septum and extends around 12-14 cm in length from the nostrils to the nasopharynx, having a total volume of 15 - 20 mL (47,56). Despite its short length, the nasal cavity has a high surface area of 150 - 200 cm^2 because of three bone structures called the turbinates or conchae (56). The turbinates are responsible for filtering, humidifying, and warming inspired air and can be divided into inferior, middle, and superior turbinates (56). The nasal cavity can also be divided into three regions: the nasal vestibule (most anterior part), the respiratory region (middle inferior part), and the olfactory region (middle superior part) (47,56) (Figure 5). The nasal vestibule consists of hairs, sebaceous, and sweat glands, not contributing to drug absorption through intranasal delivery (47,56).

The respiratory region is located in the middle and inferior turbinates, covering 80-90% of the nasal cavity area (56). It is responsible for filtering inspired air, removing particles, microorganisms, and allergens. This is mainly due to mucus secretion (goblet cells) and ciliary movements (ciliated cells) that promote mucus removal towards the nasopharynx in a process called mucociliary clearance. The respiratory region is extremely vascularized making it a possible area for systemic drug absorption (35,47,56). Moreover, it is also innervated by branches of the trigeminal nerve, which is an important structure involved in the N2B pathways later described.

The olfactory region is located on the top portion of the nasal cavity, occupying the superior turbinate and comprising 5-10% of the human nasal surface area. This region is responsible for the sense of smell and is covered by olfactory sensory neurons (35,47,56). Dendritic branches of olfactory sensory neurons extend directly into the mucus layer and are directly exposed to airborne substances that interact with odorant chemoreceptors. The non-myelinated axons of the olfactory neurons converge forming the *fila olfactoria*. It later forms the olfactory nerve, directly connecting the nasal cavity to the olfactory bulb in the brain (35,56). This neuronal network is of most importance in direct drug transport to the brain (35,47,56).

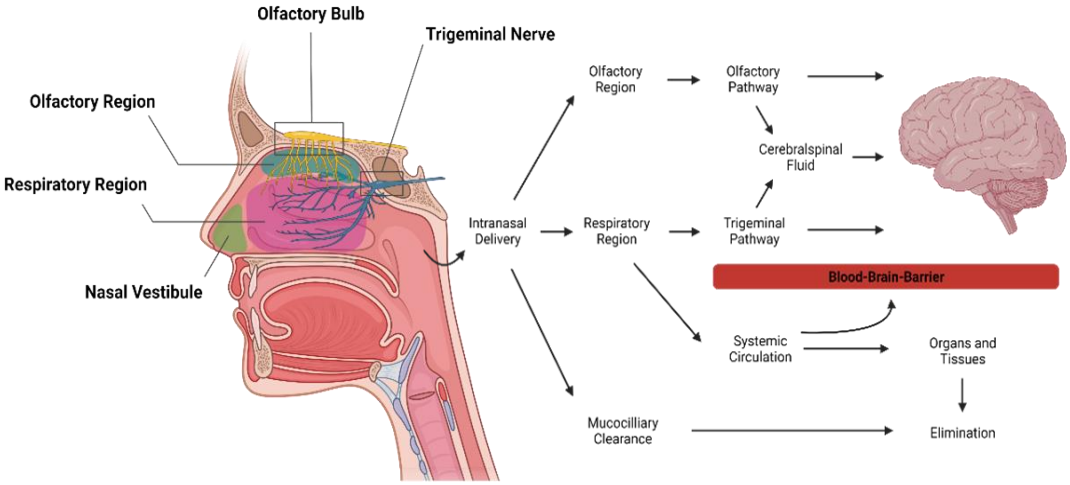

Figure 5. Schematic representation of the nasal cavity regions and nerve enervation. Different pathways drugs can take to reach the brain after being applied through intranasal administration. Created with BioRender.com.

Despite the extensive study of N2B delivery, the mechanisms involved in drug transport from the nasal epithelium to the central nervous system are still not fully elucidated. However, three major pathways have already been suggested: trigeminal pathway, olfactory pathway, and systemic pathway (47) (Figure 5).

The trigeminal pathway, as the name implies, exploits the neuronal transport of drugs through the trigeminal nerves that innervate both the olfactory and respiratory regions of the nasal cavity. Once drugs reach trigeminal branches, they will be transported and enter the brain either close to the pons or in the olfactory bulb (47,56).

The olfactory pathway is associated with the olfactory portion of the nasal cavity and the olfactory sensory neurons located in that region. After transport, drugs reach the brain through the olfactory bulb and can be then spread to the rest of the brain (47,55,56).

The mechanisms involved in the pathways employing the two neuronal networks can be divided into four different types: intra-neuronal, extra-neuronal, paracellular, and transcellular. Intra-neuronal transport starts with drug endocytosis, leading to axonal transport inside vesicles, and ends with drug exocytosis. Axonal transport has a very slow rate of 25 mm per day, not being considered the principal mechanism of drug transport. That is mostly because a faster drug delivery to the brain can be observed after intranasal administration, suggesting that other faster mechanisms might also be involved. Nevertheless, the axonal transport mechanism can still be involved in delayed-release mechanisms. Extra-neuronal transport happens when the molecules enter the tight junctions between neurons and the sustentacular cells that surround the neurons and then pass to open intracellular clefts to reach the brain. Paracellular transport happens between the tight junctions of the sustentacular cells but, instead of incorporating intracellular clefts, the drug is released to the cerebrospinal fluid in the subarachnoid space, and only then does it get delivered to the brain. This mechanism is important in hydrophilic molecules. Transcellular transport is very similar to paracellular transport, but it utilizes the inside of sustentacular cells instead of the gaps between them, either by using receptor-mediated endocytosis or passive diffusion.

Lipophilic molecules are suitable for direct transport since they passively cross the phospholipidic membrane of cells (47,55,56). Systemic pathways indirectly transport substances to the brain either by the systemic circulation or the lymphatic system.

Inhaled substances are systemically transported through the respiratory region due to the high vascularization of this area. Despite avoiding liver metabolism, this pathway requires that drugs cross the BBB, thus limiting drug delivery. However, for small and lipophilic drugs this might not impact drug delivery as much since they can bypass the BBB (47,55,56).

In spite of the major advantages of intranasal delivery, it also presents drawbacks and limiting factors like mucus barrier to drug-delivery system penetration, mucociliary clearance, enzyme degradation, and the ability to only accommodate small dose volumes (25-250 μL) limiting the route for potent drugs only (35,47,50,51,55,56).

The nasal mucus is composed of water (95%), mucins (2 ~ 3%), salts (~1%), and other components such as lipids, proteins, and DNA. Bowman's glands secrete 1.5 - 2 L of mucus per day in both respiratory and olfactory regions, which helps to humidify the nasal cavity while acting as a filter able to retain particles larger than 1 μm (47). Drug molecules need to be small enough to penetrate through the mucous mesh-like structure but, in the process, interact with the mucous composition by electrostatic, Van der

Waals's, and hydrophobic forces (47). Lipophilic drugs tend to have higher interactions with the mucus layer than hydrophilic drugs, resulting in less mucus permeation capacity (47). Motile cilia cells are present in the respiratory portion of the nasal cavity (the olfactory region only has non-motile cilia cells). They promote mucus movement in a process called mucociliary clearance, important to remove toxic substances stuck in the mucous into the nasopharynx and then the gastrointestinal tract (47). The mucous flows at a rate of about 6 mm/min, renewing the mucus layer every 10-20 minutes, meaning that drugs can rapidly be removed from the nasal cavity, leading to low absorption and bioavailability (47,57). Mucous production, viscosity, and ciliary beat frequency are variables that, depending on each individual, environmental and pathological conditions, will change the mucociliary clearance. Faster ciliary beat, higher mucous production, and lower mucous viscosity will increase mucociliary clearance while the opposite will reduce it. Intentionally altering those factors may be used as a strategy to improve mucous permeation and residence time. Some drugs and excipients have described effects on the cilia cells that reduce the ciliary beat and improve absorption by reducing mucociliary clearance (58). However, in order to be safe, those changes need to be reversible (58).

The use of absorption enhancers is another common approach to improve the overall bioavailability. Absorption enhancers include surfactants presenting high interfacial activity, enzyme inhibitors that protect drugs against enzyme degradation, cationic polymers with mucoadhesion properties and tight junction opening effects, and also tight junction modulators (57,59).

Besides adsorption enhancers, other strategies may be used to improve bioavailability and brain targeting. Nanoparticles are included in that group of strategies. They can increase residence time, mucous permeation and adhesion, drug cellular internalization, drug solubility, and stability, overcome mucociliary clearance, control drug release, and decrease drug distribution to non-target areas, leading to a reduction in systemic side effects (35,47,55,57,60). Together, all those features favor the use of nanoparticles for N2B delivery. Lipid-based nanoparticles have been widely investigated to be used in N2B delivery and include liposomes, solid lipid nanoparticles, nanostructured lipid carriers, and oil-in-water nano/microemulsions. The focus of the next topic will be on both nano and microemulsions and their potential in improving the intranasal delivery of simvastatin to target the brain.

1.4. Emulsions

Emulsions are colloidal dispersions of immiscible liquids that are formed after mixing an aqueous solution with appropriate amounts of natural or synthetic oils, surfactants, and, eventually, co-surfactants. The immiscible liquids often come in the form of an oil and an aqueous solution, mainly water. Surfactants are amphiphilic molecules, with a non-polar and polar domain in their structure. They are responsible for interacting with both the oil phase and the aqueous phase, leading to a reduction in surface tension between the two immiscible liquids. The combination between the oil phase, the aqueous phase, and surfactants can result in a variety of different systems. Those can have extremely different properties, depending on the composition itself and on the environmental conditions in which the emulsions were formed (39). Mostly, emulsions can be divided into four categories: water-in-oil (W/O), oil-in-water (O/W), water-in-oil-in-water (W/O/W), and oil-in-water-in-oil (O/W/O) (61). There are also bi-continuous systems, usually as intermediate states (39,50). In O/W emulsions, oil and surfactant clusters are dispersed in water, and the opposite happens in W/O emulsions. In any case, the surfactant has the polar head interacting with water, the non-polar tail pointing to the hydrophobic oil phase, and the hydrophilic/lipophilic balance of the surfactants is the main driving force for the type of emulsion forming (62).

A large number of drugs have very poor water solubility. For that, O/W emulsions can be used to increase drug loading, bioavailability, biocompatibility, and stability (63). That is related to the ability of the oil particles to act as reservoirs and shields for the lyophilic drugs while allowing them to be dispersed into an aqueous medium (64–67). Besides increasing drug solubility, nanometric emulsions can protect drugs against degradation (enzymatic, hydrolysis, and oxidation), increase chemical stability, control drug release profiles, and improve bioavailability (68). Further improvements can be done by altering the mucoadhesive properties of the emulsions to reduce mucociliary clearance and increase residence time in the nasal cavity thus resulting in better absorption (50,68).

Emulsions can be further divided into macroemulsions and nanoemulsions, related in their composition and name to systems known historically as microemulsions (which are fine dispersions of small nanometric size, despite their name). The improvements that both nanometric emulsion-related formulation strategies can bring to N2B delivery have made them a huge focus of study (68). Despite sharing some basic characteristics, micro and nanoemulsions have distinct physical and physicochemical features (67). The next topics will describe both in more detail.

1.4.1. Microemulsions

Microemulsions can be controversially assigned to the subgroup of nanometric emulsions, being composed of water, oils, surfactants, and cosurfactants (50). They are distinguished from nanoemulsions due to their thermodynamic stability (50,69), usually presenting smaller droplet sizes (< 100 nm). Because of the small droplet size, frequently less than 30 nm, particles do not diffract light and as a result, are usually transparent liquids (50). Due to extremely low interfacial tension, microemulsion formation is a spontaneous process (50,69) not dependent on the order of the mixture followed in its preparation. This is explained by the thermodynamics involved in microemulsions, where the free energy of the colloidal dispersions is lower than the free energy of the separated oil and aqueous phases, meaning that the microemulsion dispersion is energetically favored (66).

The potential of microemulsions has made them appealing to be used in combination with intranasal delivery to treat several different neurological disorders, such as Alzheimer's disease, Parkinson's disease, epilepsy, schizophrenia, and brain tumors (50). The focus of this work is mainly on O/W microemulsions, where small spheroid oil-surfactant droplets are dispersed within an aqueous medium since they can function as drug delivery systems for low water-soluble drugs while being biocompatibility with mucosal membranes (66). Microemulsions are important in direct drug delivery to the brain and also display good permeation to different biological membranes (50).

In *in vivo* studies allying microemulsions and intranasal delivery, a higher brain concentration of drugs together with directly targeting the brain was accomplished, reducing drug distribution to the peripheral organs and tissues (50). So, this property can be explored to reduce drug side effects when treating neurological disorders (50).

1.4.2. Nanoemulsions

Nanoemulsions are considered to be kinetically stable systems (metastable) and thermodynamically unstable, meaning that they can undergo physical destabilization (50,66). Destabilization time is usually extended due to physical factors (small size, electrostatic repulsions, and Brownian motion) that prevent flocculation, coalescence, aggregation, gravitational separation (sedimentation or creaming), and Ostwald ripening (50,69) (Figure 6).

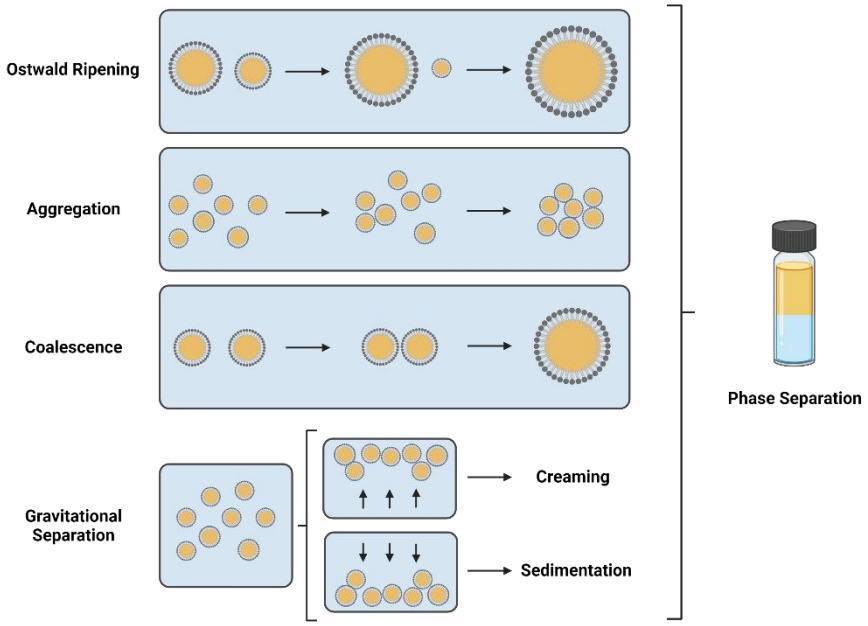

Figure 6. Mechanisms involved in nanoemulsion phase separation. Created with BioRender.com.

Nanoemulsions usually have droplet sizes of around 100 nm and can go up to 200 or 300 nm (51). However, the upper size limit is still under debate, with some studies also indicating 100 nm or 500 nm (66). This is understandably related to the authors' criteria, but also because the improved kinetic stability is not strictly dependent on size only. Light interaction with nanoemulsions droplets often results in a translucent to milky-white appearance (51). The process to obtain nanoemulsions often needs high amounts of external energy to promote the colloidal dispersion formations (50,66,69). Since nanoemulsions are thermodynamically unstable, their free energy is higher than the free energy of the different components separated, meaning the system will move towards separated phases (66). High energy methods use disruptive forces to break oil and water phases into smaller droplets and include ultra-sonification, high-pressure homogenization, and microfluidics (51,66). Fabrication techniques can also include low-energy methods (51,66), which rely on changes in environmental conditions (temperature) or composition, causing a disruption that leads to the spontaneous formation of small droplets. Phase inversion and spontaneous emulsification are two examples of low-energy methods (51,66). However, spontaneous emulsification in the nanoemulsions differs from microemulsions because it requires the surfactant to be firstly added to the oil phase before adding the aqueous phase (67).

Like microemulsions, nanoemulsions have also been applied in N2B delivery for a wide range of purposes: ischemic stroke, epilepsy, schizophrenia, migraines, infections Alzheimer's disease, Parkinson's disease, neuro-inflammations, brain tumors, and neuroprotection (51,68). Also, like in microemulsions, there are key features that make

the nanoemulsions suitable for N2B. Droplet sizes smaller than axon diameters (≈200 nm) provide direct transport through the nerve pathways while also making it harder to remove the droplets from the nasal cavity by the mucociliary clearance (51,68). The presence of surfactants and co-surfactants in nanoemulsions also has a positive effect on permeation by fluidizing endothelial membranes (51,68). A study using a chitosan/lecithin nanoparticle loaded with simvastatin (70) highlighted the previously mentioned beneficial features of lipid nanoparticles in N2B delivery. When compared with a simvastatin solution, the lipid nanoparticle increased simvastatin concentrations in the brain and decreases the overall distribution to peripheral tissues, such as the lung, liver, stomach, and heart. Direct brain targeting enables lower doses to achieve therapeutic concentrations in the brain while also decreasing possible systemic side effects.

Chapter 2

Objectives

The main objective of this work was to develop a promising formulation for the intranasal administration of simvastatin. With that in mind, we intend to demonstrate the hypothesis that the intranasal administration of this drug loaded in a suitable formulation will originate higher brain bioavailability than the oral and subcutaneous administration routes reported in the literature, allowing the reduce therapeutic doses.

Formulation strategies selected for this purpose were based on simvastatin's low water solubility and previous experience with O/W micro and nanoemulsions. The quality attributes next detailed in Table 1 were set as targets.

Table 1. Quality target product profile (QTPP).
A list of quality attributes (QAs) and their target values, required to be present in the final product, together with the respective justification.

Attribute	Target	Reason
Simvastatin dosage strength	Maximize (≥ 5.21% w/w)	A 9.09% and 5.21% concentration in the final product was previously achieved using the micro and nanoemulsion formulation, respectively. By maximizing the concentration of simvastatin in the pharmaceutical vehicle, we can administer smaller volumes with less frequency to reach the desired therapeutic concentrations. Reducing the amount of final product applied is a great advantage since it minimizes the risk of toxicity of some of its excipients.
Hydrodynamic diameter (droplet size)	< 200 nm	Smaller nanometric sizes increase the kinetic stability of nanoemulsions by reducing phenomena such as creaming, sedimentation, flocculation, aggregation, and Ostwald ripening (66,71). For successful drug permeation, the globule size should be less than 200 nm. In order to achieve even better drug absorption, smaller sizes in the order of 100 nm should be reached. The decrease in size brings another benefit by increasing retention times in the nasal cavity. Putting it into perspective sizes > 200 nm have retention times up to 4 hours and sizes < 200 nm have retention times higher than 12 hours (68). Also, to be transported by olfactory and trigeminal route particles need to be smaller than 200 nm (63)
Polydispersity index (PDI)	< 0.3, preferentially ≤ 0.1	Values lower than 0.3 are considered normal for intranasal nanocarriers. Smaller PDI values mean that the size of the particles follows a monodisperse and homogeneous distribution. A low PDI value promotes uniform drug absorption throughout the nasal cavity (72).
Zeta potential	to investigate	Values exceeding ±30 mV provide strong electric repulsion stabilization of nanometric systems. In intranasal delivery, positive zeta potential values contribute to mucoadhesive properties since

		nasal mucosa (mucin) displays a negative charge (68). Electrostatic interactions result in better residence times in the nasal cavity (63). Positively charged nanoparticles also benefit from an higher membrane-affinity, and thus better cell uptake (73). On the other hand, negatively charged particles tend to have better permeation through the mucous due to negative electrostatic repulsions while positively charged particles tend to be retained (73). This might not be a problem if there is fast drug release and diffusion through the mucosal barrier. However, if droplet direct interaction with cells is important for increased permeation/bioavailability, particle charge balance might be critical. Slightly positive or negative nanoparticles might be a good compromise between good mucoadhesion/transport across epithelial barriers and mucous penetration, leading to better overall results (73).
Viscosity	< 500 mPa·s,to further investigate	It has been previously described in the literature that a 500 mPa·s (500 cP) is the maximum viscosity for spray intranasal formulations (74). Although less mucociliary clearance and a higher residence time can be achieved with higher viscosities, higher viscosity also affects nasal absorption by reducing drug release/diffusion. Reaching an optimal viscosity for the emulsions is required to benefit from better nasal permanency without compromising absorption (75).
pH	5 (4.5 - 5.5)	The pH should be between 4 - 5 to maintain simvastatin in the lactone form since a pH > 6 promotes simvastatin hydrolysis to the open acid form (tenivastatin) (76). Adding to that, the pH needs to be maintained between 4.5 and 6.5 to reduce nasal irritation and keep the acidic environment needed for lysozyme to be active against the growth of pathogenic bacteria (77).
Osmolality	200 - 700 mOsm/Kg	Nose-to-brain formulations should have osmolality in this range to guarantee that the formulation does not damage the nasal mucosa (75). Normally nasal preparations tend to be isotonic (290 mOsm/L) but small deviations can improve some features: Hypertonic: Causes reduction of ciliary activity resulting in less clearance and better retention time (77). Hypotonic: Causes cell swelling which results in better drug absorption (77). Already commercialized products report osmolality in this range, so this can be accepted as a safe osmolality range (78). In rats, 50-600 mOsm/Kg was the range with less reported histological damaging effects. The use of hypertonic solutions is preferable to the use of hypotonic solutions (79).
Hemolysis	< 2%	In order to be considered safe, formulations need to achieve a hemolysis percentage < 2% (80), at a concentration of 0.02 mg/mL (See Supplementary Data Section S1)
Brain's drug concentration	0.1 - 5 μM, equivalent to 41.86 - 2092.8 ng/mL of simvastatin	Concerning therapeutic concentration on the brain, there is a lack of information in the literature, both for simvastatin and tenivastatin. Despite it, concentrations that achieved neuroprotection are reported for ischemic stroke *in vitro* models, both in neuronal cells (81,82) as well as brain endothelial cells (83). In neuronal models, simvastatin concentrations of 0.1 (81,82), 1 (81,82), 5 (81), and 10 μM (81) were described as having

	neuroprotection features despite one study reporting cytotoxicity for 10 μM (82) and another for 50 μM (81). In endothelial cells, a concentration of 5 μM was described as beneficial for cell function after subjection to oxygen and glucose deprivation that simulates an acute ischemic stroke (83).

A secondary objective of the present work was to better understand formulation variables in these particular micro and nanoemulsion strategies, followed by a comparison of their potential as intranasal delivery vehicles for lipophilic drugs. Therefore, facilitating future application in research of other drugs using intranasal delivery.

Chapter 3

Materials and Methods

3.1. Materials and Reagents

Kolliphor® RH 40 (Macrogolglycerol hydroxy stearate), an hydrophilic surfactant, and Vitamin E Acetate 98% (DL-alpha-tocopheryl acetate), an antioxidant lipid, were kindly offered by BASF (Ludwigshafen, Germany); Transcutol® HP (Diethylene glycol monoethyl ether), a cosolvent, and Capryol® 90 (Propylene Glycol Monocaprylate (type II) NF), a hydrophobic surfactant, were kindly offered by Gattefossé (Saint-Priest, France); Imwitor® 948 (Glyceryl Oleate), an oil, was kindly offered by IOI Oleo GmbH (Hamburg, Germany). Malic acid was acquired from Applichem (Darmstadt, Germany). Ultra-pure water was obtained from a Mili-Q® purification system from Millipore (Billerica, Massachusetts, United States of America). Simvastatin (98.03% purity) was purchased from Bld Pharmatech Ltd (Shangai, China) and kept at 4 °C under a nitrogen atmosphere during utilization. The bovine serum albumin (BSA) was acquired from Sigma-Aldrich, Inc (St. Louis, Missouri, United States of America). Polyethylene glycol 4000 (PEG), acquired to Acofarma® (Madrid, Spain), (Hydroxypropyl)methyl cellulose (HPMC, corresponding to Hypromellose Viscosity 4000 mPa·s), acquired to Acofarma® (Madrid, Spain), and Polyvinylpyrrolidone (PVP, corresponding to Povidone K30).

Cetalkonium chloride (Benzyldimethylhexadecylammonium chloride hydrate, 97%) was acquired from Acros Organics B.V.B.A (Geel, Belgium), and will be later called simply by cationic lipid. High-performance liquid chromatography (HPLC) gradient grade acetonitrile and methanol were obtained from Fisher Scientific (Leicestershire, UK) and Chem-Lab NV (Zedelgem, Belgium), respectively.

3.2. Preparation of formulations

3.2.1. Microemulsions

Although different variations of the microemulsion were tested, the preparation procedure always followed the same sequence throughout the study. First, the excipients

from the oil phase were weighed on a KERN® ABJ 120-NM precision scale (Balingen, Germany). After melting it, Kolliphor® RH 40 (40% w/w) was the first one to be weighed, due to its high viscosity. Next, Vitamin E Acetate 98% (10% w/w) and Transcutol® HP (40% w/w) were weighted and mixed with Kolliphor® RH 40 using a vortex. The excipient proportion resulted from previous work developed in the research group (84). After obtaining a homogenous mixture, simvastatin was added to the obtained oil phase, promoting its dissolution by heating it at 40 °C – 50 °C, with intermittent agitation every 5 minutes (Dry Block Heater, VWR Analogue, Pennsylvania, United States of America). Simvastatin was considered solubilized if no pellet was formed after a centrifuge pulse of 6 seconds at 4 Relative Centrifugal Force (RCF). Finally, the aqueous phase (10% w/w) composed of 30 mM malic acid buffer solution at pH 5, with or without BSA filtered through a 0.20 μm pore syringe filter (VWR International LLC, Pennsylvania, United States of America) was added to the oil phase using a precision scale. The mixture between the two phases was promoted by flicking the tube vigorously. At the present proportion of the aqueous phase (10%), a clear solution (self-microemulsifying drug delivery system), also called preconcentrate microemulsion, is obtained, with the actual microemulsion being only formed after further dispersion in water/aqueous environment (which could also happen *in vivo*). However, to simplify language, this self-microemulsifying drug delivery system will be referred to as microemulsion throughout this work.

To obtain the microemulsion containing cetalkonium chloride, a stock solution in Transcutol® HP was prepared at a concentration of 1.25%. To achieve different final concentrations of cetalkonium chloride, this solution was added to the preconcentrate during microemulsion preparation at an adequate ratio, and the amount of Transcutol® HP was reduced accordingly.

During the screening of microemulsion composition, three alternative formulations were prepared by changing the lipid-surfactant ratios of the baseline microemulsion (Table 2).

Table 2. Microemulsion excipient percentages used to prepare the oil phase.

	Transcutol® HP	Kolliphor® RH 40	Vitamin E Acetate 98%	Code
Percentage (%)	40	40	10	-
	40	35	15	-
	40	30	20	M2
	40	25	25	-

During the results and discussion section, microemulsions will be addressed using a code name that starts with ME and clarifies if they are modified or unmodified regarding vitamin E percentage (M2), simvastatin's final concentration (Simv x%), presence and concentration in the oil phase of cationic lipid (CL y%) and aqueous phase composition and concentration in the aqueous phase (BSA z%) (e.g., ME M2 Simv 10% CL 0.25%). When the aqueous phase is omitted, it is assumed the microemulsion contains malate buffer pH 5.

3.2.2. Nanoemulsions

The nanoemulsion consisted of a mixture of different excipients to create the oil phase and the aqueous phase. The oil phase pre-concentrate was composed of Capryol® 90 (50% w/w), Imwitor® 948 (33.33% w/w), and Kolliphor® RH 40 (16.67% w/w). The ideal excipient proportion resulted from previous work developed in the research group (85) and was maintained throughout this work. The aqueous phase of the nanoemulsions was a malate buffer pH 5 solution to which BSA, PEG, HPMC, and PVP were added following the preparation described in section 3.2.1. In total, the nanoemulsion was composed of 50% oil phase and 50% aqueous phase.

The preparation procedure of the nanoemulsion followed the same main steps as the microemulsions. In the oil phase weighting, the excipients were added accordingly with their viscosity: Kolliphor® RH 40 then Imwitor® 948, and finally Capryol® 90. Simvastatin solubilization followed the same procedure as the one described for microemulsions (section 3.2.1.). In nanoemulsion preparation, first only ¼ of the final aqueous phase mass was added followed by mixing, promoted by flicking the tube, and only then the other ¾ of the aqueous phase was added. Adding the aqueous phase in two steps is what causes the oil-in-water nanoemulsion to form by phase inversion emulsification (86).

To incorporate cationic lipid in the nanoemulsion, a stock solution of 1% CL in Capryol® 90 was prepared. This solution was added to the preconcentrate during nanoemulsion preparation.

In the results and discussion section, nanoemulsions will be addressed using a code name starting as NE and containing simvastatin's final concentration in the nanoemulsion (Simv x%), presence and concentration in the oil phase of cationic lipid (CL y%), and aqueous phase composition and concentration in the aqueous phase (BSA, PEG, HPMC or PVP z%) (e.g., NE Simv 5.66% CL 0.5% PVP 0.25%). When the aqueous phase is omitted, it is assumed the nanoemulsion contains malate buffer pH 5.

3.3. Formulation Characterization

3.3.1. Hydrodynamic Diameter, Polydispersity Index, and Zeta Potential Characterization

Both hydrodynamic diameter (droplet size) and PDI were measured by dynamic light scattering technique associated with cumulants method analysis. For that, a Zetasizer Nano ZS Malvern® (Malvern, United Kingdom) combined with the Zetasizer software (version 7.10) was used. Before each measurement, samples were diluted, 25-fold for microemulsions and 500-fold for nanoemulsions, in ultra-pure water filtrated through an acetate cellulose filter with a 0.2 μm pore. For each sample tested, two independent discardable plastic cuvettes were prepared and three different measurements of each were automatically performed by the equipment set at 25 °C. Measurements were always performed within 30 minutes after dilution. As measurement parameters set in Zetasizer software, water was considered as the dispersant (Refractive Index = 1.330 and Viscosity = 0.8872 cP) and the material was set to lipid (Refractive Index = 1.450).

Zeta potential characterization was done using the same equipment, with the same preparation steps but using Zetasizer Nano Series Dip Cell Kit Malver® in the measurement cuvettes. Measurements were taken at 25 °C and water was selected as the dispersant (Dielectric Constant = 78.5) and lipid as the material. When assessing the role of refrigeration in mean droplet size and PDI, formulations were placed at 4 °C overnight (at least 12 hours), and then measurements were performed exactly as stated before.

3.3.2. pH Characterization

For some formulations, the same cuvettes containing the micro and nanoemulsions diluted in filtered ultra-pure water that were used for droplet size and PDI characterization were also used to measure pH values using the MPT-2 Multi-Purpose Titrator Malvern®. After placing the pH probe inside the solution, pH was allowed to stabilize for 2 minutes before registering its value. Since samples for size characterization were always prepared in duplicate, pH was also measured in duplicate and the mean result is presented.

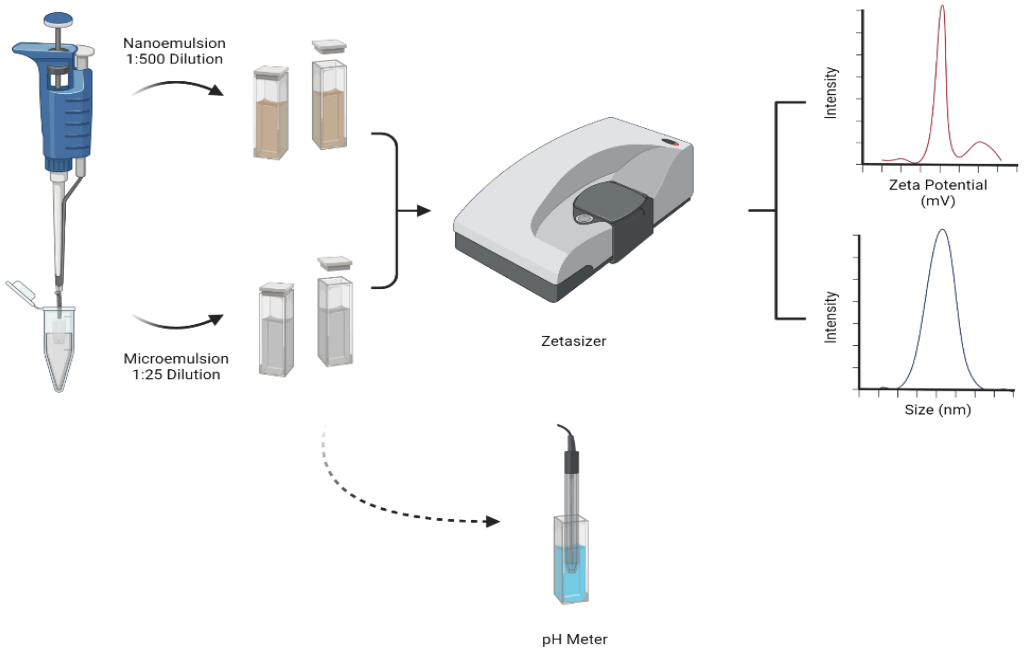

Figure 7. Micro and nanoemulsion characterization procedure regarding droplet size, PDI, zeta potential, and pH graphical representation. Created with BioRender.com.

3.3.3. Osmolality Characterization

Osmolality was measured using Osmomat® 3000 freezing point osmometer from Gonotec® GmbH (Berlin, Germany). Osmolality measurement was performed in independent triplicates. The device was previously calibrated using ultra-pure water and two standard solutions of 300 mOsmol/Kg and 850 mOsmol/Kg prepared accordingly to the European Pharmacopeia (38). Since direct measurements of both micro and nanoemulsions had values outside the calibration range, different dilutions using ultra-pure water were done to a final volume of 50 µL. The results allowed the construction of a linear regression equation, describing the behavior of the osmolality common logarithm according to the oil phase percentage.

3.3.4. Rheological Characterization

Viscosity measurements were performed at different rates [0.5 - 250 rotation per minute (rpm)] in a Brookfield DV3TRVCP® Cone Plate Viscometer (Toronto, Canada), using the CPA-40z cone spindle (viscosity range of 1.7-32700 cP) and the Rheocalc T® software (version 1.1.13). Measurements were done at a controlled temperature of 25 °C using a thermostatic water bath (MultiTemp III Thermostatic Circulator, Thermo Fisher Scientific, New Hampshire, USA). Before viscosity measurements, equipment calibration was verified using Ametek Brookfield Fluid 500 Viscosity Standard

(Middleborough, United States of America) with a standardized viscosity of 489 cP at 25 °C. During the calibration step, different sample volumes were tested. The volume used needed to be enough to cover the whole spindle surface (accessed after each measurement by visual inspection of the spindle surface and edge) while verifying specified calibration limits. Based on volume optimization, a formulation volume of 380 µL was placed on the plate, and the temperature was allowed to stabilize. Measurements were performed from high velocities, that produced a torque percentage close to 100%, to low velocities with a torque percentage close to 10%. At each velocity, viscosity was registered after the spindle had enough time to perform 5 complete rotations. For fluids with Newtonian rheological behavior, zero shear viscosity was determined at the highest torque value due to the equipment's higher resolution and precision resulting in a lower measurement error. For non-Newtonian fluids with either pseudoplastic or dilatant behaviors, zero shear viscosity was equal to the Y-intercept of the non-linear regressions based on the measurements performed at different shear rates at a constant temperature.

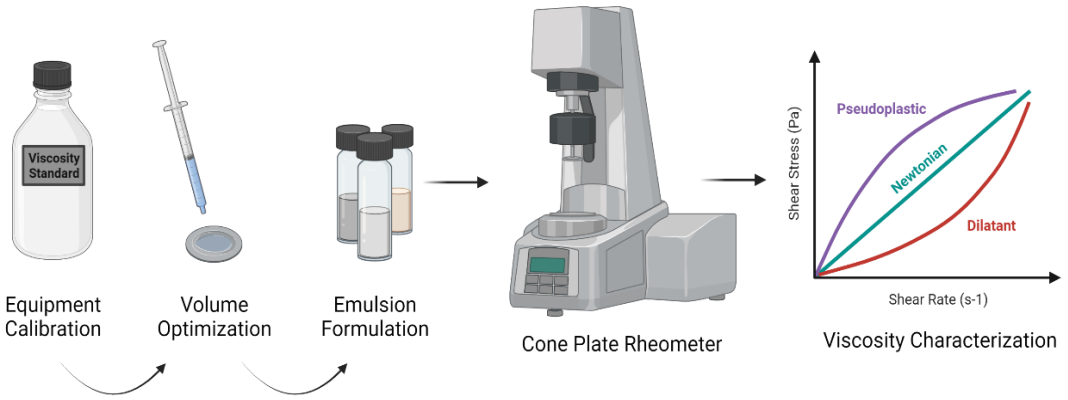

Figure 8. Rheological characterization procedure graphical representation. Created with BioRender.com.

3.4. Hemolysis Assay

The hemolysis assay procedure was performed based on the method proposed by the Nanotechnology Characterization Laboratory Method ITA-1 for the Analysis of Hemolytic Properties of Nanoparticles. Due to limitations of the cited method (explained in more detail in the Supplementary Data Incomplete Hemolysis section), the initial protocol was adjusted, and a method validation was performed.

Human blood samples in 3 mL Li-heparin tubes were kindly provided by Drª Isabel Torrão from Centro Hospitalar Universitário Cova da Beira. The hemoglobin

concentration of each sample was provided by hospital reports. Blood was stored at 4 °C for up to 48 hours. Before starting the assay, the initial hemolysis of each blood sample was determined in 0.5 mL of whole blood. For that, blood was centrifuged for 15 minutes at 800 RCF (MiniSpin® series, Eppendorf, Hamburg, Germany) and 200 µL of supernatant was mixed with 200 µL of Triton X-100 (Fisher BioReagents™, Hampton, United States of America) at a stock concentration of 0.2%. Then, 100 µL of the mixture was placed in a 96-well plate in duplicate and 100 µL of Drabkin's Solution from Chem Lab NV (Zedelgem, Belgium) was added to each well. Finally, absorbances were measured at 540 nm using an xMark™ Microplate Absorbance spectrophotometer from Bio-Rad Laboratories (Hercules, United States of America). Blank absorbance without blood (100 µL Drabkin's Solution + 100 µL PBS) was subtracted to sample absorbance values and then converted into hemolysis percentages using a standard curve produced during method validation (section 3.4.1). If the hemolysis value was less than 1%, the blood sample could be used in the hemolysis assay.

For every new blood sample, quality controls were also performed to compare the assay to the validation. The initial blood was diluted using PBS to achieve four different hemoglobin concentrations - 10 mg/mL, 5 mg/mL, 0.5 mg/mL and 0.05 mg/mL (hemolysis percentages of 100%, 50%, 5% and 0.5% respectively). To 200 µL of the blood at different concentrations were added 200 µL of Triton X-100 0.2%. Then, 100 µL of the mixture was placed in a 96-well plate in duplicate, followed by the addition of 100 µL of Drabkin's Solution, with absorbance measured at 540 nm. The absorbances obtained were then converted to hemolysis percentage using the standard curve and the experimental values were compared to the theoretical values. If one of the quality controls had a 20% discrepancy (30% for 0.5% quality control) between the experimental value and the theoretical value, the assay was not accepted and was repeated.

For the hemolysis test, the blood was diluted to a hemoglobin concentration of 10 mg/mL using PBS. In the first rack, tubes with 200 µL of test samples or controls were incubated with 200 µL of blood, and in a second rack tubes also with 200 µL of test samples were incubated with 200 µL PBS instead. All the test samples were prepared in triplicate, and the controls were prepared in quadruplicate [Triton X-100 0.2% (total hemolysis positive control)] or duplicate [Ultra-pure water (partial hemolysis intermediate control), and PBS (low hemolysis negative control)]. After adding blood or PBS, tubes were incubated at 37 °C for 30 minutes with gentle agitation at 15 minutes. After incubation, tubes were centrifuged for 15 minutes at 800 RCF (Hermle LaborTechnik GmbH - Z 323 K Universal High-Performance Centrifuge, Wehingen, Germany). Next, 100 µL of supernatant of each tube was placed in a 96-well plate in duplicate. To prepare interference controls,

150 µL of positive control were spiked with 150 µL of each concentration of the test sample, and then 100 µL were added in duplicate to the 96-well plate. Blank wells contained 100 µl of Triton X-100 0.2%. Finally, 100 µl of Drabkin's Solution was added to all the wells. An example of a final 96-well plate layout, ready to be measured, can be seen in Figure 9.

	1	2	3	4	5	6	7	8	9	10	11	12
A	Blank	TS1b	TS1b	TS1b	TS2b	TS2b	TS2b	TS3b	TS3b	TS3b	Blank	Blank
B	Blank	TS1b	TS1b	TS1b	TS2b	TS2b	TS2b	TS3b	TS3b	TS3b	Blank	Blank
C	Blank	TS1	TS1	TS1	TS2	TS2	TS2	TS3	TS3	TS3	Blank	Blank
D	Blank	TS1	TS1	TS1	TS2	TS2	TS2	TS3	TS3	TS3	Blank	Blank
E	C+	C+	H2O	C-	Blank	IEC1	IEC2	IEC3	Blank			
F	C+	C+	H2O	C-	Blank	IEC1	IEC2	IEC3	Blank			
G												
H												

Figure 9. Final 96-well plate layout with the different sample groups (with and without blood) and the multiple controls performed. TS1b-TS2b-TS3b: Test samples at different concentrations incubated with blood. TS1-TS2-TS3: Test samples incubated with PBS. C+: Triton X-100 0.2% incubated with blood. H2O: Ultra-pure water incubated with blood. C-: PBS incubated with blood. IEC1-IEC2-IEC3: Interference Controls for each concentration of the test sample.

The 96-well plate was then covered and gently agitated on the spectrophotometer plate shake function for 2 minutes before reading absorbances at 540 nm. After blank absorbance subtraction, the mean value of each test sample and control was calculated and converted to hemolysis percentage with the standard curve equation. Three independent hemolysis assays were performed for each formulation tested.

3.4.1. Hemolysis Method Validation

Linearity was tested by constructing six calibration curves using blood from six donors. For each calibration curve, twelve calibration standards covering a concentration range of 0.05 - 10 mg/mL (matching hemolysis percentages from 0% - 100%), were independently prepared. The lowest calibration standard (0.05 mg/mL) corresponded to the method's lower limit of quantification (LLOQ). Calibration curves were obtained by plotting absorbances at 540 nm, to which blank was subtracted, against the corresponding nominal hemolysis percentage. Subsequently, data was subjected to weighted linear regression analysis using different weighting factors ($1/x^2$, $1/x$, $1/\sqrt{x}$, $1/y^2$, $1/y$, and $1/\sqrt{y}$), forcing or not the curve through the origin.

Precision and accuracy were calculated, and acceptance criteria were defined as a coefficient of variation (CV) and bias percentages of ±20% for the lower limit of quantification (0.05 mg/mL), and ±15% for the rest of the concentrations. CV and bias

were calculated based on eq.1 and eq.2, respectively. The experimental value was calculated using the equation obtained by linear regression.

$$CV\ (\%) = \frac{Standard\ Deviation}{Mean} \times 100 \text{ (eq. 1)}$$

$$bias\ (\%) = \frac{|Experimental\ Value - Theoretical\ Value|}{Theoretical\ \ Value} \times 100 \text{ (eq. 2)}$$

Sensitivity was assessed through two values: limit of detection (LOD) and limit of quantification (LOQ). In this case, LOD is the smallest hemolysis percentage in the test sample that can be reliably distinguished from zero. LOQ is the lowest hemolysis percentage that can be determined with acceptable repeatability and trueness. LOD and LOQ were calculated using the following expressions (eq. 3 and eq. 4), where σ is the standard deviation of the Y-intercept of the regression line and s is the slope of the calibration curve:

$$LOD = 3.3\ \times\ \sigma \quad \text{(eq. 3)}$$

$$LOQ = \frac{10 \times \sigma}{s} \text{ (eq. 4)}$$

3.5. High-Performance Liquid Chromatography Method

3.5.1. Apparatus and Chromatographic conditions

HPLC was performed using an LC-2010A HT Liquid Chromatography system coupled with an SPD-M20A diode-array detector, automatically controlled by the LabSolutions 5.52 data acquisition software, from Shimadzu (Kyoto, Japan). Chromatographic separation was performed at 30 °C on a reversed-phase column (C18, 3 µm particle size, 55 × 4 mm) protected by a reversed-phase pre-column (C18, 5 µm particle size, 4 × 4 mm), both LiChroCART® Purospher® STAR models purchased from Merck (Darmstadt, Germany). Isocratic elution was achieved at a 1 mL/min flow rate using a mobile phase composed of 60% acetonitrile and 40% acidic water pH=5 (v/v), filtered using a Nylaflo membrane, 0.2 µm pore size (Pall, United States of America) and degassed for 30 minutes in a Labbox Labware ULTR ultrasonic bath (Barcelona, Spain) before use. Acidic water was prepared by adding orthophosphoric acid supplied by Fisher Chemical (Leicestershire, UK) to ultrapure water. The sample injection volume was 20 µL and analyte detection was performed at 238 nm in runs of 5 - 10 minutes (Figure 10).

3.5.2. Stock Solutions, Calibration Standards, and Quality Controls

A simvastatin stock solution was prepared in methanol at 2 mg/mL using a simvastatin analytical standard (99.7% purity, batch 6), purchased from the European Directorate for the Quality of Medicines & HealthCare. From this solution, an intermediate solution (I1) at 100 µg/mL was prepared by dilution in methanol. A second intermediate stock solution (I2) was prepared by diluting the I1 solution at 1 µg/mL in a nasal simulant buffer solution pH 5 (Monobasic Sodium Phosphate 7 mM, Dibasic Sodium Phosphate 3 mM, Potassium Chloride 30 mM, Sodium Chloride 107 mM, Calcium Chloride 1.5 mM, Magnesium Chloride 0.75 mM and Sodium Hydrogen Carbonate 5 mM). The different calibration standards and quality control (QC) samples were prepared by diluting either I1 or I2 solutions in the same nasal buffer solution.

3.5.3. Method Validation

Method validation was performed in accordance with the European Medicines Agency (EMA) guideline for bioanalytical method validation (87) and the Food and Drug Administration (FDA) guidance for industry on bioanalytical method validation (88). Selectivity regarding excipients in the formulation's composition was determined by running diluted micro and nanoemulsions blank samples. Linearity was tested using calibration curves independently prepared on three different days and composed of seven calibration standards covering a concentration range of 0.024925 – 4.985 µg/mL. The lowest calibration standard (0.024925 µg/mL) corresponds to the method's LLOQ. Calibration curves were obtained by plotting simvastatin's peak areas against the corresponding nominal concentration. Subsequently, data was subjected to weighted linear regression analysis using different weighting factors ($1/x^2$, $1/x$, $1/\sqrt{x}$, $1/y^2$, $1/y$, and $1/\sqrt{y}$). LLOQ intraday and interday precision and accuracy (within ±20%) were evaluated with samples prepared in quintuplicate ($n = 5$) on three independent days. Intraday accuracy and precision were evaluated by analyzing four QC samples covering different nominal concentrations (QC_{LOQ} = 0.024925 µg/mL, QC1 = 0.074775 µg/mL, QC2 = 0.4985 µg/mL, and QC3 = 4.985 µg/mL) prepared in quintuplicate in the same day. Interday accuracy and precision were assessed by analyzing the four QC samples prepared in triplicate on three consecutive days.

Finally, stability was determined by exposing QC1 and QC3 prepared in triplicate ($n = 3$) to different experimental conditions, simulating sample storage and handling. Short-term stability was tested by maintaining processed samples (diluted in the nasal buffer solution) at room temperature for 24 hours, at 32 °C for 6 hours (simulating *in vitro* drug release assays) and at 4 °C for 24 and 48 hours. For evaluation of the long-term stability

of the intermediate solutions (I1 and I2) in methanol, QC1 and QC3 solutions were prepared from freshly I1 and I2 solutions and readily analyzed. Then, I1 and I2 were left at −20 °C for 30 days. On the 30th day, new QC1 and QC3 solutions were prepared from the stored I1 and I2 methanolic solutions followed by their analysis. The obtained results of QC1 and QC3 analysis before and after being subjected to the different conditions were then compared. To be considered stable, the nominal concentration ratio before and after stability experimental conditions needed to be between 85% and 115%.

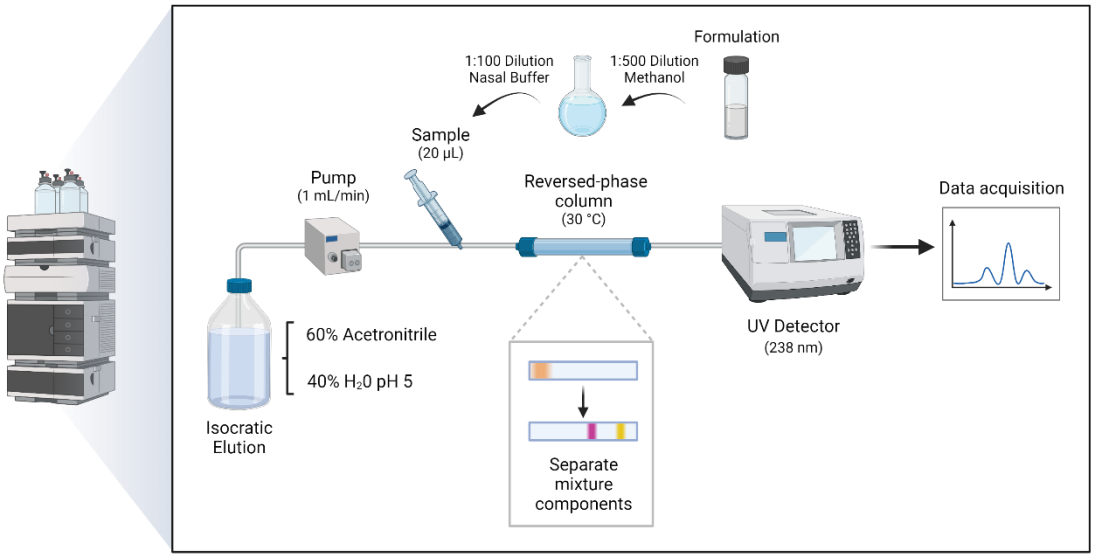

Figure 10. Graphical representation of the validated HPLC method experimental condition and procedure. Created with BioRender.com.

3.6. *In vitro* Drug Release Assay

The drug release profile was studied using horizontal Ussing chamber systems (Harvard Apparatus, NaviCyte, Hugstetten, Germany). As represented in Figure 11, it was used a setup consisting of six Ussing chambers placed on a water heating block connected to a Grant Instruments Ltd Y-28-VF thermostatic water bath circulator (Cambridge, United Kingdom).

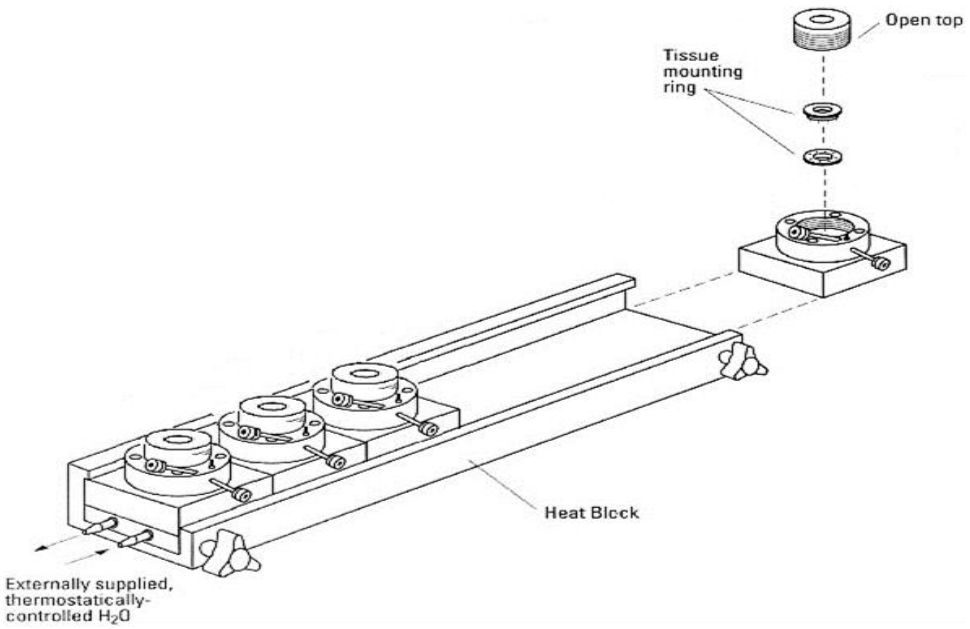

Figure 11. Horizontal Ussing chamber setup used during *in vitro* drug release assays. Adapted from Warner Instruments LLC 1988 (Hamden, United States of America)

In one of the chambers, the control chamber, a temperature sensor coupled to the magnetic stirrer (Heidolph Instruments GmbH & Co.KG EKT Hei-Con, Schwabach, Germany) was used to monitor the temperature. The water bath temperature was corrected to maintain the liquid inside the chambers at 32 °C (nasal temperature). To promote homogenization, a 2 mm micro stirring bar was placed inside the receiver chamber and agitation speed was set at 200 rpm, avoiding the formation of bubbles inside. Hydrophilic polyethersulfone Supor® membrane disc filters with a pore size of 0.2 µm (Pall Life Sciences, New York, United States of America) were used to create a physical separation between the donor chamber (top) and the receiver chamber (bottom). A nasal simulant buffer solution pH 5 (previously described) was used to fill the receiver chamber with 1.9 mL buffer. The acidic pH 5 allowed simvastatin stability to be maximized while closely mimicking the acidic nasal mucus pH of 5.5-6.5 (89).

Before starting the assay, 100 µL of nasal buffer solution was placed in the donor chamber (to promote membrane equilibrium) and the temperature was allowed to stabilize. Then, the assay would start by removing the 100 µL of nasal buffer placed in the donor chamber and then adding 100 µL of the diluted test formulation in the donor chamber. Then, at different times (15, 30, 60, 90, 120, 180, 240, 300, and 360 min), 200 µL of the receiver chamber were collected and replaced with 200 µL of nasal buffer solution to maintain the same overall volume. The collected 200 µL were directly quantified by HPLC, using the method described in section 3.4.

3.7. Chemical and Physical Stability Studies

To access chemical and physical stability, 2 mL of each tested formulation were placed at three different temperatures (4 °C, 25 °C, and 40 °C) for 4 months. At different time points (0, 1, 4, 8, 14, 21, 28, 56, and 112 days) the visual aspect of each formulation was registered, paying close attention to drug precipitation. For each formulation, droplet size, PDI, zeta potential, and pH were also characterized (as previously described). At the same time, simvastatin concentration was determined using the HPLC method previously described. In order to be quantified, samples were diluted 500-fold in methanol and then 100-fold in nasal buffer solution and then injected (Figure 10).

Degradation order was obtained based on the remaining drug concentration plotted against time. The selected formulations were independently prepared in duplicates using freshly prepared oil and aqueous phases.

3.8. *In vivo* Pharmacokinetic Studies

Animal experimentation was conducted using adult male Wistar Han rats from the Centro de Investigação Ciências da Saúde (CICS-UBI) certified animal facility. Animals were housed under controlled environmental conditions with 12-hour light/dark cycles, 20 ± 2 °C temperatures, and 50 ± 5% relative humidity. Standard 4RF21 rodent food (Mucedola, Italy) and tap water were supplied *ad libitum*. Animals' ages ranged between 8 and 11 weeks, with weights between 213 and 378 grams. All animal procedures were done in conformity with the regulations from the European Directive 2010/63/EU, regarding the protection of laboratory animals used for scientific purposes and obtained favorable acceptance by the Local Animal Ethics Committee (animal procedure project entitled "*Avaliação pré-clínica de novas formulações de ação neuroprotetora*"). The protocol was submitted to the competent national authority [Portuguese National Authority for Animal Health, Phytosanitation and Food Safety (DGAV – Direção Geral de Alimentação e Veterinária)].

Before intranasal administration of formulations, each rat was anesthetized using an induction chamber filled with Ecuphar IsoFlo® isoflurane (Sintra, Portugal), an inhalant anesthetic agent, at a 5% (v/v) rate combined with oxygen 1000 mL/min. Oxygen flow was maintained using a Philips EverFlo™ Oxygen Concentrator (Pennsylvania, United States of America) and isoflurane was vaporized and controlled with a Midmark VIP 3000® Veterinary Vaporizer (Dayton, United States of America).

Intranasal administrations were performed immediately and approximately 1 minute after removing the animal from the aesthesia induction chamber. Rats were laid in a supine head-back positioning under a rolled pillow, with volumes being administered using a 50 µL Hamilton syringe (Nevada, United States of America) coupled with a Braun Introcan®-W Certo (19 mm) flexible catheter (Melsungen, Germany). Administration volumes were split between the two nasal cavities, and the catheter was inserted until half of it was placed inside the nostril. After administration and recovery from the anesthetic effect, rats were placed in their respective cage.

In the first pharmacokinetic study, there were two experimental groups, 9 animals each, with three rats ($n= 3$) per time point (30, 120, and 360 minutes). In one group, 'Nanoemulsion Simvastatin 9,94% Cationic Lipid 0,5% Malate Buffer', and in the other, 'Microemulsion M2 Simvastatin 10,87% Cationic Lipid 0,25% Malate Buffer', were administered intranasally. The dose was 15 mg/Kg of simvastatin for both groups. To calculate the respective formulation volumes, simvastatin concentration in the formulations was quantified using the previously described HPLC method, and the formulation's density was experimentally estimated (0,9758 mg/µL for the nanoemulsion and 1,0076 mg/µL for the microemulsion) by weighting a precise 1 mL volume of the formulations with a 1000 µL Hamilton syringe. Administered volumes ranged between 35 and 48 µL for the nanoemulsion and 32 and 42 µL for the microemulsion.

In the second pharmacokinetic study, there were different time pointes (15, 30, 60, and 360 minutes) and five experimental groups, each receiving one of 5 formulations:

1. Nanoemulsion Simvastatin 8,79% Cationic Lipid 0,5% Malate Buffer
2. Nanoemulsion Simvastatin 8,92% Malate Buffer
3. Nanoemulsion Simvastatin 7,86% Cationic Lipid 0,5% PVP 0,25%
4. Microemulsion M2 Simvastatin 9,62% Cationic Lipid 0,25% Malate Buffer
5. Tenivastatin 17,74% Solution HPMC 1%

The animal distribution between the groups (up to 3 animal/time-point) was made to use all the available animals while maximizing new information gathered and complementing the first *in vivo* assay results.

After euthanasia under anesthesia at the specific time points, the brains were collected, cleaned with a cold NaCl 0.9% solution and paper towel to remove blood from their surface, snap-frozen using liquid nitrogen, and transferred to a -80 °C New Brunswick Scientific U570 -86 Freezer (Hamburg, Germany).

Simvastatin and tenivastatin quantification were performed by a third-party HPLC-MS/MS service provider (*Servicio de Análisis Elemental, Cromatografía y Masas*, University of Salamanca, Salamanca Spain). Sample transport was done in dry ice. The service provider described that frozen samples were homogenized on dry ice using an IKA-Werke® GmbH Ultra-Turrax® (Staufen, Germany), and 50 mg of the triturated sample were extracted using 500 µL of methanol while sonicated for 10 minutes. After extracted, the solution was filtered and diluted in ultrapure water (10-fold dilution). The extract was purified in a Discovery C18 Solid Phase Extraction cartridge and eluted with methanol. The solvent was then evaporated, and the sample was reconstituted in 500 µL of mobile phase before injection in the HPLC system. The method achieved good linearity for both tenivastatin and simvastatin with respective correlation coefficients (r^2) of 0.998348 and 0.997176 in the concentration interval of 5 to 50 ng/mL giving an LLOQ of 5 ng/mL in the diluted sample (50 to 500 ng/mL in the brain homogenate).

3.9. Statistical Analysis

Graphics and statistical data analysis were performed using GraphPad Prism® version 8.01 software.

In the micro and nanoemulsion screening, hemolysis assay, osmolality characterization, HPLC method validation, *in vitro* drug release assay, rheological characterization, chemical and physical stability studies, and *in vivo* pharmacokinetic studies data is presented as mean ± standard deviation.

In the hemolysis statistical analysis of the significant differences between the different formulations, different concentrations, and to the negative control group was evaluated by two-way ANOVA analysis followed by a Sidak's multiple comparisons test. To determine the hemolytic category of each formulation (safe, moderate hemolytic, and

hemolytic), a one-sample t-test was used to compare the mean hemolysis value to the lower and upper limit values of each category.

In the osmolality characterization section, a logarithmic transformation of the data was performed before linear regression analysis.

In *in vitro* drug release assay, drug release was determined based on initial drug strength. The drug release rate was calculated through three different models. In zero-order, a linear regression analysis was done. In first order, the remaining drug percentage (Y) was calculated by subtracting the drug release percentage to 100, and then Y was transformed by calculating its common logarithm. Linear regression was then applied. In the Higuchi model (90) both time (X) and drug release percentage (Y) were transformed by calculating the square root of X and by dividing Y by the area of the membrane used during the assay (0.64). Only points within 60% of the cumulative drug release percentage were considered. Linear regression was then applied after the transformations. The best fit was determined by comparing the correlation coefficients (r2) of the different models' linear regressions.

During rheological characterization, Newtonian behavior (dilatant/pseudoplastic) was determined by fitting a linear regression (Newtonian), an exponential growth equation non-linear regression (dilatant), or a second-order polynomial non-linear regression (pseudoplastic), to the "shear rate *vs* shear stress" data, and then comparing correlation coefficients. Zero shear viscosity of non-Newtonian pseudoplastic fluids was calculated by fitting a one-phase decay non-linear regression to the "viscosity vs shear rate" data and determining the zero of the function (Y when X = 0).

In chemical and physical stability studies, statistical analysis of the significant differences between mean droplet size and PDI between formulations and throughout time was evaluated by two-way ANOVA followed by Turkey's multiple comparison test. Time and temperature impact on simvastatin chemical stability was evaluated by two-way ANOVA. To determine the kinetic order of simvastatin degradation at different temperatures, three models were used. In the zero-order model, a linear regression analysis was done after plotting simvastatin concentration (Y) against time (X). In the first-order model, Y was transformed by calculating its common logarithm and plotted against X, and then linear regression analysis was done. In the second-order model, Y was transformed dividing 1 by Y and plotting it against X, and then a linear regression was done. The best fit was determined by comparing the correlation coefficient.

Chapter 4

Results and Discussion

4.1. Nanoemulsion's Composition Screening

Increasing simvastatin concentration in nanoemulsions was the first main goal established during the screening. Prior to the present work, another member of the research group achieved a 5.21% w/w simvastatin concentration, using the same nanoemulsion composition, before precipitation started to happen when loaded with higher concentrations (5.66%) (85). An approach to this problem was to add higher concentrations of BSA that might improve simvastatin solubilization while also being an active agent in brain targeting (91). BSA is able of binding poorly soluble drugs, such as simvastatin, and enhance its solubility and stability due to the buffer capacity in the pH ranges of 5.2 – 7 (92). BSA seems to bind to simvastatin in a 1:1 mol ratio due to very strong hydrophobic and hydrogen bond interactions (91,93).

The impact of different BSA concentrations in the water phase (2%, 4%, 6%, 7.5%, and 8%) of nanoemulsions was evaluated by droplet size and PDI characterization (Figure 12).

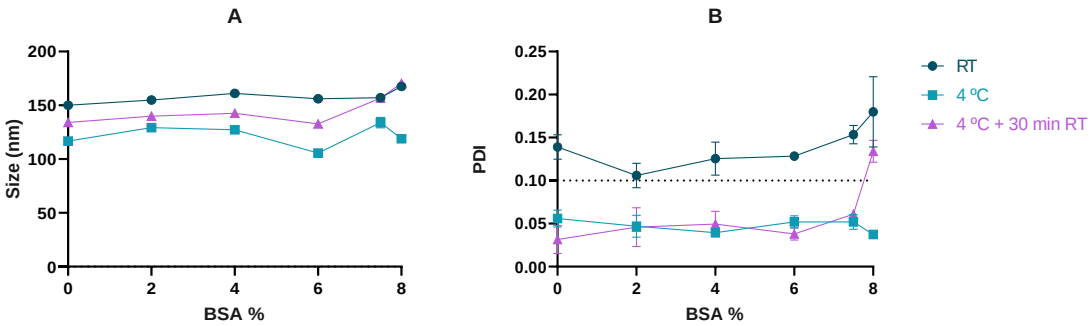

Figure 12. Influence of albumin (BSA) concentration on nanoemulsions' droplet size (A) and PDI (B). Formulations contained simvastatin at 5.66%. Measures were performed at room temperature (RT), after refrigeration (4 °C), and 30 minutes at RT after being refrigerated. Data corresponds to the mean ± standard deviation of two independent dilutions of one formulation.

At 25 °C, the mean droplet size was very similar among all formulations. On the other hand, stronger differences in the PDI values were observed. BSA at 2% originated a lower PDI compared to the nanoemulsion without BSA, but PDI was still over 0.1, our preferred

target. At higher BSA concentrations, PDI values increased but still were within the homogenous range (PDI < 0.2).

After refrigeration, mean droplet size and PDI decreased in all the formulations, becoming extremely homogenous (PDI < 0.1). The effect of refrigeration remained at least for 30 minutes after being left at room temperature. This meant that, for refrigerated nanoemulsion, any BSA concentrations could have been used to try to increase simvastatin's concentration. Nevertheless, BSA at 6% seemed to be the best option since it achieved the lowest size of 105.6 ± 1.41 nm, with a very low PDI of 0.052 ± 0.007.

A series of simvastatin increments was then performed to determine the maximum amount of simvastatin capable of being loaded without precipitation when using the BSA 6% solution as the aqueous phase (Figure 13).

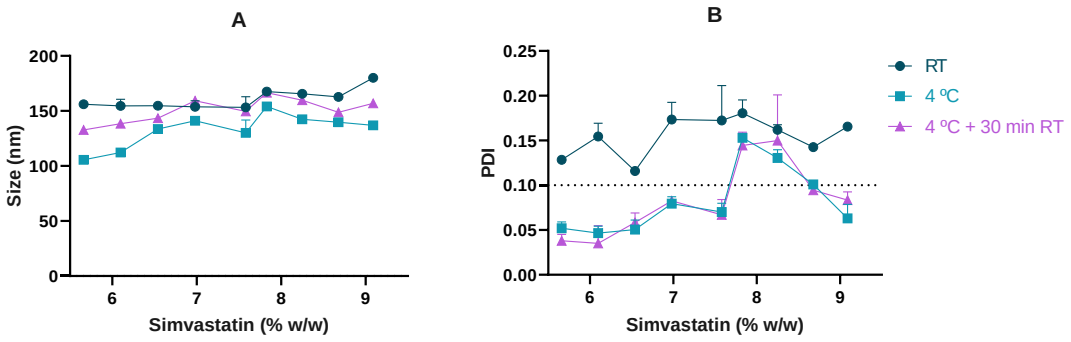

Figure 13. Influence of simvastatin concentration on nanoemulsions' droplet size (A) and PDI (B). Albumin in the aqueous phase was set at 6%. Measures were performed at room temperature (RT), after refrigeration (4 °C), and 30 minutes at RT after being refrigerated. Data correspond to the mean ± standard deviation of two independent dilutions of one formulation.

Simvastatin increments produced an overall increase in droplet size. At room temperature, all the simvastatin concentrations had PDI higher than 0.1, but still being homogenous (PDI < 0.2). Once again, refrigeration of the nanoemulsions produced a decrease in both droplet size and PDI, an effect extended for at least 30 minutes back at room temperature regarding PDI. A final concentration of 9.09% of simvastatin was reached, equaling the starting concentration encapsulated in the microemulsion. Higher concentrations of 9.50% and 9.91% were also attained. However, those were impossible to characterize since simvastatin started to precipitate after the dilution needed to perform the measurements. Those nanoemulsions probably were in a supersaturated state that, after dilution, promoted the simvastatin crystallization in the form of macroscopic needle-like crystals and, in later stages, round agglomerates. The observed macroscopic precipitate matches with information previously described in literature

when simvastatin is loaded in a supersaturated self-nanoemulsifying drug delivery system (94). That could possibly be caused by cosurfactant interaction changes after dilution, leading to loss of simvastatin solubilization and consequent precipitation (95).

At this point, it was clear that nanoemulsions needed refrigeration to have good size properties. Nevertheless, the physical stability of the formulation with higher simvastatin concentrations would be compromised. At 4 °C, formulations with concentrations higher than 7.41% would precipitate in 1-2 days. In order to further improve the characteristics of nanoemulsions, BSA was once again tested at different concentrations but, this time, only with 7.41% of simvastatin (Figure 14).

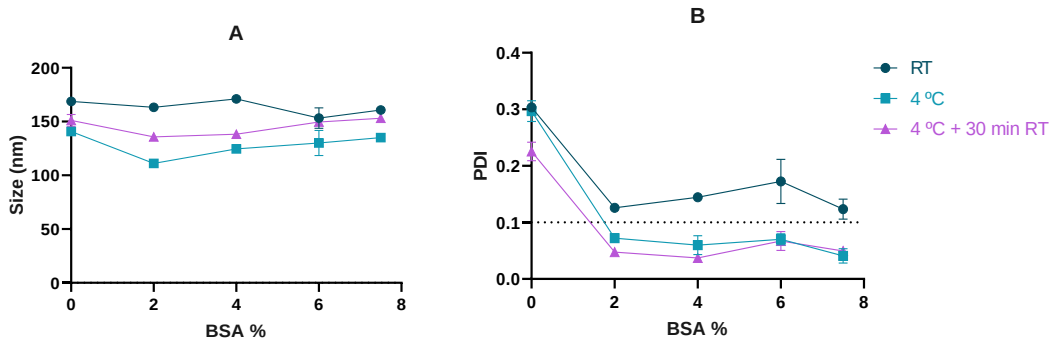

Figure 14. Influence of albumin (BSA) concentration on nanoemulsions' droplet size (A) and PDI (B). Formulation contained simvastatin at 7.41% and BSA at 0%, 2%, 4%, 6%, and 7.5%. Measures were performed at room temperature (RT), after refrigeration (4 °C), and 30 minutes at RT after being refrigerated. Data corresponds to the mean ± standard deviation of two independent dilutions of one formulation.

At 7.41% simvastatin, it was no longer possible to have a homogenous emulsion without using BSA, even after refrigeration. Even at the lowest concentration (2%) of BSA in the aqueous phase, PDI values decrease, demonstrating the importance of BSA as a stabilizing agent. Once again, by cooling the nanoemulsions with BSA, it was possible to obtain extremally homogenous droplet size (PDI < 0.1).

After improving simvastatin concentration and size properties, the next problem that emerged was the poor physical stability of the refrigerated nanoemulsions. To determine the role of BSA in delaying this effect, different concentrations of BSA were used with nanoemulsions containing simvastatin at 5.66% or 7.41%. Formulations were daily observed until precipitation occurrence. To prove the role of temperature in the loss of physical stability, this test was conducted at room temperature and 4 °C (Table 3).

Table 3. Precipitation day at room temperature (RT) and 4 °C of different nanoemulsions containing albumin (BSA) at different concentrations (0%, 2%, 4%, and 7.5%) and simvastatin at 5.66% or 7.41%.

Nanoemulsions		Precipitation Day	
Simvastatin	BSA	RT	4 °C
5.66%	0%	> 30	> 30
	7.5%	> 30	> 30
7.41%	0%	9	1
	2%	9	1
	4%	24	2
	7.5%	> 30	6

RT, room temperature

With 5.66% simvastatin concentration, both formulations had physical stability (absence of drug precipitation) at least for 30 days at room temperature and 4 °C. It means that at lower simvastatin concentrations, BSA does not play a major role in increasing physical stability. This difference compared to the previous results reported by Mariana Fernandes of the same investigation group (85) might be due to variation in the weighting of the drug. At 7.41%, the role of temperature in speeding up simvastatin's precipitation is visible because all formulations achieved better stability at room temperature than at 4 °C. Using BSA at a concentration of 2% did not seem to affect physical stability because it had exactly the same precipitation day as the nanoemulsion without BSA (9 days at room temperature and 1 day at 4 °C). However, at BSA concentrations of 4% and 7.5%, physical stability at room temperature increased to 24 days and over 30 days when at room temperature and 2 days and 6 days at 4 °C, respectively. Despite 6 days being a considerable a short amount of time, the use of BSA at 7.5% could delay precipitation for 5 more days than when no BSA was used, proving the role of BSA in simvastatin solubilization/stabilization.

After gathering important information about the behavior of nanoemulsions, two strategies were selected to be further tested: for nanoemulsions containing simvastatin at 5.66%, BSA at lower concentrations of 2% and 4% would be used. For simvastatin 7.41%, higher BSA concentrations of 4% and 6% would be used.

In spite of showing good potential, other alternatives were also tested. The main reason relied on the BSA cost itself and its challenging safety, stability, and possible approval problems later during pharmaceutical development stages (96,97).

PEG was incorporated in the aqueous phase since the group experience and literature evidence report an increase in emulsions stability (98), permeation through mucus layers, and it is considered safe and biocompatible (99). Alternatively, CL was

incorporated in the oil phase and was tested in order to achieve cationic nanoemulsions. In fact, electrostatic interactions between CL and the negatively charged mucus layer of the nasal cavity (100), could allow less clearance, possibly increasing formulations' residence time and absorption. This principle was applied in nanoemulsions for ophthalmic drug delivery (101). Some studies applied it to nasal delivery using the cationic polymer chitosan to establish the electrostatic interactions (102–104).

PEG was used in two concentrations - 1% and 4% - while CL was used at 0.5% (based on previous experience in the research group (105)). The impact of the varying composition (BSA, PEG, and CL) in formulations droplet size and physical stability at 4 °C was determined and compared (Figure 15).

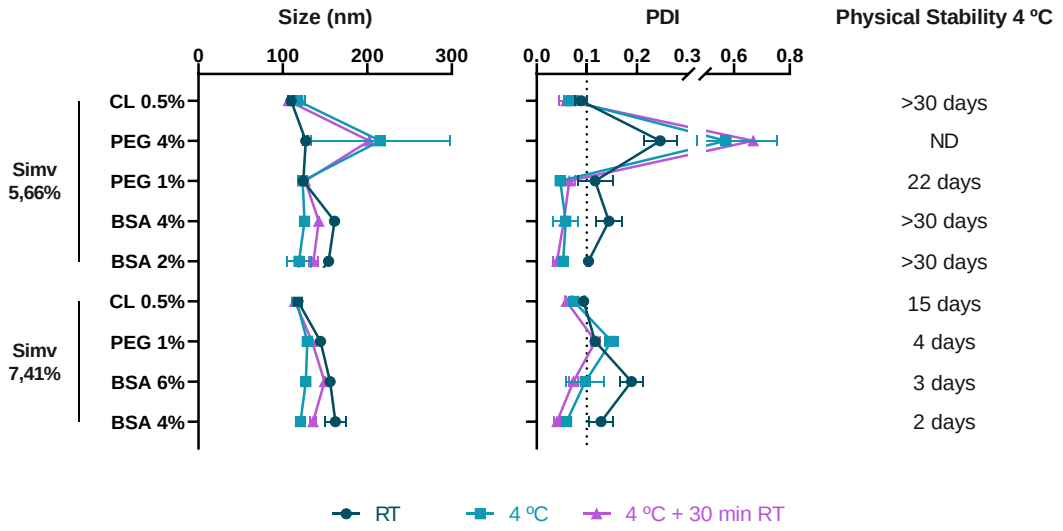

Figure 15. Influence of albumin (BSA), PEG, and cationic lipid (CL) on nanoemulsions' mean droplet size, PDI, and physical stability at 4 °C.
Simvastatin (Simv) concentrations varied between 5.66% w/w and 7.41% w/w) as indicated. Measures were performed at room temperature (RT), after refrigeration (4 °C), and 30 minutes at RT after being refrigerated. Mean droplet size and PDI data correspond to the mean ± standard deviation of two independent dilutions of one formulation. ND, Not determined.

Stability results using PEG at 4% are not plotted because, after adding the aqueous phase to the oil phase, instead of the usual translucent-amber color and fluid aspect, an opaque white and very thick emulsion was formed, making it hard to identify if there was any drug precipitation.

Regarding droplet sizes, all the strategies resulted in optimal droplets' mean sizes under 200 nm. In terms of PDI, after refrigeration, only the nanoemulsion with simvastatin at 7.41% and PEG at 1% did not reach extremely homogenous values (PDI >0.1). For both nanoemulsions, better values were achieved at room temperature than after

refrigeration. PEG 1% worked well when using simvastatin at 5.66% obtaining a PDI of 0.047 ± 0.004.

Nanoemulsions with cationic lipid led to surprising results with both concentrations of simvastatin tested. The PDI values were already extremely homogenous at room temperature (PDI of 0.089 ± 0.012 with simvastatin at 5.66% and PDI of 0.094 ± 0.001 with simvastatin at 7.41%). Nevertheless, these values were even better after refrigeration (PDI of 0.069 ± 0.014 with simvastatin at 5.66% and PDI of 0.074 ± 0.001 with simvastatin at 7.41%). An increased drug loading capacity using cetalkonium chloride was also reported in studies for ocular administration (106,107). From all the strategies explored, only the addition of cationic lipid resulted in nanoemulsions with the desired size features without refrigeration, meaning it could be used right after preparation.

In terms of physical stability, the BSA strategies displayed similar precipitation days to the previously tested formulations. PEG 1% originated less stability compared to BSA in nanoemulsions containing 5.66% of simvastatin. Still, at 7.41% better stability was obtained compared with both BSA strategies. This means that PEG can be a possible alternative when trying to stabilize the emulsion and solubilize simvastatin, despite the PDI not meeting the requirements. Nanoemulsions with CL had once again very good results by achieving stability for 15 days at 7.41% and over 30 days at 5.66% simvastatin concentrations. Combining the cationic lipid results with the previously stated BSA problems, the BSA strategy started to fall behind.

In conclusion, from the initial screening, the following nanoemulsions displayed high potential to be further studied: 'NE Simv 5.66%', 'NE Simv 5.66% CL 0.5%', and 'NE Simv 7.41% CL 0.5%'.

4.2. Microemulsion's Composition Screening

The first step in the screening phase was to increase simvastatin concentration in the microemulsion preconcentrate. To achieve it, BSA was initially tested at a concentration in the aqueous phase of 6%, associated with a simvastatin concentration of 9.09%. This formulation displayed great results with a mean droplet size of 19.5 ± 0.06 nm and a PDI of 0.05 ± 0.01. Results are plotted in Figure 16, in comparison to the equivalent microemulsion without simvastatin. However, refrigeration induced drug precipitation

overnight. This might be a problem regarding simvastatin chemical stability since simvastatin requires storage at 4 °C.

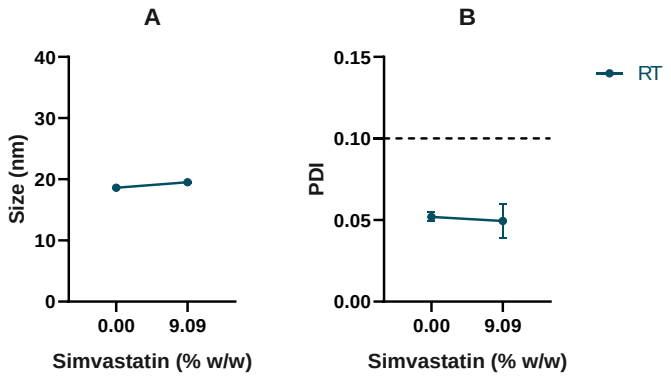

Figure 16. Microemulsions' droplet size (A) and PDI (B) containing albumin (BSA) at 6% with (9.09%) and without simvastatin.
Measurements were performed at room temperature (RT). Mean droplet size and PDI data correspond to the mean ± standard deviation of two independent dilutions of one formulation.

Two simvastatin increments were then tested: 10% and 11.11%. At those concentrations, simvastatin solubilization was not possible and precipitation started to happen right after adding the aqueous phase.

Since the microemulsion only contains 10% of the aqueous phase, this meant BSA was only at a final concentration of 0.6%. To try to improve the good solubilization and stability properties of BSA, three formulations with higher aqueous phase (20%, 35%, and 40%) were tested. This strategy did not solve the problem because, by altering the formulation's initial proportion, all three formulations jellified.

CL was a good alternative found to BSA during nanoemulsion screening, so the next step was to test it on the microemulsion. CL was tested at four different final concentrations: 0.1%, 0.2%, 0.25% and 0.3%. Therefore, by incorporating a positively charged component in the microemulsion, we expected to increase the zeta potential possibly promoting mucoadhesion.

Simultaneously, we also tried to modify the lipid-to-surfactant ratio, increasing the lipid percentage (Vitamin E) from 10% to 25%, while reducing the co-surfactant percentage (Transcutol ® HP). The three different proportions used were summarized in Table 2 in section 3.2.1. With those modifications, it was expected that more simvastatin could be solubilized in the lipid portion. Due to the antioxidant features of vitamin E, increasing its percentage could also be beneficial to simvastatin's chemical stability (108).

Simvastatin is easily oxidized even if stored in the powder form at 4 °C. So, to reduce oxidation, it needs to be stored in a nitrogen atmosphere at 4 °C.

Microemulsions with and without the modifications were tested with CL at different final concentrations (0.1%, 0.2%, 0.25% and 0.3%). Droplet sizes and PDI results from the different microemulsions are plotted in Figure 17. With some CL concentrations, size measurement was not possible due to precipitation after formulation dilution, thus being excluded. Unlike simvastatin's precipitate that forms needle-like structures, the precipitate obtained formed large macroscopic spheres with an appearance closer to cream formation. Since precipitation only happened for larger CL concentrations (0.25% and 0.3%), this might be related to CL, which is a lipophilic component with low water solubility.

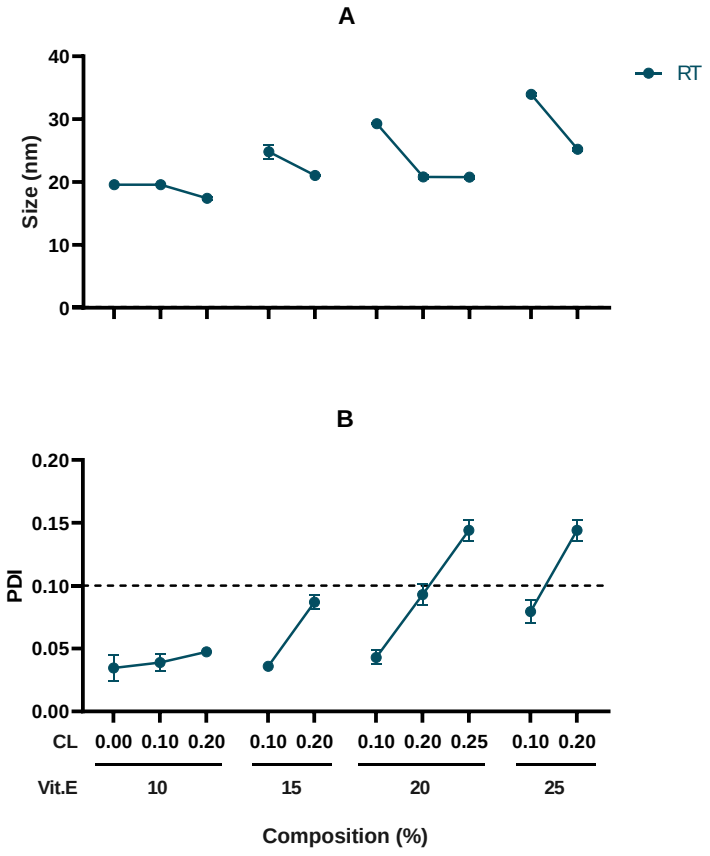

Figure 17. Influence of vitamin E (Vit.E) and cationic lipid (CL) on microemulsions' mean droplet size (A) and PDI (B).
Simvastatin (Simv) concentration used was 9.09% (w/w). Measurements were performed at room temperature (RT). Mean droplet size and PDI data correspond to the mean ± standard deviation of two independent dilutions of one formulation.

Increasing CL concentration seemed to decrease droplet size and increase heterogeneity in both microemulsions with and without modifications. Despite not achieving extremely

homogenous results (PDI of 0.144 ± 0.008), 20% Vitamin E allowed the highest CL concentration (0.25%) without precipitation. Similarly to microemulsion containing vitamin E at 15% plus CL at 0.1% or 0,2%, and to that with vitamin E 10% plus CL at 0.1%, microemulsion with vitamin E at 20% also achieved extremely homogenous PDI results. The microemulsion containing vitamin E at 20% (M2) was selected because of the higher CL incorporation while maintaining similar results to the Vitamin E at 10% and 15% microemulsions.

The M2 microemulsion was tested without CL and with an additional CL concentration of 0.15% (Figure 18). Since the main objective of modifying the microemulsion composition was to obtain higher simvastatin concentrations, the three increments were done to the initial 9.09% simvastatin concentration, resulting in 10%, 10.71%, and 11.5%. Again, some microemulsions precipitated after dilution and are not shown.

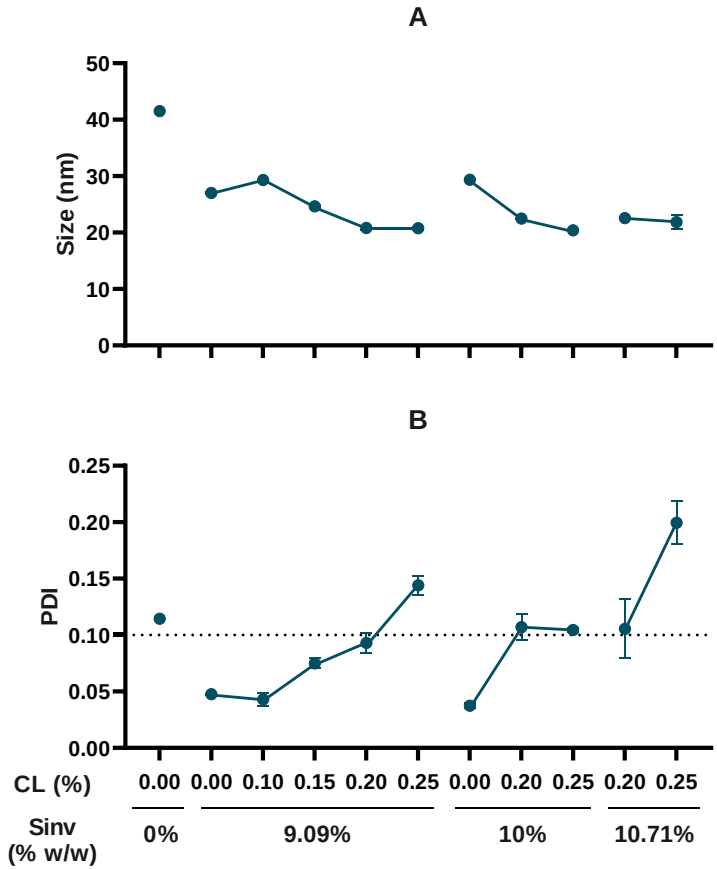

Figure 18. Influence of cationic lipid (CL) and simvastatin (Simv) on M2 microemulsions' mean droplet size (A) and PDI (B).

Measurements were performed at room temperature. Data correspond to the mean ± standard deviation of two independent dilutions of one formulation. The results of the M2 microemulsions with 9.09% simvastatin and CL concentrations of 0.1%, 0.2%, and 0.25% are plotted in the graph only for comparison purposes since the measurements are the same as those plotted in Figure 17.

These results demonstrate that, without CL, the modification for M2 worked better with simvastatin than without simvastatin. Comparing the M2 microemulsion without simvastatin with the 'ME M2 Simv 9.09%', it can be observed that adding simvastatin resulted in a particle droplet size decrease (41,52 ± 0.32 nm to 27.02 ± 0.27 nm) and an increase in homogeneity (PDI=0.115 ± 0.002 to PDI=0.048 ± 0.001). Once again, adding CL resulted in a decrease in droplet sizes and an increase in the microemulsion heterogeneity.

The M2 modification achieved the main goal by allowing simvastatin to be increased to 10.71%. At 11.5%, simvastatin solubilization in the oil phase was significantly harder to achieve, with crystals formed right after the dilution needed for measurements. At a simvastatin concentration of 10%, it was possible to obtain an extremely homogenous emulsion (PDI=0.038 ± 0.002) without CL. With CL at 0.2% and 0.25%, PDI values were close to the 0.1 mark, with 0.107 ± 0.011 and 0.105 ± 0.002 respectively. At 10.71%, the microemulsion without CL did not result, once again due to simvastatin precipitation. Still, with CL at 0,2%, it was achieved a PDI of 0.106 ± 0.026, similar to the 10% concentration.

Zeta potential of the unmodified and M2 microemulsions was also measured to determine if the incorporation of CL resulted in positively charged microemulsions. Only measurements that met quality criteria were considered and the resulting data is plotted in Figure 19.

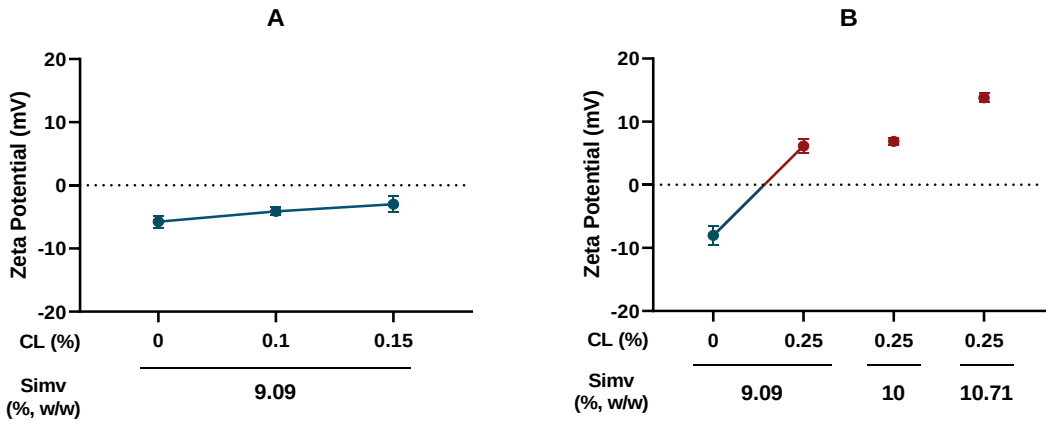

Figure 19. Influence of cationic lipid (CL) and simvastatin (Simv) on the zeta potential of microemulsions containing Vitamin E 10% (A) and Vitamin E 20% (B).
Measurements were performed at room temperature. Zeta potential data correspond to the mean ± standard deviation of two independent dilutions of one formulation.

Since microemulsions are thermodynamically stable, zeta potential optimization is intended to optimize absorption features rather than physical stability (± 30mV). Zeta potential values increased with the increase of CL. In fact, CL concentration had a statistical significance ($p<0.0001$) in zeta potential increase for both unmodified and modified formulation after ordinary one-way ANOVA analysis. However, the ± 10 mV zeta potential threshold needed for the formulation to be considered cationic or anionic (109) was only reached in the 'ME M2 Simv 10.71% CL 0.25%'. Focusing on the more promising formulations regarding size and PDI results (Figure 18), the 'ME M2 Simv 9.09% CL 0.25%' and the 'ME M2 Simv 10% CL 0.25%' revealed a zeta potential of 6.16 ± 1.17 mV and 6.89 ± 0.62 mV, respectively. It resulted in an overall increase of 14.18 mV and 14.91 mV when compared to the 'ME M2 Simv 9.09%', which had a zeta potential of -8.02 ± 1.54 mV. Despite not achieving cationic formulations, the overall increase in surface charge could result in better mucoadhesive properties, maintaining good mucus permeability and diffusion. In fact, an *in vitro* study using porcine gastrointestinal mucus (110) achieved the highest mucus diffusion when using neutral nanoparticles. The slightly positive surface charge of the M2 microemulsions could be beneficial in terms of mucoadhesion without compromising mucus diffusion, which is facilitated by higher negative charges reducing the interaction with the mucus (111).

For the microemulsion with vitamin E at 10%, only negative zeta potentials were obtained regardless of the CL concentration.

Therefore, the use of the M2 modification seemed to be beneficial due to the improvement of zeta potential and increase in simvastatin concentration, while maintaining relatively good size and PDI.

4.3. Hemolysis Assay

As previously described, after applying the formulation in the nasal cavity, simvastatin can be directly transported to the brain through the trigeminal and olfactory nerve pathways. Additionally, it can also be systemically transported due to the high vascularization of the nasal mucosa. Assuming that the micro and nanoemulsion droplets might also be partially absorbed through the systemic route this last transport route makes the evaluation of the hemolytic potential of micro and nanoemulsions an important step in assessing the safety of the formulations.

Hemolysis assays were performed using human blood from different donors with different initial concentrations of hemoglobin (Table 4). The heterogeneity of the blood samples gives robustness to the results since it represents a wider range of possible sensitivities to the formulations in the study.

Table 4. Blood pool hemoglobin concentrations and initial hemolysis.

Blood Samples	Hemoglobin (mg/mL)	Initial Hemolysis (%)	
1	135	0.35	Blood used in Assays
2	153	0.27	
3	133	0.20	
4	129	0.66	
5	121	0.18	
6	130	0.20	
7	136	0.58	
8	140	0.09	
9	129	0.62	
10	135	0.17	
11	138	0.34	
12	146		Blood used in Validation
13	140		
14	157		
15	133		
16	135		
17	135		

A total of five different formulation strategies were tested in the hemolysis assay - two nanoemulsions, and three microemulsions. The different formulations were tested with and without simvastatin to separate the hemolytic potential of simvastatin from the hemolytic potential of the excipients. To obtain the same excipient concentration between groups with and without simvastatin, formulations with simvastatin suffered a mass correction (increasing the mass weighted) in the stock solution preparation accounting for the simvastatin mass being weighted during this stage.

Considering nanoemulsions, the formulations tested were ‘NE Simv 5.66%’ and ‘NE Simv 5.66% CL 0.5%’. Microemulsions included were ‘ME Simv 9.09%’, ‘ME Simv 9.09% CL 0.25%’, and ‘ME M2 Simv 9.09% CL 0.25%’.

Besides simvastatin and excipient hemolytic powers, this group configuration also allowed the comparison between formulations with and without CL. For the case of the microemulsions, it allowed the assessment of the M2 modification (increase in vitamin E content) impact on hemolysis.

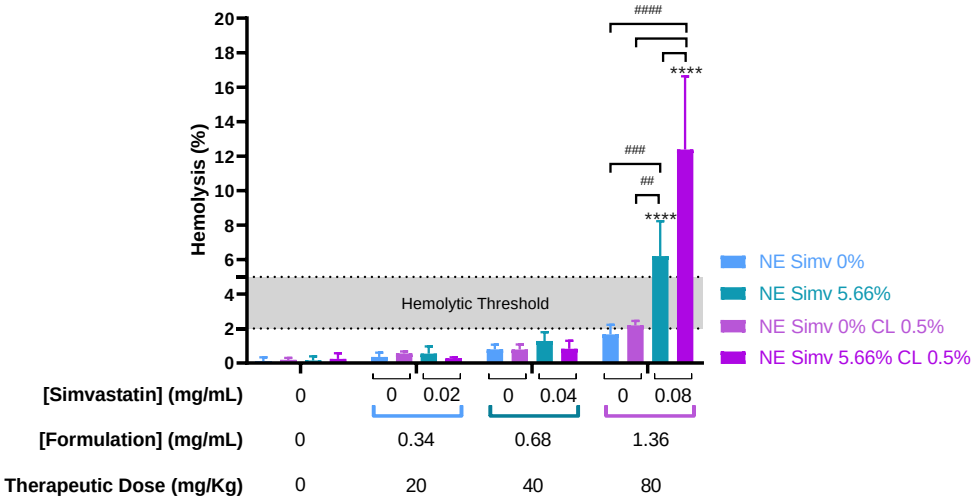

Figure 20. Nanoemulsion hemolysis results using different formulation strategies with and without cationic lipid (CL) and with (5.66%) or without (0%) simvastatin.
In total, three different formulation concentrations were incubated with blood corresponding to three different simvastatin concentrations, and therapeutic doses. Data correspond to the mean ± standard deviation of three independent formulation baches. Statistical significance differences after two-way ANOVA followed by Sidak's multiple comparisons test with the negative control (C-) and differences between test groups are highlighted by * and # symbols, respectively. */#: p< 0.05, **/## p<0.01, ***/### p<0.001, and ****/#### p<0.0001.

Starting with nanoemulsions results (Figure 20), only formulations with simvastatin at the higher therapeutic dose (80 mg/Kg) showed a significant statistical difference from the negative control (PBS). At that equivalent therapeutic dose, there were also differences between the two formulations tested with and without simvastatin. Interesting, simvastatin itself demonstrated a hemolytic potential at higher concentrations (0.08 mg/mL) since for lower simvastatin concentrations (0.02 and 0.04 mg/mL) no statistical differences were found between formulations with and without simvastatin. For the theoretical simvastatin concentration group (0.02 mg/mL), there even was a decrease in hemolysis when comparing the 'NE Simv 0% CL 0.5%' with the 'NE Simv 5.66% CL 0.5%'. That could be interpreted as the complete opposite of what was said about the higher concentration. Nevertheless, at that concentration, the hemolysis percentages are very close to the LOQ of the assay meaning that the obtained difference it's most certainly explained by the accuracy itself. In fact, simvastatin itself

has a hemolytic potential demonstrated by a study that incubated erythrocytes for 48 hours with different simvastatin concentrations (0.5, 1, 1.5, and 2 μg/mL). The results of that study demonstrated that the three highest concentrations induced significant hemolysis (approximately 12% for 1 μg/mL, 18% for 1.5 μg/mL, and 22% for 2 μg/mL) when compared to the negative control group (112).

This also confirms the importance of the drug being encapsulated in a delivery system versus the drug being freely dispersed in solution. Despite using a different drug (primaquine), Wu *et. al.* (113) described a major hemolysis decrease when the drug was encapsulated in a nanoemulsion system.

Another important conclusion possible to observe at simvastatin higher concentrations is that the incorporation of CL in the formulation had an impact on hemolysis since the 'NE Simv 5.66% CL 0.5%' showed a hemolysis increase when compared to the same formulation without the CL. This might be related to the increase in positively charged surface potential caused by the CL. This hypothesis is supported by the literature since this mechanism has been proposed and generally agreed upon as a possible reason for hemolysis induction (114,115). In fact, results using positively charged PLGA/chitosan nanoparticles proved to be more hemolytic than the negatively charged PLGA nanoparticles (116). This is also highlighted by different studies that used primary amines (positive charged) on the surface of dendrimers, where the hemolysis increase was directly related to the amine concentration. In those cases, by simply blocking primary amines and neutralizing the cationic surface charge, the hemolytic potential suffered a major decrease as reviewed by Dobrovolskaia *et. al.* (114).

Excipients also had an important role in hemolysis, exhibited by the increase of hemolysis percentages with the increase in formulation concentration in the group without simvastatin and CL. Within the excipients, surfactants might play an important role in hemolysis induction. Surfactants can interact with erythrocytes' phospholipid membranes, causing their reorganization and leading to loss of cell integrity and hemolysis (115,117). For non-ionic surfactants such as Kolliphor® RH 40, two mechanisms of hemolysis induction have been described: osmotic hemolysis and membrane solubilization (115,117). Osmotic hemolysis occurs just like erythrocyte hemolysis when in a hypotonic medium, where water uptake leads to cell swelling until the membrane can no longer resist the internal force and breaks. In this case, surfactants interact with the phospholipid membranes leading to K^+/Na^+ imbalance (K^+ loss and Na^+ uptake) causing water to enter the cell to balance the osmotic pressure resulting in lysis (115,117). Membrane solubilization is caused by surfactant micelles, rather than

surfactant monomers (osmotic hemolysis). In this case, micelles interact and remove important components of membranes such as lipids and proteins, leading to membrane disruption and hemolysis (115,117).

Regarding excipients, despite the hemolysis increase, the effect does not appear to be the most important in hemolysis since it does not reflect a statistically significant difference between the 'NE Simv 0%' to the negative control group. This led us to conclude that simvastatin, CL, and the excipients themselves have an impact on hemolysis, but it is simvastatin and CL or the combination of both that mostly contributes to it.

To categorize the formulations containing simvastatin as safe (<2%), moderate hemolytic (2%-5%), and hemolytic (>5%), a one-sample t-test was used to compare if the mean hemolysis values of which group were statistically different from the hemolysis limits of the different categories. 'NE Simv 5.66% CL 0.5%' is considered safe for both 20 mg/Kg and 40 mg/Kg therapeutic doses, and moderate hemolytic or hemolytic for 80 mg/Kg. 'NE Simv 5.66%' is considered safe in therapeutic doses of 20 mg/Kg, moderate hemolytic for 40 mg/Kg, and hemolytic for 80 mg/Kg. In conclusion for the theoretical therapeutic dose, both nanoemulsions tested were safe.

Regarding hemolysis, microemulsion results (Figure 20) evidently demonstrated a safer hemolytic profile compared with that of nanoemulsions. This can be partially explained by the higher simvastatin solubilization capacity and the respective final concentrations achieved in microemulsions, leading to less formulation necessary to obtain the same final therapeutic concentrations. As discussed before, since formulation concentration itself seems to have an impact on hemolysis, this can be one of the explanations for the safer hemolytic profile of the microemulsions. Another important factor to consider is the safety differences between excipient composition and ratios. Regarding this topic, microemulsion formulation itself looks to be safer than nanoemulsion, being further discussed during the analysis of the microemulsion hemolysis results.

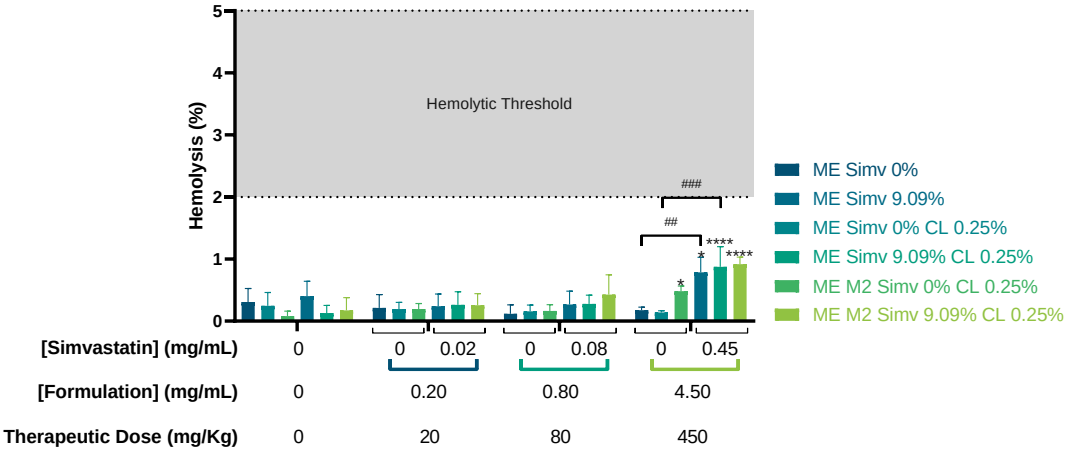

Figure 21. Microemulsion hemolysis results using a combination of different formulation strategies with and without cationic lipid (CL), with different vitamin E percentages in the pre-concentrate (M2) and also with (5.66%) or without (0%) simvastatin.
In total three different formulation concentrations were incubated with blood corresponding to three different simvastatin concentrations, and therapeutic doses. Data correspond to the mean ± standard deviation of three independent formulation baches. Statistical significance differences after two-way ANOVA followed by Sidak's multiple comparisons test with the negative control (C-) and differences between test groups are highlighted by * and # symbols, respectively. */#: $p < 0.05$, **/## $p<0.01$, ***/### $p<0.001$, and ****/#### $p<0.0001$.

All the microemulsions tested proved to be safe for therapeutic doses up to 450 mg/Kg, a value that is 22.5-fold higher than the starting theoretical therapeutic dose. This is proven by the results of the one-sample t-test, in which the mean hemolysis of all groups in all concentrations are statistically different than 1.99% and thus considered safe (<2% hemolysis).

Despite microemulsions' safety, a further analysis like that performed for nanoemulsions can be done to isolate and determine the main reasons for the hemolytic effects of microemulsions. The differences are once again best observed at the higher concentration tested and, for that, the discussion will be specially addressed to the 450 mg/Kg therapeutic dose. At that therapeutic dose, all the microemulsion groups with simvastatin showed a significant statistical difference from the negative control (PBS), just like in the nanoemulsions. However, in this case, the 'ME M2 Simv 0% CL 0.25%' also exhibited a significant statistical difference. Since the two other groups without simvastatin did not show any difference from the control group, this might indicate that the higher percentage of vitamin E can possibly be responsible for higher hemolysis potential. Contrastingly, the 'ME M2 Simv 9.09%' did not demonstrate significantly higher hemolysis than the other two formulations with simvastatin. In fact, the statistical analysis did not indicate significant differences between the three groups with simvastatin. By observing the other two therapeutic concentrations, the second approach

regarding the impact of vitamin E in hemolysis seems much more plausible due to the similar hemolysis of the three groups without simvastatin.

Just like what was discussed for nanoemulsions, simvastatin seems to have an important impact on hemolysis. However, in this case, the effect is seen throughout all therapeutic doses and especially at the higher dose. At 450 mg/Kg, both the 'ME Simv 9.09%' and 'ME Simv 9.09% CL 0.25%' groups had statistical differences from the respective groups without simvastatin. Despite showing higher hemolysis than the respective groups without simvastatin, the 'ME M2 Simv 9.09% CL 0.25%' did not have a statistical difference.

For microemulsions, the incorporation of CL did not affect the hemolysis potential since no statistical difference was obtained between the 'ME Simv 9.09%' and the 'ME Simv 9.09% CL 0.25%'.

Microemulsion excipients did not appear to have an impact on hemolysis, since no increase in hemolysis percentages occurred with the increase in formulation concentration in the group without simvastatin and CL. This is the major difference between nanoemulsions and microemulsions results. Despite not having an equal formulation concentration that can be directly compared, at a 4.5 mg/mL, the 'ME Simv 0%' had and hemolysis of only 0.18% and was considered safe after performing a one-sample t-test. This points to the conclusion that it is also safe for lower concentrations and, for that reason, it can be compared with the ones used for nanoemulsions. At a lower formulation concentration of 1.36 mg/mL, 'NE Simv 0%' had hemolysis of 1.67%. After performing a one-sample t-test to the upper limit of safety (1.99), the test concluded that there was no statistical difference, meaning the value cannot be taken as safe, but possible as moderate hemolytic. All the above results led to the conclusion that microemulsion excipient content is safer than nanoemulsion content.

During the hemolysis assays, three other control groups were performed to assure the assay was well performed and to give robustness to the obtained results. A positive control using Triton X-100 at a concentration of 0.2% was used to identify if complete or almost complete hemolysis were possible to achieve. Ultra-pure water was used as an intermediate positive control group for lower hemolysis percentages since the hemolysis percentages of ultra-pure water were around 30 % (Figure S3 in Supplementary Data Section S3). Finally, an interference control evaluated if the formulations could be interfering with the hemolysis quantification (Figure S4 in Supplementary Data, Section S3). By these results, it was confirmed that, despite a slight variability, both complete

and intermediate hemolysis could be achieved in all the tests performed and that the formulations were not interfering with hemolysis quantification.

To close the hemolysis discussion, it is important to refer to why higher concentrations of the microemulsions were not tested to determine where they start to lose safety and become slightly hemolytic or even hemolytic. This is linked to the poor water solubility of simvastatin that, even when loaded in the microemulsion at higher concentrations, starts to precipitate after PBS dilution. So, higher concentrations could not be used due to drug precipitation which will lead to invalid assay results.

4.3.1. Validation

Regarding linearity, a linear equation with a good coefficient of correlation (r^2) was obtained using the six standard curve replicates:

$$y = 0.00931x + 0.001615\ ,\ r^2 = 0.9999.$$

Precision and accuracy were tested using different weighting factors and forcing the linear regression to go through the origin. Of the total five different weighting methods, $1/x^2$ without forcing to pass through the origin displayed the best precision and accuracy, having the lowest sum of CV% and bias (Table 5). That weighting factor also produced the best LOD and LOQ (Table 5). It also provided a very good quantification value that enabled us to distinguish small differences in the hemolysis percentage and, consequently, increase the robustness of the assay.

Table 5. Precision, accuracy, and sensitivity (LOD and LOQ) using $1/x^2$ weighting factor without forcing to go through the origin.

H_{nom} (%)	H_{exp} (Mean ± SD %)	Precision (% CV)	Accuracy (% bias)	Sensitivity (Hemolysis %)	
100	100,07 ± 2.41	2.4	1.10	LOD	LOD
70	70,50 ± 2.66	3.8	1.14	0.05	0.05
50	49,59 ± 1.33	2.7	2.44		
40	39,94 ± 1.12	2.8	1.71		
30	30,22 ± 0.88	2.9	1.10		
20	20,51 ± 0.58	2.8	1.04		
10	10,19 ± 0.21	2.0	0.77		
5	5,09 ± 0.20	3.9	0.48		
2	1,90 ± 0.09	4.6	7.37		
1	0,95 ± 0.13	13.3	3.43		
0.5	0.50 ± 0.09	17.6	7.14		

H_{nom}, nominal hemolysis; H_{exp}, experimental hemolysis; CV, coefficient of variance; SD, standard deviation; LOD, limit of detection; LOQ, limit of quantification.

4.4. Osmolality Characterization

Osmolality is especially important regarding the safety and compatibility of the emulsions with the nasal cavity. In addition, osmolality values can also modify formulation residence time and drug absorption. Before being tested *in vivo* and based on the good properties displayed in the screening phase, one microemulsion and one nanoemulsion were characterized regarding osmolality. The formulations tested were the: 'ME M2 Simv 9.09% CL 0.25%' and 'NE Simv 5.66% CL 0.5%'.

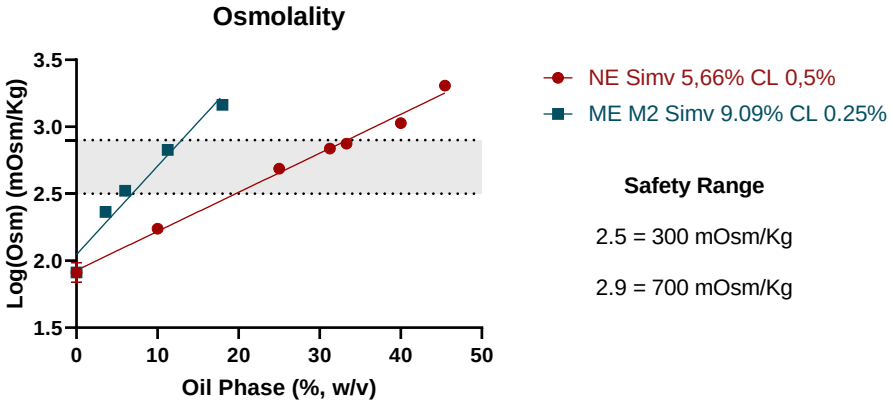

Figure 22. Micro and nanoemulsion oil phase percentage (w/v) impact on osmolality natural logarithm.

Formulations were increasingly diluted using ultrapure water in order to determine osmolality in the nasal cavity safety range (300-700 mOsm/Kg).Based on each dilution ($n = 3$), osmolality did not seem to follow a linear distribution. By applying a logarithmic function, it achieved better linearity. For that, the linear regression equation was done using the logarithmic osmolality values. Results of this transformation and linear regression are plotted in Figure 22 and equation information is summarized in Table 6.

Table 6. Result of the linear regression for the micro and nanoemulsion osmolality using the osmolality natural logarithm.

Formulation	Linear regression equation		
	Slope	Y-intercept	r^2
Microemulsion	0.06589	2.046	0.9586
Nanoemulsion	0.02914	1.928	0.9928

The differences between the oil phase percentage of micro and nanoemulsions are explained by the composition of the formulations themselves. Microemulsions consist of 90% of the oil phase and 10% of the aqueous phase, while nanoemulsions have 50% oil phase and 50% aqueous phase. This meant that, when applying the same dilution to both, microemulsions would always have a higher oil phase and also have higher osmolality

values. Using the obtained equations for both formulations, it is possible to calculate the dilutions required to reach safety for the upper (700 mOsm/Kg) and lower (300 mOsm/Kg) limit of osmolality. Both values are considered hypertonic compared to the physiological normal blood plasma osmolality range of 285-295 mOsm/Kg (118,119).

Starting with the nanoemulsion, 31.43% of the oil phase would have an osmolality of 700 mOsm/Kg, with 18.79% of the oil phase having an osmolality of 300 mOsm/Kg. That can be translated into a dilution of 2.66-fold and 1.59-fold, respectively.

For the microemulsion, 12.11% oil phase would have an osmolality of 700 mOsm/Kg and 6.52% of the oil phase would have an osmolality of 300 mOsm/Kg, converting into dilutions of 4.13-fold and 7.67-fold, respectively. So, to be safe, the microemulsion needs a higher dilution. Despite being too hypertonic to use without dilution, we should consider that, after instillation in the nasal cavity, the formulations would be spread through the nasal mucosa (78). So, during this process, the formulations would possibly be diluted in the multiple secretions contained in the area. The nasal cavity also has a very high surface area (120) because of the microvilli (121), where the formulations can spread and dilute. Described volumes used in intranasal delivery are around 100 µl. Assuming the value of 700 mOsm/Kg to achieve safety, the nanoemulsion needed to dilute in a volume of 59 µl and the microemulsion in a volume of 313 µl.

A possible solution to achieve better osmolality and reduce the required dilution could be replacing the malate buffer with a pH=5 buffer with less osmolality. Malate buffer had a mean osmolality value of 83 mOsm/Kg meaning the formulations had an osmolality contribution from the buffer itself. By decreasing aqueous phase osmolality, overall formulation osmolality would also be reduced.

4.5. HPLC Method Validation

Selectivity was assured since, at simvastatin retention time (RT), both the micro and nanoemulsion blank samples had an absence of interferences, enabling simvastatin selective quantification (Figure 23).

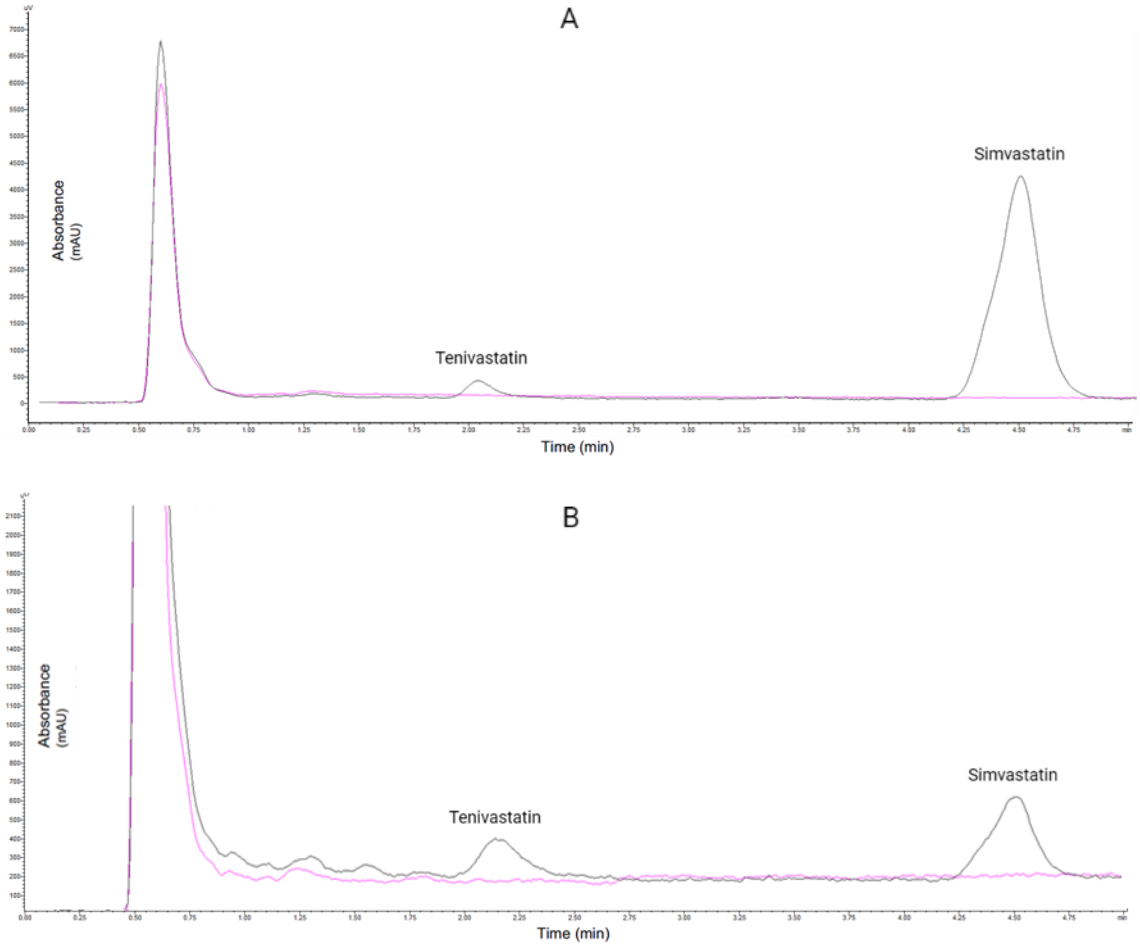

Figure 23. Chromatograms of microemulsion M2 with cationic lipid at 0.25% (A) and nanoemulsion with cationic lipid at 0.5% (B) containing simvastatin (blue chromatogram) overlaid with blank samples of the two formulations without simvastatin (pink chromatogram).
Tenivastatin was present in the samples used (simvastatin interconversion and/or degradation) and can also be detected for both formulations using the HPLC method conditions.

Calibration curves prepared on the three different days of validation showed linearity for the range of concentrations used (0.024925-4.985 µg/mL). After testing different weighting factors, $1/x^2$ was selected for exhibiting the best linearity and coefficient of determination (r^2=0.9928) (Table 7).

Table 7. Linearity using $1/x^2$ as the weighting factor.

Equation (y= ax + b)		
Slope (a)	Y-Intercept (b)	r^2
33158.8276	56.5151	0,9928

The $1/x^2$ weighting factor also achieved the best overall intraday and interday precision and accuracy (Table 8).

Table 8. Intra and interday precision (% CV) and accuracy (% bias) values obtained for quality control (QC) samples at the lower limit of quantification (QC_{LLOQ}), and at the low (QC1), middle (QC2), and high (QC3) concentration levels representative of the calibration ranges.

Quality Controls		Interday (n=3)			Intraday (n=5)		
	Cnom (µg/mL)	Cexp (Mean ± SD µg/mL)	Precision (% CV)	Accuracy (% bias)	Cexp (Mean ± SD µg/mL)	Precision (% CV)	Accuracy (% bias)
QC_{LLOQ}	0.024925	0.023 ± 0.001	3.2	-6.5	0.025 ± 0.001	4.7	-0.2
QC1	0.074775	0.068 ± 0.007	10.1	-8.6	0.075 ± 0.006	8.4	-0.1
QC2	0.4985	0.536 ± 0.02	3.6	7.5	0.491 ± 0.033	6.7	-1.6
QC3	4.985	5.341 ± 0.088	1.6	7.1	5.644 ± 0.192	3.4	13.2

Cnom, nominal concentration; Cexp, experimental concentration; CV, coefficient of variance; SD, standard deviation.

Sensitivity was recognized after the LLOQ value was established at 0.024925 µg/mL, which demonstrated acceptable precision and accuracy (Table 8) within the range established by the EMA and FDA guidelines. Taking the acceptance criteria from the previously mentioned guidelines, the present method showed to be precise and accurate for simvastatin quantification with the intraday and interday CV and bias values calculated for QC1, QC2, and QC3 meeting the mentioned international guidelines (Table 8).

Finally, stability was assessed at different storage and handling conditions. Except for samples stored at 4 °C for 48 hours, no significant loss of simvastatin was observed, with concentration values between the acceptance criteria earlier defined (Table 9).

Table 9. Stability (values in percentage) of simvastatin at low (QC1) and high (QC3) concentrations of the calibration range in processed samples in nasal buffer pH 5 and stock samples prepared in methanol.

Stability (%)		
	QC1	QC3
Cnom (µg/mL)	0.074775	4.985
Processed Samples		
Autosampler (RT, 24 hours)	93.1	93.6
4 °C (24 hours)	99.6	102.1
4 °C (48 hours)	NS	NS
32 °C (6 hours)	98.5	107.4
Stock Samples		
-20 °C (1 month)	96.9	102.7

Cnom, nominal concentration; RT, room temperature; NS, not stable.

4.6. *In vitro* Drug Release Assay

During this type of assay, it is important to maintain drug solubility controlled since, as the test goes on, simvastatin starts to be released from the emulsion's oil/lipophilic environment to the nasal buffer solution that acts as an aqueous solution where simvastatin solubility is reduced. So, to prevent drug saturation and precipitation, sink conditions need to be verified. According to the European Pharmacopeia (38), this translates into using simvastatin concentrations 3 to 10 times lower than its solubility in nasal simulant buffer, assuming all the drug is released.

So, before performing the *in vitro* drug release assays, a test to determine simvastatin solubility in the nasal simulant buffer solution was conducted. Simvastatin was added to nasal buffer at 122 µg/mL (10-fold its water solubility). The solution with excess powder was thoroughly mixed and equilibrated for 1 hour at 32°C, then centrifuged at 12 RCF for 10 minutes to promote precipitate deposition. The supernatant was then removed, diluted 10-fold, and quantified using the HPCL method previously described. This test indicated a simvastatin solubility in the nasal buffer of 23.34 µg/mL, at 32 °C.

In preliminary assays, a nanoemulsion and a microemulsion containing 2.4 mg/g (0.24% w/w) were diluted 10-fold in nasal buffer with 100 µL of that dilution added to the donor chamber. The concentration of simvastatin in the donor solution was quantified by HPLC, indicating that an initial mass of 40.95 µg and 47.71 µg were present in the donor chamber, respectively for the nanoemulsion and the microemulsion.

In the receptor chamber, a maximum of 10.97 µg/mL was reached during this assay. That value is not ideal concerning sink conditions since it is close to the solubility limit. Still, the obtained data is informative, and the drug release profile is shown in Figure 24.

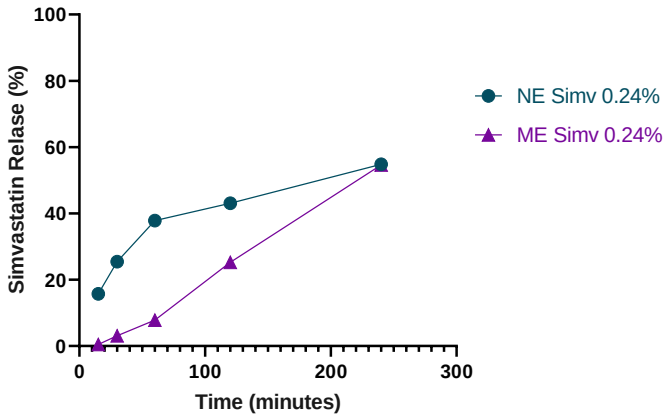

Figure 24. Simvastatin percentual drug release profile between 15 and 240 minutes from a diluted micro and nanoemulsion without cationic lipid and containing simvastatin at 0.24% (w/w).

Simvastatin release was not complete in both formulations tested after 240 minutes, with both achieving similar drug release percentages (54.84% and 54.62% respectively for the nanoemulsion and the microemulsion). Despite the similar final release percentage, the release profile was very different between the two formulations. The nanoemulsion had a faster simvastatin release of 37.08%within the first 60 minutes, starting to slow down and only releasing 17.76% in the following 180 minutes. The microemulsion had almost an opposite simvastatin release profile, with a slower release of 7.85% in the first 60 minutes of the assay but releasing 46.77% over the following 180 minutes.

In terms of release kinetics, nanoemulsion had the best correlation to the Higuchi Model (90) while the microemulsion displayed a better correlation to the zero-order release kinetics. The results of the three models tested are displayed in Figure 25.

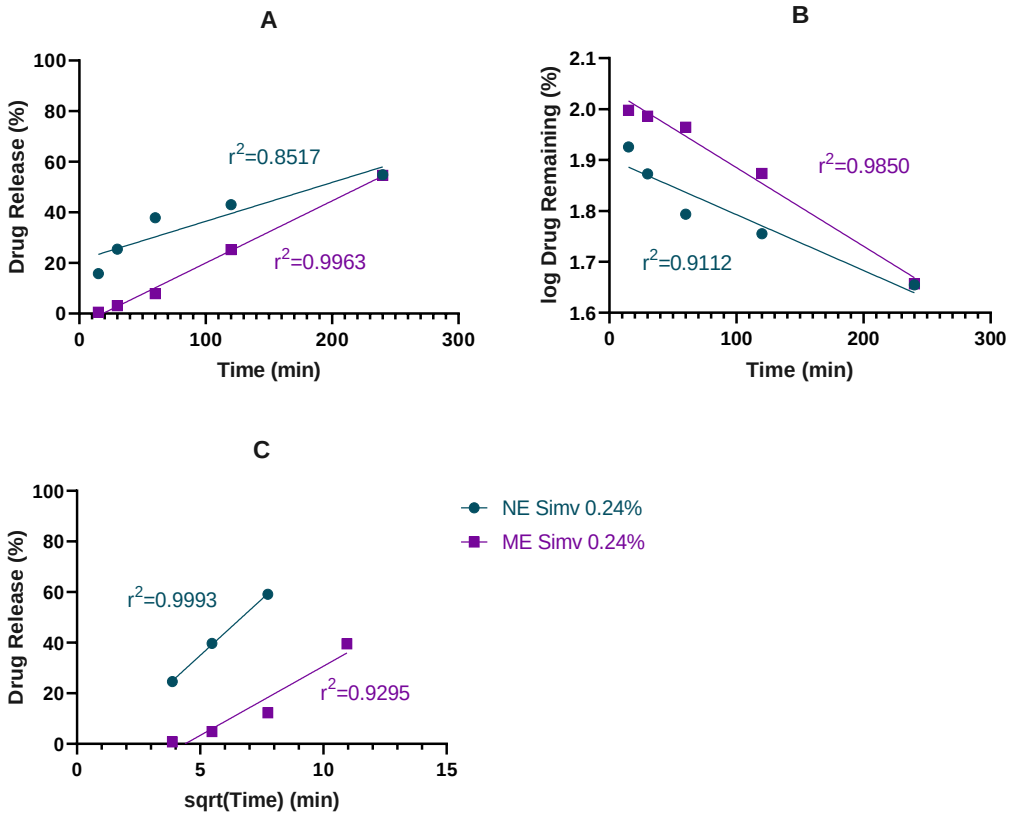

Figure 25. Drug release data of both formulations fitted with a linear regression to various kinetic models. (A) Zero-order release; (B) First-order release; (C) Higuchi Model release, only considering points within 60% of the total drug release.

Several hypotheses can be discussed to explain the obtained released profiles for both formulations. It is described that viscosity can affect drug release. However, since the

formulations were diluted 10-fold in nasal buffer, here the viscosity is expected to be low and not very different between the two formulations. Simvastatin has two different ways of passing through the membrane: it can either be transported inside the emulsion's oil droplets, or it can be released from the droplets and freely pass the membrane. Due to its high lipophilicity, simvastatin is most likely to be solubilized inside the oil droplets of the two emulsions. So, droplet size and homogeneity might also play a role in the different release profiles. Microemulsion's smaller sizes (<30 nm) and high homogeneity (PDI<0.1) could better pass through the membrane pores than the nanoemulsion droplets which have bigger sizes (<200 nm) and are slightly more heterogeneous, making it harder for the droplets to cross the membrane. By the release rate of nanoemulsion, it is expected that the principal mechanism involved is the simvastatin release from the oil droplets to the aqueous solution which then freely passes the membrane. The smaller size of simvastatin itself would facilitate diffusion that justifies the initial higher concentrations detected in the receiving chamber until equilibrium (plateau). For the case of microemulsions, the slower release but sustained rate can be explained by the drug being transported while still encapsulated, having a slower initial release but also extending the equilibrium. Another parameter that can affect the release rate is osmolality, and indeed the diluted microemulsion at 10% should have significantly higher osmolality (512 mOsm/Kg) than the diluted nanoemulsion at 5% oil phase (169 mOsm/Kg), as seen in section 4.4., and be hyperosmotic relatively to the nasal buffer of the recipient chamber.

After the preliminary assay and based on the results achieved in the screening phase and the hemolysis assay, the following formulations were selected to be tested: nanoemulsion with and without CL (0.5%) and the M2 microemulsion with CL (0.25%). In order to comply with the sink conditions, an initial simvastatin concentration of 5 mg/g (0.5% w/w) was used for nanoemulsions, and an 8 mg/g (0.8% w/w) concentration was used for the microemulsion. After a 10-fold dilution (100 mg of formulation in 10 mL of nasal buffer), a concentration of, respectively, 50 µg/mL and 80 µg/mL were expected from nano and microemulsion. In the 100 µL added to the donor chamber, a total of 5 µg or 8 µg of simvastatin could be released into a volume of 1,9 m. It means that a maximum concentration of 2.6 µg/mL and 4.2 µg/mL would be expected, which is about 8-fold and 5-fold lower than 23.34 µg/mL, respecting sink conditions. In the receiver chamber, a maximum of 2.8 µg/mL and 1.5 µg/mL was reached during the assay using the microemulsion and the nanoemulsion, respectively. Those values respect the sink conditions since they are 8-15 times lower than simvastatin's solubility in the nasal buffer. A simvastatin solution at 5 mg/g was prepared in Transcutol® HP and used as a positive control since in solution the drug release should be very fast and complete.

Once again simvastatin release was not complete in any of the formulations. Most surprisingly, the release of simvastatin from the positive control group (5 mg/g in Transcutol® HP) was only 23,26% (Figure 26).

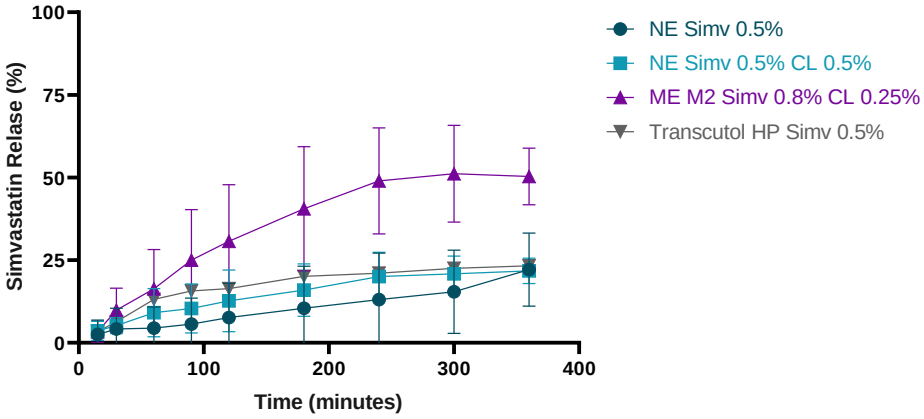

Figure 26. Simvastatin percentual drug release profile.
Samples were taken between 15 and 360 minutes. Three different formulations (two nanoemulsions with and without cationic lipid, and a microemulsion M2 with cationic lipid) were testes, as well as a simvastatin solution prepared in Transcutol® HP.

This indicated that drug adsorption to either the membrane and/or the Ussing chamber itself must be occurring in a proportion that significantly biases the results. Nanoemulsions results were also surprisingly different from those obtained in the preliminary assay, with both nanoemulsions achieving values close to the 23% mark, with the NE Simv 5 mg/g reaching 22,17% and the NE Simv 5 mg/g CL 0,5% reaching 21,73%. On the other hand, the microemulsion reached the highest release percentage of 51,16%. Comparing the only formulation used in both tests (nanoemulsion without CL) the final simvastatin concentration in the donor chamber was the only change, 40.95 µg in the preliminary and 5 µg in the second test. In fact, it can be hypothesized that, with a must lower initial mass, mass loss by adsorption must be now much more significant.

No information about similar results using Ussing chambers was found in the literature. However, in other drug release models using a dialysis apparatus, drug adsorption to the polymeric membrane has been reported as a problem (122,123). A study using cellulose membranes also described the adsorption of methyl orange to the membranes. That study also found that the quantity adsorbed increased with the concentration increase until saturation was reached but the relative amount adsorbed decreased with higher concentrations of methyl orange (124). The fact that the microemulsion did not suffer the effect to the same extent might be due to the higher 8 µg of simvastatin in the donor chamber.

A study using simvastatin-loaded chitosan/lecithin lipid nanoparticles also obtained similar results when performing *in vitro* release studies (70). In the mentioned study, the formulation was compared against a simvastatin suspension. After the initial 6 hours, it released 35.6%±4.2%, increasing to about 50% after 24 hours while the simvastatin solution reached the plateau at 21% after the 8-hour mark. The membrane's impact on the results is also discussed by the study, stating that the membrane can hinder drug release and create an additional barrier to the diffusion of simvastatin.

To clarify the drug adsorption a simple test could be performed by filling the Ussing chamber with donor solution (with simvastatin) letting it stabilize for a certain period, and then replacing it with nasal buffer and letting it stabilize (125). If the drug adsorbed to any of the Ussing chamber components, it would possibly be detected in the nasal buffer solution after HPLC analysis.

4.7. Rheological Characterization

Aiming to determine the overall behavior of the micro and nanoemulsions, rheological characterization was initially accessed using formulations without simvastatin. For this, a NE Simv 0% CL 0.5% and a ME M2 Simv 0% CL 0.25% were used (Figure 27).

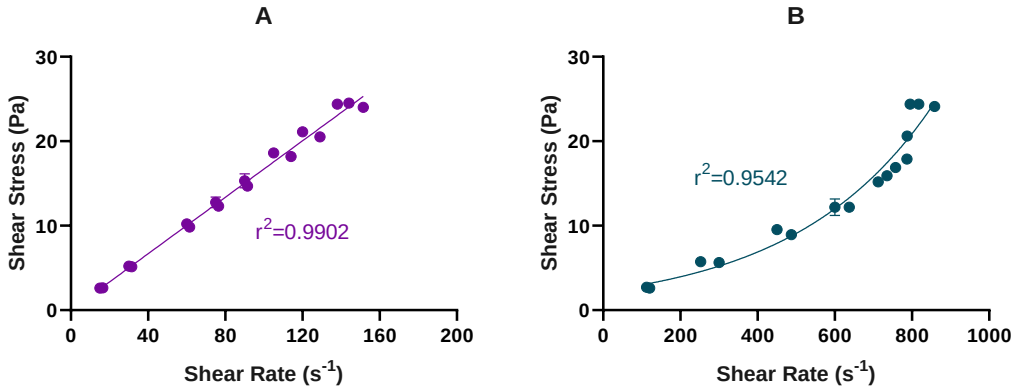

Figure 27. Rheological characterization of formulations.
Shear stress *vs* shear rate profiles of a micro (A) and nanoemulsion (B) without simvastatin with regression fits (linear regressions and exponential growth equation non-linear regression, respectively). ME M2 Simv 0% CL 0.25% and NE Simv 0% CL 0.5% were used to perform measurements at 25 °C.

A linear regression and a non-linear regression (exponential growth equation) were fitted to the shear stress values against the shear rate of the microemulsion (Figure 27A) and nanoemulsion (Figure 27B), respectively. The nanoemulsion without simvastatin

behaves as a dilatant/shear thickening non-Newtonian fluid, translating into higher viscosity when higher forces are applied. A zero shear viscosity of 28.14 ± 1.50 mPa·s was obtained considering the mean Y-intercept of the polynomial non-linear regression equations. On the other hand, the microemulsion acts as a Newtonian fluid (unchanging viscosity regardless of the force applied), with a viscosity of 168.48 ± 9.29 mPa·s. While performing the *in vivo* pharmacokinetic studies (using the same formulations but with simvastatin) it was noticed that animals receiving the microemulsion intranasally had better volume retention in the nasal cavity, contrary to the animals receiving the nanoemulsion that often sneezed out the formulation possibly due to the lower viscosity. To address this problem, two polymers were added to the aqueous phase in order to increase nanoemulsion viscosity: PVP and HPMC. Results of the formulation viscosities employing those agents are plotted in Figure 28.

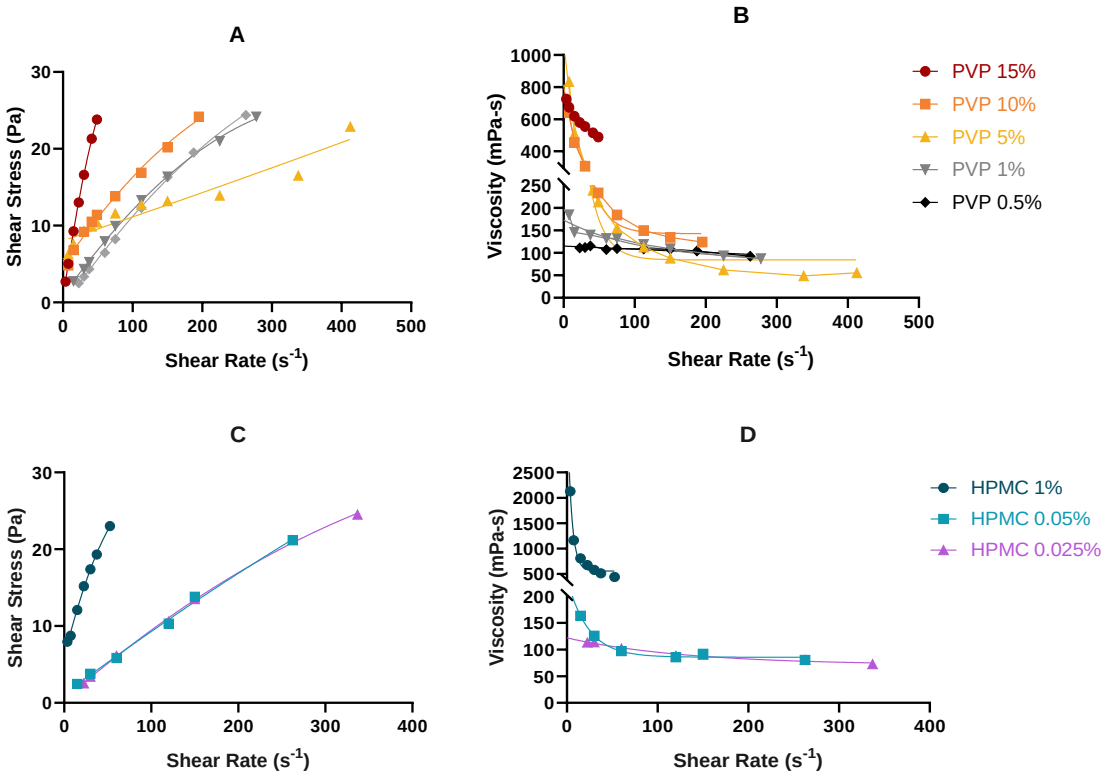

Figure 28. Nanoemulsion shear stress and viscosity profiles, using PVP (A and B) and HPMC (C and D) in the aqueous phase.

Different polymer concentrations were tested. Data corresponds to a single measurement for each polymer concentration and was fitted with second-order polynomial non-linear regression (A and C), or one phase decay non-linear regressions (B and D). Measurements were performed at 25 °C.

All these modified nanoemulsions had a pseudoplastic/shear-thinning non-Newtonian behavior, with lower viscosities for higher shear rates. This was an interesting result since

adding a viscous agent changed the non-Newtonian fluid behavior of the nanoemulsion from dilatant/shear thickening to pseudoplastic/shear thinning. Zero shear viscosities were calculated based on the Y-intercept from the one-phase decay non-linear regressions. PVP 1% and 0.5% had acceptable viscosity values of 173.2 mPa·s and 115.2 mPa·s, respectively. HPMC 0.05% resulted in a viscosity of 233.8 mPa·s and HPMC 0.025% of 121.9 mPa·s, meaning that a possible intermediate concentration could have a closer viscosity to the target 168.48 mPa·s of the microemulsion.

The next step was to test those concentrations in formulation with simvastatin. A microemulsion and nanoemulsion with, respectively, 9.09% and 5.66% of simvastatin, and without viscous agents were tested to obtain baseline values. Similar profiles (represented in Figure 29) were obtained, with viscosity values of 24.62 mPa·s for the nanoemulsion and 125.31 mPa·s for the microemulsion containing simvastatin. Despite it, the microemulsion presented a lower viscosity value when compared with the same formulation without simvastatin.

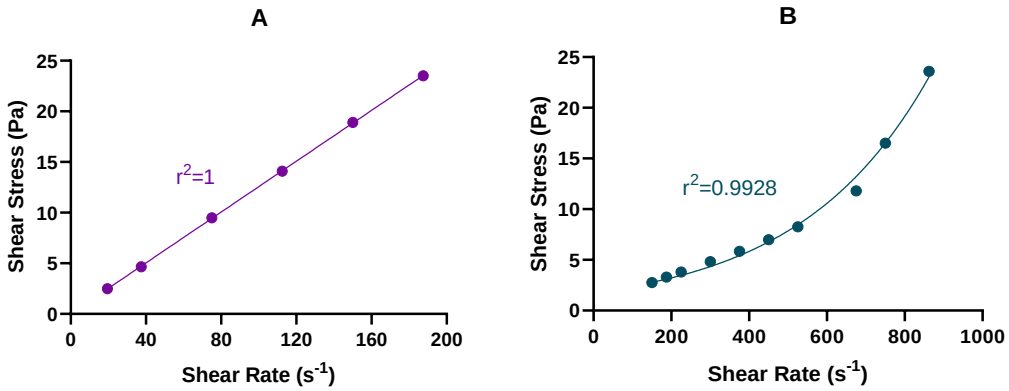

Figure 29. Shear stress *vs* shear rate profiles of a micro (A) and nanoemulsion (B) with simvastatin with regression fits (linear regressions and exponential growth equation non-linear regression, respectively). ME M2 Simv 9.09% CL 0.25% and NE Simv 5.66% CL 0.5% were used to perform measurements at 25 °C.

Since the microemulsion tested *in vivo* was loaded with simvastatin, a target range of zero shear viscosity was set between 125 mPa·s and 200 mPa·s. Compared with the viscosity values without simvastatin, viscosity was much higher than what was expected. (Figure 30).

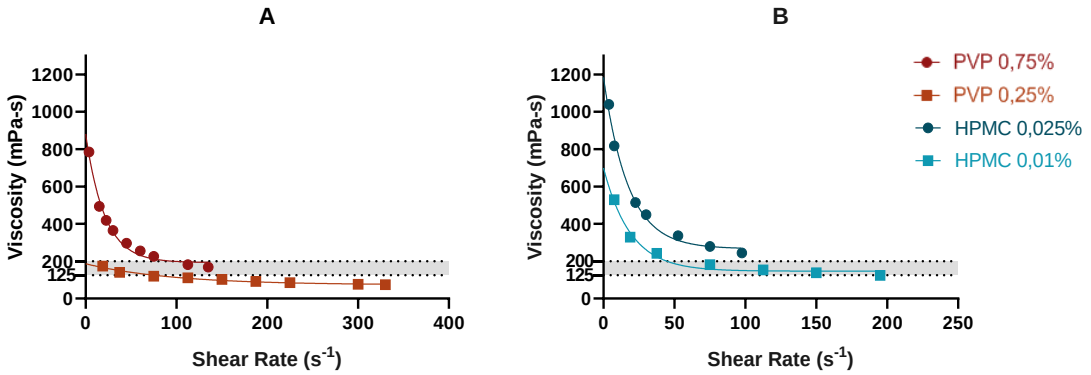

Figure 30. Viscosity *vs* shear rate profiles of nanoemulsions with simvastatin (5.66%) containing PVP (A) HPMC (B) with regression fits (one-phase decay non-linear regression).
Measurements were performed at 25 °C.

Based on the previous results, the nanoemulsion with PVP at 0.75% was expected to have a viscosity between 173.2 mPa·s and 115.2 mPa·s but, instead, it had a viscosity of 881.1 mPa·s. The concentration of PVP was reduced to 0.25% obtaining a viscosity of 186.2 mPa·s within the target range. Despite using half the concentration of PVP, viscosity was still higher than that in the formulations without simvastatin and PVP at 0.5%. Similar results were also obtained for the nanoemulsions with HPMC 0.025% and 0.01%, with respectively zero shear viscosity values of 1184 mPa·s and 699.8 mPa·s, both higher than the target range or even the literature maximum target value of 500 mPa·s (74).

PVP 0.25% was selected for further characterization of nanoemulsions mean droplet sizes and PDI. Despite not achieving desired zero shear viscosity values, HPMC 0.01% was also selected as a possible candidate for further studies since at higher shear rates it had viscosity values between the target range. After refrigeration, the 'NE Simv 5.66% CL 0.5% PVP 0.25%' had a mean size of 123.2 ±2.83 nm and PDI of 0.258 ± 0.047. On the other hand, the 'NE Simv 5.66% CL 0.5% HPMC 0.01%' had a mean droplet size of 101.4 ± 0.71 nm and PDI value of 0.099 ± 0.009. Despite the high PDI value outside the extremely homogenous mark (PDI > 0.1), the PVP nanoemulsion exhibit the same visual aspect as other good nanoemulsions previously prepared - a translucid white color that changes to an amber color when placed between a light source. However, after the 500-fold dilution needed for the measurement, precipitation slowly started to happen. The precipitation only stopped when a 50-fold dilution was rather used and, with this dilution, a droplet size of 125.7 nm and a PDI of 0.178 were obtained. Since the main objective during this study was to optimize the nanoemulsion viscosity, the values achieved with a lower dilution (that was not the optimal dilution for the nanoemulsions),

combined with the visual good aspect of the formulation, provided enough confidence to select it as a potential formulation for *in vivo* tests.

4.8. Chemical and Physical Stability Studies

In total, four formulation strategies (two independent batches each) were tested during chemical and physical stability characterization:

A. NE Simv 5.66%

B. Oil Phase NE Simv 5.66% (without aqueous phase)

C. ME M2 Simv 9.09% CL 0.25%

D. NE Simv 5.66% CL 0.5%

Formulations A and B aimed to determine if better stability by simvastatin hydrolysis reduction could be achieved by storing the nanoemulsion preconcentrate (without an aqueous phase). For that reason, they were only characterized regarding chemical stability.

Physical stability was assessed by visual inspection, droplet size, and PDI measurements over time. After phase separation was observed, the day in which it happened was registered. Then, the formulations were mixed to promote phase unification in order to characterize droplet size and PDI. This meant formulations displaying phase separation for multiple times over the assay duration (Table 10).

The visual aspect and simvastatin precipitation time are summarized in Table 10. Representative photos of the formulations' visual aspect in the different conditions are given in Figure 31. The correspondence is given by superscript letters. Visual inspection is very important since it is possible to predict mean size and PDI measurements just by the aspect of the formulations. This is especially true in the nanoemulsions, where the translucid with amber color aspect (e) often translates in extremely homogenous PDI (<0.1) and small mean droplet sizes.

Table 10. Visual aspect characterization of formulations stored at different temperature conditions (25 °C, 40 °C, and 4 °C) at the beginning (t=0) and end (t=112) of the assay, phase separation days, and simvastatin's precipitation day.

Formulation	T (°C)	Visual Aspect		Physical destabilization signs observed (days)	
		initial	by day 112	Phase Separation	Precipitation
ME M2 Simv 9.09% CL 0.25%	25	Transparent [a]	Transparent [a]	-	112 [d]
	40	Transparent [a]	Yellowish [b]	-	112 [d]
	4	Transparent [a]	Cloudy Translucid [c]	-	1 [d]
NE Simv 5.66% CL 0.5%	25	Translucid with Amber color [e]	Opaque White without Amber color [f]	14, 21, 28, 56, 112 [h]	-
	40	Translucid with Amber color [e]	Opaque Milky White with Amber color [g]	4, 8, 14, 21, 28, 56, 112 [h]	-
	4	Translucid with Amber color [e]	Translucid with Amber color [e]	-	-

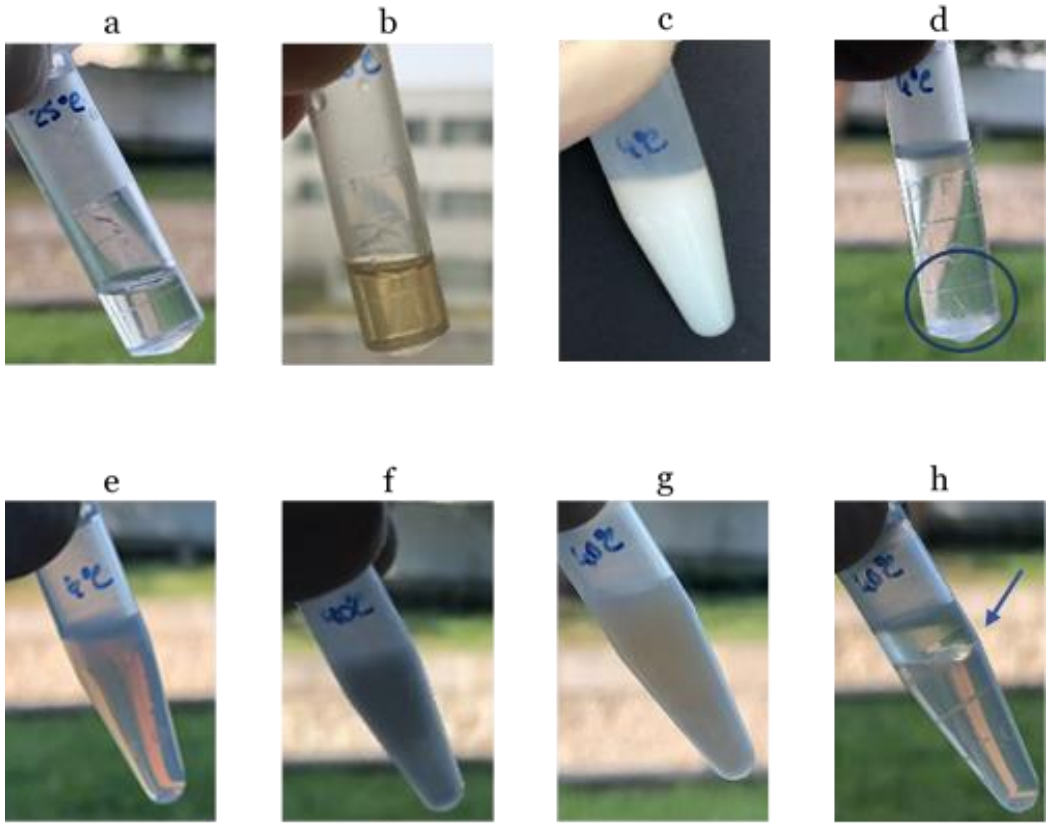

Figure 31. Different micro and nanoemulsion visual aspects. Transparent (a), yellowish (b), cloudy translucid (c), simvastatin's precipitate (highlighted by the circle) (d), translucid with amber color (e), opaque white without amber color (f), opaque milky white with amber color (g), phase separation highlighted by the arrow (h).

Droplet size and PDI results of the formulation 'ME M2 Simv 9.09% CL 0.25%' and 'NE Simv 5.66% CL 0.5%' are plotted in Figure 32. Since in 'ME M2 Simv 9.09% CL 0.25%' drug precipitation occurred after one day at 4 °C, the formulations stored at this temperature were excluded from droplet size and PDI characterization.

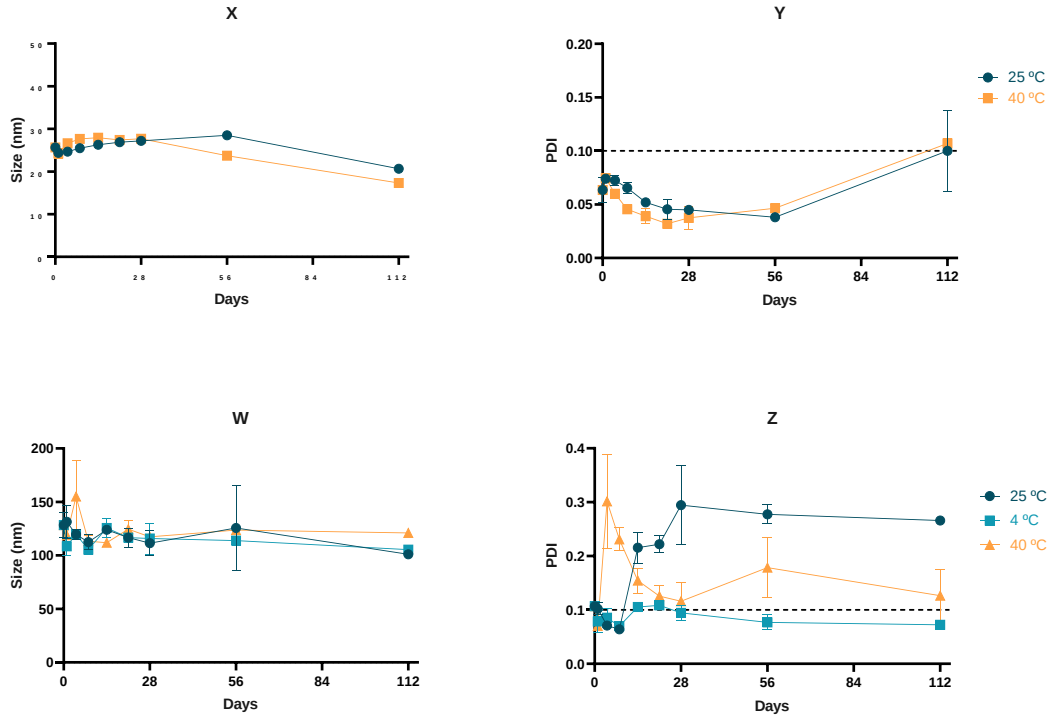

Figure 32. Formulations' droplet size characterization over time.
Formulation 'ME M2 Simv 9.09% CL 0.25%' droplets' mean size (X) and PDI (Y) and formulation 'NE Simv 5.66% CL 0.5%' droplet's mean size (W) and PDI (Z). Data correspond to the mean ± standard deviation of the two independent batches. Three storage temperatures were tested (25 °C, 40 °C, and 4 °C) at different time points (0, 1, 4, 8, 14, 21, 28, 56, and 112 days).

As already expected, the microemulsion (preconcentrate) did not show any signs of phase separation during the four months. Regarding formulations at 25 °C and 40 °C, both size and PDI remain stable throughout the time, except for the last measurement, where PDI increased due to simvastatin precipitation at both temperatures. Comparing droplet sizes and PDI at t=0 and t=56 (before precipitation), there is no statistically significant difference between the two, indicating stability. On the other hand, the comparison with t=112 is statistically significant. Considering the two batches' mean, the microemulsion started with a size of 25.65 ± 0.014 nm and PDI of 0.064 ± 0.012 nm which kept being stable until 56 days. After 112 days, droplet sizes decreased to 20.66 ± 0,21 nm (25 °C) and 17.32 ± 0.141 nm (40 °C), and PDI increased to 0.1 ± 0.038 (25 °C) and 0.107 ± 0.003 (40 °C). Droplet size decrease and PDI increase after 112 days were probably due to simvastatin precipitation, decreasing droplet size but increasing overall

heterogeneity. The temperature had no impact on both size and PDI, once again proving the thermodynamic stability of microemulsions reported in the literature (66).

Contrary, the 'NE Simv 5.66% CL 0.5%' nanoemulsions displayed early phase separation (creaming) and full phase separation at both 25 °C and 40 °C. Temperature accelerated this phenomenon with phase separation happening after 4 days at 40 °C, while at 25 °C it only happened after 14 days. This thermodynamic instability is responsible for the major PDI increase at the respective phase separation days. In contrast, at 4 °C, the nanoemulsions did not display phase separation and the PDI was stable during the 112 days. On day 0, the mean droplet size and PDI of the nanoemulsion batches were 128.4 ± 11.46 nm and 0.107, respectively. After 112 days, droplet sizes decrease to 101.1 ± 2.4 nm (25 °C), 105.5 ± 1.77 (4 °C) and 121.05 ± 3.75 nm (40 °C), while PDI increased to 0.266 ± 0.003 nm (25 °C) and 0.127 ± 0.049 nm (40 °C), but decreased to 0.073 ± 0.008 at 4 °C. No simvastatin precipitation occurred in the nanoemulsions in contrast to what happened in the microemulsions. After ANOVA analysis, droplet size and PDI did not vary significantly with time and temperature, both with a 95% confidence interval ($p<0.05\%$). However, it was the interaction between both variables that achieved higher statistical significance, with a 99.9% confidence interval ($p<0.001$). Altogether, the results are in accordance with the nanoemulsion definition of being thermodynamically unstable while having some degree of kinetic stability (metastable). At 4 °C, the kinetic stability is improved being a positive factor considering the refrigeration effect on sizes and PDI previously discussed and already hypothesized regarding the role temperature plays on simvastatin chemical stability.

During the assay, zeta potential and pH were also measured (Table 11).

Table 11. Zeta potential and pH characterization of formulations stored at different temperature conditions (25 °C, 40 °C, and 4 °C) at the beginning (t=0), after 28 days (t=28), and at the end of the assay (t=112).

Formulation	T (°C)	pH			Zeta Potential (mV)		
		t=0	t=28	t=112	t=0	t=28	t=112
ME M2 Simv 9.09% CL 0.25%	25	5.32 ± 0.26	5.11 ± 0.11	5.52 ± 0.08	2.98 ± 2.1	-	-
	40		4.90 ± 0.06	5.45 ± 0.04		-	-
	4		5.16 ± 0.08	5.22 ± 0.05		-	-
NE Simv 5.66% CL 0.5%	25	5.76 ± 0.05	5.67 ± 0.21	5.07 ± 0.06	26.48 ± 6.18	-6.87 ± 9.81	-38.52 ± 3.04
	40		5.48 ± 0.06	4.93 ± 0.41		-23.02 ± 6.87	-14.07 ± 2.84
	4		5.93 ± 0.08	5.71 ± 0.18		26.48 ± 6.18	2.82 ± 3.14

pH was kept acidic for all the formulations at the three temperatures, remaining lower than 6. That is particularly important to keep simvastatin in the lactone form (76). The formulations also achieved pH in the range of 4.5 - 6.5 needed to maintain nasal cavity pH and also to reduce possible nasal toxicity (77).

After multiple attempts, microemulsions did not achieve quality in zeta potential measurements after 28 and 112 days, so zeta potential results could not be accepted. Nanoemulsions had cationic zeta potential values at 0 days (> +20 mV) with microemulsion D2 close to the literature reported value for good physical stability due to electrostatic interaction of (± 30 mV). Both D1 and D2 had a statistically significant decrease in zeta potential after 28 days at 25 °C and 40 °C possibly due to the loss of physical stability. No significant statistical changes were obtained at 4 °C for both formulations, translating the stable behavior of the formulations at that temperature. After 112 days, all the formulations at all temperatures exhibited a statistically significant decrease in zeta potential, compared to the value at the previous time. Overall, both time and temperatures had a major influence on the stability regarding zeta potential values, which was demonstrated by statistical significance with $p<0,0001$.

Simvastatin chemical stability was also followed throughout 112 days (Figure 33). Regarding formulation B, both batches presented simvastatin precipitation after 4 days at 25 °C and 40 °C, which explains the abrupt decrease in simvastatin concentration. Temperature influenced the degradation of formulations A, C, and D. In the three groups, a statistically significant difference was obtained (two-way ANOVA followed by Turkey's multiple comparison test) between 4 °C and 40 °C, and between 25 °C and 40 °C in formulation D. This demonstrates the impact that refrigeration can have on slowing simvastatin degradation in formulations. Formulation B did not show any statistical difference between the temperatures, possibly because of the simvastatin precipitation at 25 °C and 4 °C. Despite the lack of difference between the different temperatures, for all formulations temperature and time variables displayed statistical significance (regular two-way ANOVA) in simvastatin concentration.

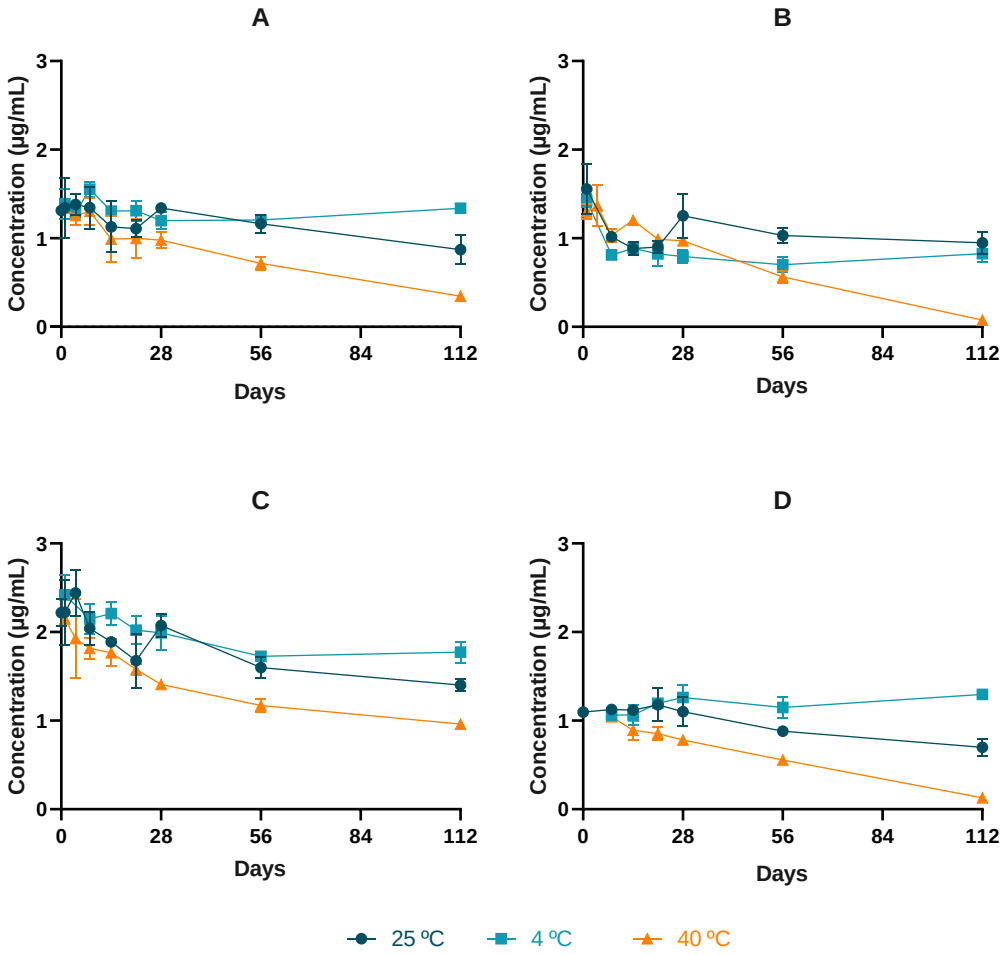

Figure 33. Simvastatin's concentration over time using the four different formulation strategies. Simvastatin was formulated in a 'NE Simv 5.66%' (A), Oil Phase 'NE Simv 5.66%' (B), 'ME M2 Simv 9.09% CL 0.25%' (C), and 'NE Simv 5.66% CL 0.5%' (D). Data correspond to the mean ± standard deviation of the two independent batches. Three storage temperatures were tested (25 °C, 40 °C, and 4 °C) at different time points (0, 1, 4, 8, 14, 21, 28, 56, and 112 days).

Regarding formulations A and B, storing the nanoemulsion as preconcentrate did not result in better chemical stability. The hypothesis that hydrolysis could be reduced by removing the aqueous phase continues to be plausible, but the overall degradation was worst (especially at 40 °C). Simvastatin degradation is pH-dependent, with studies reporting higher degradation at alkaline pH values (42,44,126). Removing the aqueous phase means the pH control by the malate buffer at pH 5 is also removed, promoting a pH shift and, consequently, simvastatin degradation. Despite the lack of an aqueous phase, the simple moisture present in the air (42) (formulations not stored in a container closure system) can induce simvastatin hydrolysis. This hypothesis is in accordance with results from Álvarez-Lueje *et. al.* (42) where simvastatin hydrolysis degradation at 40 °C was lower at acid pH of 3 and 5, and exponentially increased when using pH 6, 7, and 8.

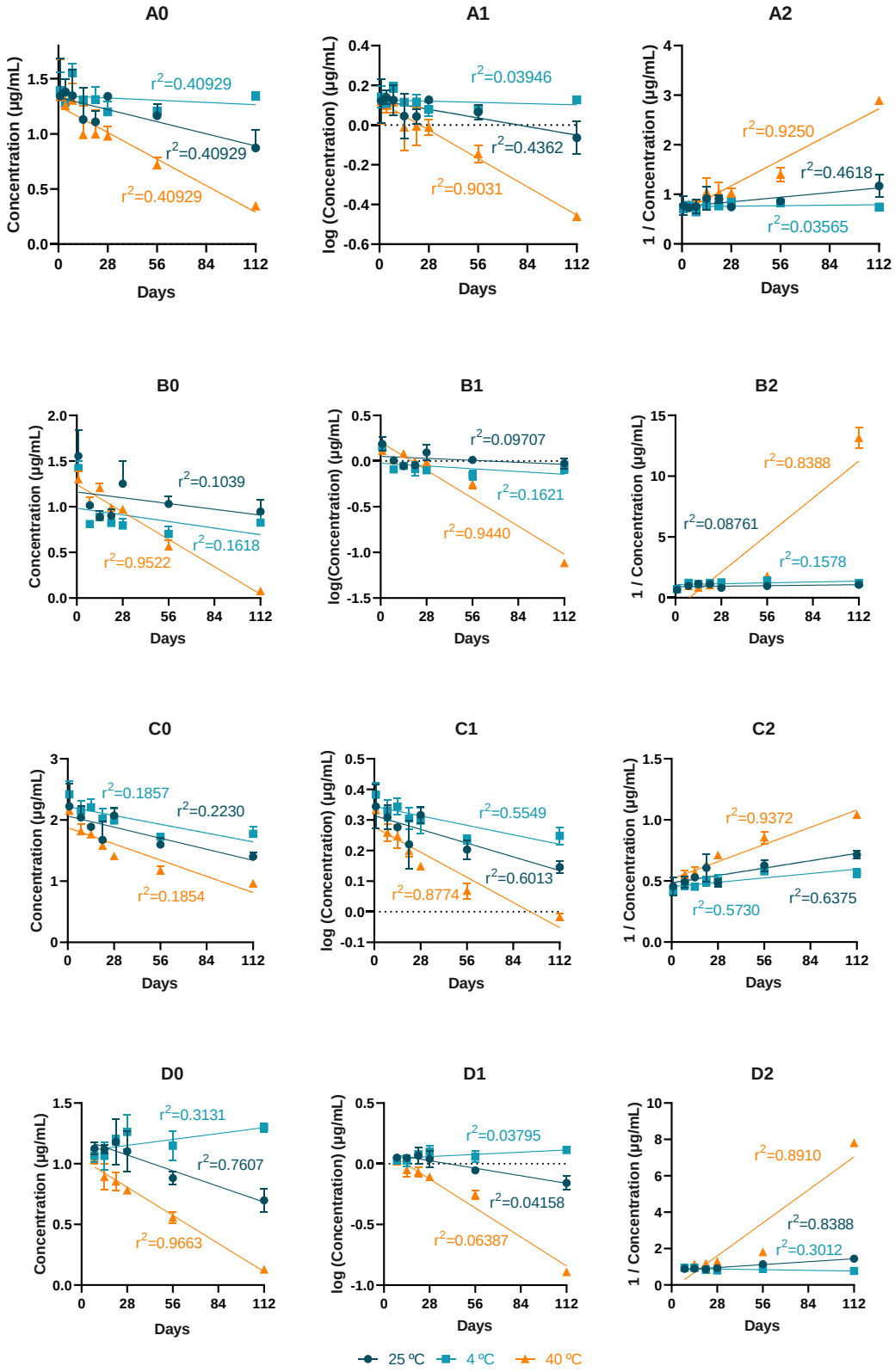

Figure 34. Simvastatin's degradation order kinetics in the formulations A (A), B (B), C (B), and D (D). Data correspond to the mean ± standard deviation of the two independent batches, at the three temperatures tested (25 °C, 40 °C, and 4 °C) over time (0, 1, 4, 8, 14, 21, 28, 56, and 112 days) and is fitted with a linear regression for zero-order (0) kinetics, first-order kinetics (1) and second-order kinetics (2) with the corresponding number next to identifying letter of the four formulations.

The drug degradation order kinetics were tested for all the formulations at the three temperatures by fitting linear regressions and evaluating the coefficient of correlation (r^2) (Figure 34). Only linear regressions for the temperature of 40 °C showed good correlation coefficients in the 4-month period. Formulations B and D display a zero-order drug degradation; formulation A displayed the first-order profile; and formulation C a second-order kinetic. Based on the behaviors at 40 °C (accelerated degradation condition), we can hypothesize that the overall degradation at the other two temperatures is slower but follows the same kinetics.
Besides simvastatin's concentration decrease throughout the 4 months, another piece of evidence confirming the chemical instability of the drug was the formation of new peaks. Those were especially predominant at 40 °C where simvastatin displayed higher degradation. Data and discussion regarding this topic is presented in Supplementary Data section S.4.

It is important to address two issues regarding the chemical stability assay. The first one is the high variability between measurements and replicates which is explained mainly by variability in pipetting methanol solutions during the dilution needed for quantification. One part of the pipetting problem was related to user inexperience, with better assay precision being achieved in the latest sample times (less variability) after better handling and understanding of all the factors impacting a rigorous pipetting, such as pipette and pipette tip position, equal up and down repetitions and also temperature stabilization before pipetting. The previously mentioned factors are especially important when it comes to pipetting organic solvents (methanol) with a regular micropipette (not suited to organic solvents). Methanol tends to drip from the pipette tip and the simple change in tip supplier can induce changes in the volume pipetted. The second issue that needed to be addressed is the fact that formulations were stored in Eppendorf tubes and not in ready-to-commercialize containers. Despite being protected by light (to avoid photodegradation), the tubes can allow evaporation and gas changes, which can have an impact on drug degradation. In robust studies to assess chemical stability and shelf life of ready-to-commercialize products, the assay is performed in the final optimized container closure system. The EMA guideline ICH Q1E (127) sets a maximum 5% change in drug content from its initial value to be considered stable. Due to sample variability and the preliminary conditions of the study, the same acceptance criteria cannot be applied to our study. Thus, the main conclusion was that at 4 °C simvastatin displayed the best stability despite drug content reduction.

4.9. *In vivo* Pharmacokinetic Studies

A first preliminary *in vivo* experiment was performed to compare brain levels of simvastatin and tenivastatin after intranasal administration. Additionally, it also intended to understand if the selected strategies allowed to achieve detectable drug levels in the brain. Animals were randomly divided into two groups, one intranasally receiving a nanoemulsion, and the other a microemulsion. In these assays, only three-time points and three animals ($n = 3$) per time point were contemplated. Due to budget constraints, only brain levels, and not plasma levels, were investigated. Tree animals from the nanoemulsion group (one at each time point) were excluded from quantification since a large amount of formulation volume was expelled after intranasal administration. The first prominent result was that tenivastatin was not detected in any of the quantified samples (Table 12). This was surprising considering that the enzyme responsible for the conversion of simvastatin to tenivastatin is present in rats' brains (128). A possible explanation for the absence of tenivastatin detection could be the drug efflux transport mechanisms responsible for quickly removing statins from the brain (129). A well-studied example is the P-glycoprotein efflux transporter which is present in the BBB, neurons, and other brain cell types (130). Nevertheless, literature reports that tenivastatin can actually be detected in animals' brains. One example of that is the Karin *et. al.* (131) study that reported levels of both simvastatin (14.7 ± 12.5 pmol/g, equivalent to 6.15 ng/g) and tenivastatin (50.1 ± 59.6 pmol/g, equivalent to 21.87 ng/g) in mice' brains after a 3 day 100 mg/kg simvastatin oral administration. Campos-Martorell *et. al.* (132) also reported having quantified tenivastatin and simvastatin at 2 and 4 hours after an intravenous administration of a tenivastatin solution to Wistar rats, even though the quantified concentrations are not mentioned. No tenivastatin concentrations are mentioned but the detection range for the ultra-performance liquid chromatography-tandem mass spectrometer (UHPLC-MS/MS) method used was between 4 ng/mL to 40 ng/mL in the brain homogenate. Wencui Yin *et. al.* (133) performed detection and characterization of simvastatin and its metabolites in different rat biological tissues, including the brain. In this case, the authors did not detect either simvastatin or tenivastatin in the brain after 1 hour of administering a single 100 mg/kg oral dose. It is hard to compare our results with the results of the previously stated studies since different doses and routes of administration were used. Contrary to the intranasal 15 mg/Kg dose used in our study, Wencui Yin *et. al.* (133) and Karin *et. al.* (131) administered, by gavage, an oral dose of 100 mg/Kg. For that dose and administration, higher simvastatin to tenivastatin conversion due to the hepatic metabolism can be expected. The comparison with Campos-Martorell *et. al.* (132) study is also difficult since

it is the drug in the active form (tenivastatin) that is administered instead of the pro-drug (simvastatin). Despite it, all the provided information is important to understand that tenivastatin can be transported to the brain, even though literature is usually unclear on that matter. In fact, it is reported that, due to a hydrophilic profile, statin acid forms (such as tenivastatin) are associated with lower BBB permeation, especially when compared to lipophilic statins (such as simvastatin). Hydrophilic statins need to be transported by organic anionic transporters and monocarboxylic acid transporters, while lipophilic statins passively cross the brain barriers (129,130,134).

Table 12. Quantification of simvastatin and tenivastatin at different times (30, 120, and 360 minutes) after intranasally administering a 15 mg/kg dose of simvastatin formulated in a micro and nanoemulsion. ME M2 Simv 10.87% CL 0.25% and a NE Simv 9.94% CL 0.5% were used as the administered formulations.

Formulation	Time (min)	Animal	Simvastatin (ng/g)		Tenivastatin (ng/g)
			Individual value	Mean ± SD	Individual value
Nanoemulsion	30	n1	130	153 ± 32.53	ND
		n2	176		ND
	120	n1	ND	0	ND
		n2	ND		ND
	360	n1	ND	0	ND
		n2	ND		ND
Microemulsion	30	n1	30.2	33.6 ± 35.42	ND
		n2	70.6		ND
		n3	ND		ND
	120	n1	ND	0	ND
		n2	ND		ND
		n3	ND		ND
	360	n1	154.1	182.87 ± 107.48	ND
		n2	301.8		ND
		n3	92.7		ND

ND, Not detected; SD, standard deviation.

Regarding our results (Table 12), after intranasal administration, lower simvastatin to tenivastatin conversion is expected, since liver metabolism is bypassed. Consequently, lower tenivastatin concentration is expected to reach the brain. Despite the possibility of simvastatin being also metabolized in the brain, if the efflux transport of simvastatin surpasses its metabolism rate, only a very low concentration of tenivastatin, outside of the detection range of the HPLC-MS/MS method used, might be present in the brain at a certain time.

That explanation can be supported by studies reporting that simvastatin is actually a subtract for the P-glycoprotein efflux transporter present in BBB. An example is a study by Cuiping Chen *et. al.* (135) that did not detect tenivastatin after simvastatin and tenivastatin were administered at 3 mg/Kg subcutaneously. This study only detected simvastatin at 30 minutes (191 ± 33 ng/mL using knockout mice for the mdr1a/b gene and 43 ± 46 ng/mL in wild-type mice) after administering simvastatin, even though samples were also collected after 90 and 180 minutes of administration. The method used by the authors has an LLOQ for both simvastatin and tenivastatin of 10 ng/mL in the brain homogenate (lower than the one used for our samples) (135). The study by Cuiping Chen *et. al.* (135) study is important because the knockout model used demonstrated that P-glycoprotein acts as an efflux transporter, removing simvastatin from the brain. Another important conclusion was that conversion from simvastatin to tenivastatin was observed when the lactone form was administered (detected in the plasma) but the conversion from acid form to lactone was not detected in plasma, liver, and brain. The results contrasted with statin results in humans and they could be partially attributed to the difference in species (mice *vs* humans) and/or the subcutaneous route of administration (normally the oral route is used in humans).

The subcutaneous route is closest to the intranasal route. For that reason, the simvastatin concentrations obtained will be discussed in comparison to the last-mentioned study. Despite using a dose 5-times lower than the one used in our study, after 30 minutes of administration, simvastatin concentrations match with the obtained results for the microemulsion (53.15 ± 38.32 ng/mL), but the nanoemulsion obtain a concentration 3,55-fold higher at the same time point. These results are in accordance with the different *in vitro* release profiles (see section 4.6), where the nanoemulsion had a faster release at 30 minutes compared to the slower microemulsion release. However, the concentration at 6 hours using the microemulsion is puzzling since no simvastatin could be found at 2 hours and reappeared 4 hours later.

A second *in vivo* test was performed using a lower dose (10 mg/Kg) to try to confirm and clarify some of the previous *in vivo* results and to compare further formulation behavior *in vivo*. Once again, no tenivastatin was quantified in rats' brains, even when administering a tenivastatin solution (results not reported).

For all simvastatin formulations, the prodrug was detected at the first three-time points (15, 30, and 60 minutes) but not at 6 hours, with concentrations decreasing in all the formulations from 30 minutes to 1 hour (Figure 35). Combining this information with the preliminary study results, simvastatin brain concentrations seem to have a rapid

increase, followed by a fast decrease in the first 1 - 2 hours after administration. Contrary to what occurred in the first preliminary *in vivo* study, after intranasal administration of the microemulsion, the maximum concentration in the brain was not observed after 6 hours post-dose, with results being in accordance with those obtained for the other formulations. Despite no statistically significant difference, probably due to the low number of replicates, important hypothesis can be speculated to guide future investigation. From the three nanoemulsions strategies used, the NE 8.79% CL 0.5% had the lowest initial concentration (49.67 ± 12.5 ng/mL) but obtain the highest concentration at 30 minutes (131.3 ± 27.43 ng/mL). Compared with the nanoemulsion without CL, the presence of CL seems to slow but also prolongate the delivery of simvastatin to the brain. This might be due to interaction with the mucus that, on one hand, can hamper the mucus permeation capacity of the nanoemulsions but, on the other hand, might increase retention time and facilitates absorption through the membranes. Increasing the viscosity did not produce improvements when compared with the NE Simv 8.79% CL 0.5% at 30 minutes but had a slightly better result than the NE Simv 8.92% at 30 minutes. Once again, the nanoemulsion seems to be a better alternative than the microemulsion, with higher concentrations reached at 30 minutes, like in the preliminary test.

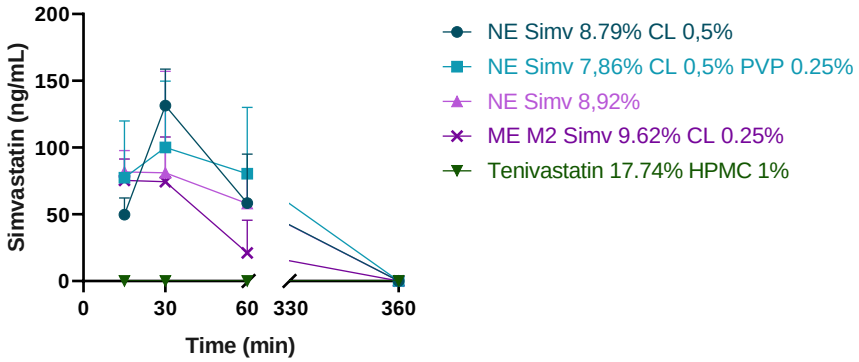

Figure 35. Quantification of brain simvastatin at different times (15, 30, 60, and 360 minutes) after intranasally administering a 10 mg/kg dose of simvastatin formulated in different micro and nanoemulsion and a viscous (HPMC 1%) tenivastatin solution at 17.74%.
ME M2 Simv 9.62% CL 0.25%, a NE Simv 8.79% CL 0.5%, a NE Simv 7.86% CL 0.5% PVP 0.25%, and a NE Simv 8.92% were used as the administered formulations. Data correspond to the mean ± standard deviation of three animals ($n = 3$) for each time point, except at 360 minutes where in the NE Simv 8.79% CL 0.5% only two animals were used and in the and NE Simv 8.92% where no animals were used.

Despite using a lower dose to reduce the administration volume (10 mg/Kg), and thus give better chances for intranasal absorption, in this second study simvastatin concentrations in the brain were similar to those obtained when using 15 mg/Kg.

Moreover, our obtained concentrations were still higher than the concentrations previously mentioned for other *in vivo* studies using oral administration with a 10-fold higher dose (100 mg/Kg). Correlating the information gathered in the *in vivo* tests with the *in vitro* concentrations reported in the literature (see Table 1, section 2), our strategy might be promising to obtain neuroprotection concentrations (within 41.86 and 418.6 ng/mL). However, the reported *in vitro* vascular effect concentration (2092.8 ng/mL) was not reached in rats' brains in any of our studies. Still, that could possibly be reached in the blood after intranasal delivery and should be a matter of future investigation.

Chapter 5

Conclusion

Considering all compositions and the different attributes evaluated during this work, the nanoemulsion strategy containing CL at 0.5% seems to be the most promising formulation for simvastatin intranasal administration. The nanoemulsion fulfilled the quality attributes set in the QTPP (see Table 1, section 2), such as drug strength, mean droplet size, PDI, hemolytic safety, viscosity, and pH. A good compromise between drug strength and physical stability was obtained, with the nanoemulsion containing simvastatin at 5.66% being stable at 4 °C for 4 months. The better physical stability at 4 °C and the improvement of size and PDI properties proved to be an advantage over the microemulsion strategy since refrigeration contributed to less simvastatin chemical degradation. The preliminary *in vivo* assays also demonstrated that this formulation, when intranasally administered, might represent a possible alternative to the oral and subcutaneous administration of simvastatin, with similar/better results even administrating lower doses.

However, further studies need to be conducted to fully understand and characterize the selected nanoemulsion. It would be important to identify the major simvastatin degradation products in order to develop strategies to effectively reduce simvastatin's degradation. Understanding the reasons beyond the incomplete drug release profile of simvastatin using horizontal Ussing Chambers is another topic that needs further study and optimization, to develop a suitable assay to predict *in vivo* drug release. Mucoadhesion, drug permeation, and nasal mucosa safety could also be addressed as factors to characterize and optimize in the future, with a special emphasis and priority on mucosa safety.

Finally, understanding how simvastatin and tenivastatin brain and plasma pharmacokinetics and functional studies correlate between them is a key aspect to improve the applicability of simvastatin in ischemic stroke and neuroprotection. Since tenivastatin is the active form of simvastatin responsible for promoting all the pleiotropic effects described as possible being neuroprotective, it is surprising how little information there is in the literature about its direct role, with most of the studies only focusing on simvastatin administered doses and not tenivastatin achieved concentrations. In fact, tenivastatin quantification in the brain with increased sensitivity, and characterization

of its plasmatic profile may be of great interest. In addition, its conjugation with dose-effect studies and *in vitro* studies of tenivastatin in neuroprotection assays might finally clarify therapeutic concentrations required, and whether systemic delivery, rather than brain direct delivery, is required for a neuroprotective effect of simvastatin/tenivastatin.

It is also important to mention that all the knowledge and experience produced while optimizing and characterizing the different micro and nanoemulsions can be applied in the future to formulate other lipophilic drugs. In fact, the present work is already facilitating the application of the present drug delivery technology in research performed in the lab with different drugs and with different aims.

References

1. Katan M, Luft A. Global Burden of Stroke. Semin Neurol. 2018 Apr 1;38(2):208–11.
2. Barthels D, Das H. Current advances in ischemic stroke research and therapies. Biochim Biophys acta Mol basis Dis. 2020 Apr 1;1866(4):165260.
3. Squizzato A, Romualdi E, Dentali F, Ageno W. Statins for acute ischemic stroke. Cochrane database Syst Rev. 2011 Aug;(8):CD007551.
4. Christophe B, Karatela M, Sanchez J, Pucci J, Connolly ES. Statin Therapy in Ischemic Stroke Models: A Meta-Analysis. Transl Stroke Res. 2020 Aug;11(4):590–600.
5. Hanson LR, Frey WH 2nd. Intranasal delivery bypasses the blood-brain barrier to target therapeutic agents to the central nervous system and treat neurodegenerative disease. BMC Neurosci. 2008 Dec;9 Suppl 3(Suppl 3):S5.
6. Grysiewicz RA, Thomas K, Pandey DK. Epidemiology of ischemic and hemorrhagic stroke: incidence, prevalence, mortality, and risk factors. Neurol Clin. 2008 Nov;26(4):871–95, vii.
7. Kuriakose D, Xiao Z. Pathophysiology and Treatment of Stroke: Present Status and Future Perspectives. Int J Mol Sci. 2020;21(20).
8. Machado-Pereira M, Santos T, Ferreira L, Bernardino L, Ferreira R. Challenging the great vascular wall: Can we envision a simple yet comprehensive therapy for stroke? J Tissue Eng Regen Med. 2018 Jan;12(1):e350–4.
9. Correa-Paz C, da Silva-Candal A, Polo E, Parcq J, Vivien D, Maysinger D, et al. New Approaches in Nanomedicine for Ischemic Stroke. Pharmaceutics. 2021;13(5).
10. Montaño A, Hanley DF, Hemphill JC 3rd. Hemorrhagic stroke. Handb Clin Neurol. 2021;176:229–48.
11. Liu K, Khan H, Geng X, Zhang J, Ding Y. Pharmacological hypothermia: a potential for future stroke therapy? Neurol Res. 2016;38(6):478–90.
12. Maida CD, Norrito RL, Daidone M, Tuttolomondo A, Pinto A. Neuroinflammatory Mechanisms in Ischemic Stroke: Focus on Cardioembolic Stroke, Background, and Therapeutic Approaches. Int J Mol Sci. 2020 Sep;21(18).
13. Datta A, Sarmah D, Mounica L, Kaur H, Kesharwani R, Verma G, et al. Cell Death Pathways in Ischemic Stroke and Targeted Pharmacotherapy. Transl Stroke Res. 2020;11(6):1185–202.
14. Paul S, Candelario-Jalil E. Emerging neuroprotective strategies for the treatment

of ischemic stroke: An overview of clinical and preclinical studies. Exp Neurol. 2021;335:113518.
15. Sirtori CR. The pharmacology of statins. Pharmacol Res. 2014 Oct;88:3–11.
16. Robinson JG. Simvastatin: present and future perspectives. Expert Opin Pharmacother. 2007 Sep;8(13):2127–59.
17. Stancu C, Sima A. Statins: mechanism of action and effects. J Cell Mol Med. 2001;5(4):378–87.
18. Pedersen TR, Tobert JA. Simvastatin: a review. Expert Opin Pharmacother. 2004;5(12):2583–96.
19. Pedersen TR. Pleiotropic effects of statins: evidence against benefits beyond LDL-cholesterol lowering. Am J Cardiovasc drugs drugs, devices, other Interv. 2010;10 Suppl 1:10–7.
20. MRC/BHF Heart Protection Study of cholesterol lowering with simvastatin in 20,536 high-risk individuals: a randomised placebo-controlled trial. Lancet (London, England). 2002 Jul;360(9326):7–22.
21. Cimino M, Balduini W, Carloni S, Gelosa P, Guerrini U, Tremoli E, et al. Neuroprotective Effect of Simvastatin in Stroke: A Comparison Between Adult and Neonatal Rat Models of Cerebral Ischemia. Neurotoxicology. 2005;26(5):929–33.
22. Group SSSS. Randomised trial of cholesterol lowering in 4444 patients with coronary heart disease: the Scandinavian Simvastatin Survival Study (4S). Lancet. 1994;344:1383–9.
23. Liao JK. Clinical implications for statin pleiotropy. Curr Opin Lipidol. 2005 Dec;16(6):624–9.
24. Jeong A, Suazo KF, Wood WG, Distefano MD, Li L. Isoprenoids and protein prenylation: implications in the pathogenesis and therapeutic intervention of Alzheimer's disease. Crit Rev Biochem Mol Biol. 2018;53(3):279–310.
25. Bar-Sagi D, Hall A. Ras and Rho GTPases: A Family Reunion. Cell. 2000;103(2):227–38.
26. Zhao J, Zhang X, Dong L, Wen Y, Cui L. The many roles of statins in ischemic stroke. Curr Neuropharmacol. 2014 Dec;12(6):564–74.
27. Endres M, Laufs U, Liao JK, Moskowitz MA. Targeting eNOS for stroke protection. Trends Neurosci. 2004 May;27(5):283–9.
28. Endres M, Laufs U, Huang Z, Nakamura T, Huang P, Moskowitz MA, et al. Stroke protection by 3-hydroxy-3-methylglutaryl (HMG)-CoA reductase inhibitors mediated by endothelial nitric oxide synthase. Proc Natl Acad Sci U S A. 1998 Jul;95(15):8880–5.

29. Sironi L, Cimino M, Guerrini U, Calvio AM, Lodetti B, Asdente M, et al. Treatment With Statins After Induction of Focal Ischemia in Rats Reduces the Extent of Brain Damage. Arterioscler Thromb Vasc Biol. 2003;23(2):322–7.
30. Oesterle A, Liao JK. The Pleiotropic Effects of Statins - From Coronary Artery Disease and Stroke to Atrial Fibrillation and Ventricular Tachyarrhythmia. Curr Vasc Pharmacol. 2019;17(3):222–32.
31. Hess DC, Fagan SC. Pharmacology and clinical experience with simvastatin. Expert Opin Pharmacother. 2001 Jan;2(1):153–63.
32. Bove M, Fogacci F, Cicero AFG. Pharmacokinetic drug evaluation of ezetimibe + simvastatin for the treatment of hypercholesterolemia. Expert Opin Drug Metab \& Toxicol. 2017;13(10):1099–104.
33. Climent E, Benaiges D, Pedro-Botet J. Hydrophilic or Lipophilic Statins? Front Cardiovasc Med. 2021;8.
34. Gänger S, Schindowski K. Tailoring Formulations for Intranasal Nose-to-Brain Delivery: A Review on Architecture, Physico-Chemical Characteristics and Mucociliary Clearance of the Nasal Olfactory Mucosa. Pharmaceutics. 2018;10(3).
35. Uchegbu I, Wang Z, Xiong G, Tsang A, Schatzlein A. Nose to brain delivery. J Pharmacol Exp Ther. 2019;370:jpet.119.258152.
36. Schachter M. Chemical, pharmacokinetic and pharmacodynamic properties of statins: an update. Fundam Clin Pharmacol. 2005 Feb;19(1):117–25.
37. Murtaza G. Solubility enhancement of simvastatin: a review. Acta Pol Pharm. 2012;69(4):581–90.
38. European Pharmacopoeia. 10th ed. Strasbourg: Council of Europe; 2020.
39. McClements DJ. Enhanced delivery of lipophilic bioactives using emulsions: a review of major factors affecting vitamin{,} nutraceutical{,} and lipid bioaccessibility. Food Funct. 2018;9(1):22–41.
40. Tamilvanan S. Oil-in-water lipid emulsions: implications for parenteral and ocular delivering systems. Prog Lipid Res. 2004;43(6):489–533.
41. Karwal R, Garg T, Rath G, Markandeywar TS. Current Trends in Self-Emulsifying Drug Delivery Systems (SEDDSs) to Enhance the Bioavailability of Poorly Water-Soluble Drugs. Crit Rev Ther Drug Carrier Syst. 2016;33(1):1–39.
42. Álvarez-Lueje A, Valenzuela C, Squella JA, Núñez-Vergara LJ. Stability Study of Simvastatin under Hydrolytic Conditions Assessed by Liquid Chromatography. J AOAC Int. 2019;88(6):1631–6.
43. Luo Y, Xu L, Tao X, Xu M, Feng J, Tang X. Preparation, characterization, stability and in vitro-in vivo evaluation of pellet-layered Simvastatin

nanosuspensions. Drug Dev Ind Pharm. 2013 Jul;39(7):936–46.
44. Malenović A, Jančić-Stojanović B, Ivanović D, Medenica M. Forced Degradation Studies of Simvastatin using Microemulsion Liquid Chromatography. J Liq Chromatogr \& Relat Technol. 2010;33(4):536–47.
45. Mitra R, Pezron I, Chu WA, Mitra AK. Lipid emulsions as vehicles for enhanced nasal delivery of insulin. Int J Pharm. 2000;205(1):127–34.
46. Danaei M, Dehghankhold M, Ataei S, Hasanzadeh Davarani F, Javanmard R, Dokhani A, et al. Impact of Particle Size and Polydispersity Index on the Clinical Applications of Lipidic Nanocarrier Systems. Pharmaceutics. 2018;10(2).
47. Lee D, Minko T. Nanotherapeutics for Nose-to-Brain Drug Delivery: An Approach to Bypass the Blood Brain Barrier. Pharmaceutics. 2021;13(12).
48. Brown RC, Lockwood AH, Sonawane BR. Neurodegenerative Diseases: An Overview of Environmental Risk Factors. Environ Health Perspect. 2005;113(9):1250–6.
49. Crowe TP, Greenlee MHW, Kanthasamy AG, Hsu WH. Mechanism of intranasal drug delivery directly to the brain. Life Sci. 2018;195:44–52.
50. Froelich A, Osmałek T, Jadach B, Puri V, Michniak-Kohn B. Microemulsion-Based Media in Nose-to-Brain Drug Delivery. Pharmaceutics. 2021;13(2).
51. Bonferoni MC, Rossi S, Sandri G, Ferrari F, Gavini E, Rassu G, et al. Nanoemulsions for “Nose-to-Brain” Drug Delivery. Pharmaceutics. 2019;11(2).
52. Pardridge WM. Blood–brain barrier delivery. Drug Discov Today. 2007;12(1):54–61.
53. Kabanov A V, Batrakova E V. New technologies for drug delivery across the blood brain barrier. Curr Pharm Des. 2004;10(12):1355–63.
54. Shepardson NE, Shankar GM, Selkoe DJ. Cholesterol Level and Statin Use in Alzheimer Disease: II. Review of Human Trials and Recommendations. Arch Neurol. 2011;68(11):1385–92.
55. Battaglia L, Panciani PP, Muntoni E, Capucchio MT, Biasibetti E, De Bonis P, et al. Lipid nanoparticles for intranasal administration: application to nose-to-brain delivery. Expert Opin Drug Deliv. 2018 Apr;15(4):369–78.
56. Lochhead JJ, Thorne RG. Intranasal delivery of biologics to the central nervous system. Adv Drug Deliv Rev. 2012;64(7):614–28.
57. Ghadiri M, Young PM, Traini D. Strategies to Enhance Drug Absorption via Nasal and Pulmonary Routes. Pharmaceutics. 2019;11(3).
58. Jiao J, Zhang L. Influence of Intranasal Drugs on Human Nasal Mucociliary Clearance and Ciliary Beat Frequency. Allergy Asthma Immunol Res. 2019 May;11(3):306–19.

59. Rassu G, Ferraro L, Pavan B, Giunchedi P, Gavini E, Dalpiaz A. The Role of Combined Penetration Enhancers in Nasal Microspheres on In Vivo Drug Bioavailability. Pharmaceutics. 2018 Oct;10(4).
60. Sonvico F, Clementino A, Buttini F, Colombo G, Pescina S, Stanisçuaski Guterres S, et al. Surface-Modified Nanocarriers for Nose-to-Brain Delivery: From Bioadhesion to Targeting. Pharmaceutics. 2018 Mar;10(1).
61. Kale S, Deore S. Emulsion Micro Emulsion and Nano Emulsion: A Review. Syst Rev Pharm. 2016;8:39–47.
62. McClements DJ. Encapsulation, protection, and delivery of bioactive proteins and peptides using nanoparticle and microparticle systems: A review. Adv Colloid Interface Sci. 2018;253:1–22.
63. Nguyen TT, Nguyen TTD, Tran N-M-A, Van Vo G. Lipid-Based Nanocarriers via Nose-to-Brain Pathway for Central Nervous System Disorders. Neurochem Res. 2022;47(3):552–73.
64. Khan AY, Talegaonkar S, Iqbal Z, Ahmed FJ, Khar RK. Multiple emulsions: an overview. Curr Drug Deliv. 2006 Oct;3(4):429–43.
65. Chen H, Khemtong C, Yang X, Chang X, Gao J. Nanonization strategies for poorly water-soluble drugs. Drug Discov Today. 2011;16(7):354–60.
66. Mcclements DJ. Nanoemulsions versus microemulsions: terminology, differences, and similarities. Soft Matter. 2012;8:1719–29.
67. Anton N, Vandamme TF. Nano-emulsions and micro-emulsions: clarifications of the critical differences. Pharm Res. 2011 May;28(5):978–85.
68. Bahadur S, Pardhi DM, Rautio J, Rosenholm JM, Pathak K. Intranasal Nanoemulsions for Direct Nose-to-Brain Delivery of Actives for CNS Disorders. Pharmaceutics. 2020;12(12).
69. Garavand F, Jalai-Jivan M, Assadpour E, Jafari SM. Encapsulation of phenolic compounds within nano/microemulsion systems: A review. Food Chem. 2021;364:130376.
70. Clementino A, Batger M, Garrastazu G, Pozzoli M, Del Favero E, Rondelli V, et al. The nasal delivery of nanoencapsulated statins - an approach for brain delivery. Int J Nanomedicine. 2016;11:6575–90.
71. Iyer V, Cayatte C, Guzman B, Schneider-Ohrum K, Matuszak R, Snell A, et al. Impact of formulation and particle size on stability and immunogenicity of oil-in-water emulsion adjuvants. Hum Vaccines \& Immunother. 2015;11(7):1853–64.
72. Costa CP, Moreira JN, Sousa Lobo JM, Silva AC. Intranasal delivery of nanostructured lipid carriers, solid lipid nanoparticles and nanoemulsions: A

current overview of in vivo studies. Acta Pharm Sin B. 2021;11(4):925–40.
73. Wu L, Shan W, Zhang Z, Huang Y. Engineering nanomaterials to overcome the mucosal barrier by modulating surface properties. Adv Drug Deliv Rev. 2018;124:150–63.
74. Nakamura F, Ohta R, Machida Y, Nagai T. In vitro and in vivo nasal mucoadhesion of some water-soluble polymers. Int J Pharm. 1996;134(1):173–81.
75. Deruyver L, Rigaut C, Lambert P, Haut B, Goole J. The importance of pre-formulation studies and of 3D-printed nasal casts in the success of a pharmaceutical product intended for nose-to-brain delivery. Adv Drug Deliv Rev. 2021;175:113826.
76. Nováková L, Šatínský D, Solich P. HPLC methods for the determination of simvastatin and atorvastatin. TrAC Trends Anal Chem. 2008;27(4):352–67.
77. Scherließ R. Nasal formulations for drug administration and characterization of nasal preparations in drug delivery. Ther Deliv. 2020 Mar;11(3):183–91.
78. Marx D, Williams G, Birkhoff M. Intranasal Drug Administration — An Attractive Delivery Route for Some Drugs. In: Vallisuta O, Olimat S, editors. Drug Discovery and Development. Rijeka: IntechOpen; 2015.
79. Pujara CP, Shao Z, Duncan MR, Mitra AK. Effects of formulation variables on nasal epithelial cell integrity: Biochemical evaluations. Int J Pharm. 1995;114(2):197–203.
80. ASTM F 756-00. Standard practice for assessment of hemolytic properties of materials. Philadelphia. Am Soc Test Mater. 2000;(January):5.
81. Sohn H-M, Hwang J-Y, Ryu J-H, Kim J, Park S, Park J-W, et al. Simvastatin protects ischemic spinal cord injury from cell death and cytotoxicity through decreasing oxidative stress: in vitro primary cultured rat spinal cord model under oxygen and glucose deprivation-reoxygenation conditions. J Orthop Surg Res. 2017 Feb;12(1):36.
82. Lim JH, Lee J-C, Lee YH, Choi IY, Oh Y-K, Kim H-S, et al. Simvastatin prevents oxygen and glucose deprivation/reoxygenation-induced death of cortical neurons by reducing the production and toxicity of 4-hydroxy-2E-nonenal. J Neurochem. 2006;97(1):140–50.
83. Reuter B, Rodemer C, Grudzenski S, Meairs S, Bugert P, Hennerici MG, et al. Effect of simvastatin on MMPs and TIMPs in human brain endothelial cells and experimental stroke. Transl Stroke Res. 2015 Apr;6(2):156–9.
84. Meirinho S, Rodrigues M, Ferreira CL, Oliveira RC, Fortuna A, Santos AO, et al. Intranasal delivery of lipid-based nanosystems as a promising approach for

brain targeting of the new-generation antiepileptic drug perampanel. Int J Pharm. 2022 Jun;622:121853.
85. Fernandes MC. Desenvolvimento de uma emulsão O/A de sinvastatina para administração intranasal. Universidade da Beira Interior; 2019.
86. Kumar A, Li S, Cheng C-M, Lee D. Recent Developments in Phase Inversion Emulsification. Ind \& Eng Chem Res. 2015;54(34):8375–96.
87. Corr. Guideline on bioanalytical method validation. 1922;44(July 2011):1–23.
88. Booth BP, Simon WC. Analytical method validation. New Drug Dev Regul Paradig Clin Pharmacol Biopharm. 2016;(May):138–59.
89. England RJA, Homer JJ, Knight LC, Ell SR. Nasal pH measurement: a reliable and repeatable parameter. Clin Otolaryngol \& Allied Sci. 1999;24(1):67–8.
90. Higuchi T. Mechanism of Sustained-Action Medication. Theoretical Analysis of Rate of Release of Solid Drugs Dispersed in Solid Matrices. J Pharm Sci. 1963 Dec;52:1145–9.
91. Wang J, Zhang B. Bovine Serum Albumin as a Versatile Platform for Cancer Imaging and Therapy. Curr Med Chem. 2018;25(25):2938–53.
92. Khoder M, Abdelkader H, ElShaer A, Karam A, Najlah M, Alany RG. Efficient approach to enhance drug solubility by particle engineering of bovine serum albumin. Int J Pharm. 2016;515(1):740–8.
93. Shi J-H, Wang Q, Pan D-Q, Liu T-T, Jiang M. Characterization of interactions of simvastatin, pravastatin, fluvastatin, and pitavastatin with bovine serum albumin: multiple spectroscopic and molecular docking. J Biomol Struct Dyn. 2017;35(7):1529–46.
94. Bannow J, Yorulmaz Y, Löbmann K, Müllertz A, Rades T. Improving the drug load and in vitro performance of supersaturated self-nanoemulsifying drug delivery systems (super-SNEDDS) using polymeric precipitation inhibitors. Int J Pharm. 2020;575:118960.
95. Thomas N, Holm R, Garmer M, Karlsson JJ, Müllertz A, Rades T. Supersaturated Self-Nanoemulsifying Drug Delivery Systems (Super-SNEDDS) Enhance the Bioavailability of the Poorly Water-Soluble Drug Simvastatin in Dogs. AAPS J. 2013;15(1):219–27.
96. Hassanin I, Elzoghby A. Albumin-based nanoparticles: a promising strategy to overcome cancer drug resistance. Cancer drug Resist (Alhambra, Calif). 2020;3(4):930–46.
97. Kianfar E. Protein nanoparticles in drug delivery: animal protein, plant proteins and protein cages, albumin nanoparticles. J Nanobiotechnology. 2021 May;19(1):159.

98. Niu Z, Thielen I, Loveday SM, Singh H. Emulsions Stabilised by Polyethylene Glycol (PEG) 40 Stearate and Lactoferrin for Protection of Lactoferrin during In Vitro Digestion. Food Biophys. 2021;16(1):40–7.
99. Zaichik S, Steinbring C, Jelkmann M, Bernkop-Schnürch A. Zeta potential changing nanoemulsions: Impact of PEG-corona on phosphate cleavage. Int J Pharm. 2020;581:119299.
100. Leal J, Smyth HDC, Ghosh D. Physicochemical properties of mucus and their impact on transmucosal drug delivery. Int J Pharm. 2017 Oct;532(1):555–72.
101. Daull P, Lallemand F, Garrigue J-S. Benefits of cetalkonium chloride cationic oil-in-water nanoemulsions for topical ophthalmic drug delivery. J Pharm Pharmacol. 2014 Apr;66(4):531–41.
102. Prego C, García M, Torres D, Alonso MJ. Transmucosal macromolecular drug delivery. J Control Release. 2005;101(1):151–62.
103. Dyer AM, Hinchcliffe M, Watts P, Castile J, Jabbal-Gill I, Nankervis R, et al. Nasal delivery of insulin using novel chitosan based formulations: a comparative study in two animal models between simple chitosan formulations and chitosan nanoparticles. Pharm Res. 2002 Jul;19(7):998–1008.
104. Casettari L, Illum L. Chitosan in nasal delivery systems for therapeutic drugs. J Control Release. 2014;190:189–200.
105. Pais Bulha R. Desenvolvimento e otimização de nanoemulsões catiónicas. Universidade da Beira Interior; 2021.
106. Torres-Luna C, Hu N, Tammareddy T, Domszy R, Yang J, Wang NS, et al. Extended delivery of non-steroidal anti-inflammatory drugs through contact lenses loaded with Vitamin E and cationic surfactants. Contact Lens Anterior Eye. 2019;42.
107. Bengani LC, Chauhan A. Extended delivery of an anionic drug by contact lens loaded with a cationic surfactant. Biomaterials. 2013;34(11):2814–21.
108. Niki E, Abe K. CHAPTER 1. Vitamin E: Structure, Properties and Functions: Chemistry and Nutritional Benefits. In: Food Chemistry, Function and Analysis. 2019. p. 1–11.
109. Barhoum A, García-Betancourt ML, Rahier H, Van Assche G. Chapter 9 - Physicochemical characterization of nanomaterials: polymorph, composition, wettability, and thermal stability. In: Barhoum A, Makhlouf ASH, editors. Emerging Applications of Nanoparticles and Architecture Nanostructures. Elsevier; 2018. p. 255–78. (Micro and Nano Technologies).
110. Laffleur F, Hintzen F, Shahnaz G, Rahmat D, Leithner K, Bernkop-Schnürch A. Development and in vitro evaluation of slippery nanoparticles for enhanced

diffusion through native mucus. Nanomedicine. 2014;9(3):387–96.
111. Pereira de Sousa I, Steiner C, Schmutzler M, Wilcox MD, Veldhuis GJ, Pearson JP, et al. Mucus permeating carriers: formulation and characterization of highly densely charged nanoparticles. Eur J Pharm Biopharm. 2015;97:273–9.
112. Al Mamun Bhuyan A, Nüßle S, Cao H, Zhang S, Lang F. Simvastatin, a Novel Stimulator of Eryptosis, the Suicidal Erythrocyte Death. Cell Physiol Biochem Int J Exp Cell Physiol Biochem Pharmacol. 2017;43(2):492–506.
113. Wu K-W, Sweeney C, Dudhipala N, Lakhani P, Chaurasiya ND, Tekwani BL, et al. Primaquine Loaded Solid Lipid Nanoparticles (SLN), Nanostructured Lipid Carriers (NLC), and Nanoemulsion (NE): Effect of Lipid Matrix and Surfactant on Drug Entrapment, in vitro Release, and ex vivo Hemolysis. AAPS PharmSciTech. 2021;22(7):240.
114. Dobrovolskaia MA, Aggarwal P, Hall JB, McNeil SE. Preclinical Studies To Understand Nanoparticle Interaction with the Immune System and Its Potential Effects on Nanoparticle Biodistribution. Mol Pharm. 2008;5(4):487–95.
115. Guo S, Shi Y, Liang Y, Liu L, Sun K, Li Y. Relationship and improvement strategies between drug nanocarrier characteristics and hemocompatibility: What can we learn from the literature. Asian J Pharm Sci. 2021;16(5):551–76.
116. Chatzitaki A-T, Jesus S, Karavasili C, Andreadis D, Fatouros DG, Borges O. Chitosan-coated PLGA nanoparticles for the nasal delivery of ropinirole hydrochloride: In vitro and ex vivo evaluation of efficacy and safety. Int J Pharm. 2020;589:119776.
117. Manaargadoo-Catin M, Ali-Cherif A, Pougnas J-L, Perrin C. Hemolysis by surfactants — A review. Adv Colloid Interface Sci. 2016;228:1–16.
118. Espay AJ. Chapter 23 - Neurologic complications of electrolyte disturbances and acid–base balance. In: Biller J, Ferro JM, editors. Neurologic Aspects of Systemic Disease Part I. Elsevier; 2014. p. 365–82. (Handbook of Clinical Neurology; vol. 119).
119. Brinkman JE, Dorius B, Sharma S. Physiology, Body Fluids. In Treasure Island (FL); 2022.
120. Ramvikas M, Arumugam M, Chakrabarti SR, Jaganathan KS. Chapter Fifteen - Nasal Vaccine Delivery. In: Skwarczynski M, Toth I, editors. Micro and Nanotechnology in Vaccine Development. William Andrew Publishing; 2017. p. 279–301. (Micro and Nano Technologies).
121. Gizurarson S. Anatomical and histological factors affecting intranasal drug and vaccine delivery. Curr Drug Deliv. 2012 Nov;9(6):566–82.
122. D'Souza S. A Review of *In Vitro* Drug Release Test Methods for Nano-Sized

Dosage Forms. Keck CM, editor. Adv Pharm. 2014;2014:304757.
123. D'Souza SS, DeLuca PP. Development of a dialysis in vitro release method for biodegradable microspheres. AAPS PharmSciTech. 2005 Oct;6(2):E323-8.
124. Kinget R, Bontinck A-M, Herbots H. Problems of dialysis techniques in the study of macromolecule binding of drugs. Int J Pharm. 1979;3(2):65–72.
125. Fortuna A, Alves G, Falcão A, Soares-da-Silva P. Evaluation of the permeability and P-glycoprotein efflux of carbamazepine and several derivatives across mouse small intestine by the Ussing chamber technique. Epilepsia. 2012 Mar;53(3):529–38.
126. Yulianita R, Sopyan I, Muchtaridi M. Forced Degradation Study of Statins: A Review. Int J Appl Pharm. 2018;10(6):38–42.
127. EMA. Note For Guidance On Evaluation Of Stability Data (CPMP/ICH/420/02). Ema. 2003;(August 2002):1–17.
128. Pai H V, Upadhya SC, Chinta SJ, Hegde SN, Ravindranath V. Differential metabolism of alprazolam by liver and brain cytochrome (P4503A) to pharmacologically active metabolite. Pharmacogenomics J. 2002;2(4):243–58.
129. Johnson-Anuna LN, Eckert GP, Keller JH, Igbavboa U, Franke C, Fechner T, et al. Chronic administration of statins alters multiple gene expression patterns in mouse cerebral cortex. J Pharmacol Exp Ther. 2005 Feb;312(2):786–93.
130. Wood WG, Eckert GP, Igbavboa U, Müller WE. Statins and neuroprotection: a prescription to move the field forward. Ann N Y Acad Sci. 2010 Jun;1199:69–76.
131. Thelen KM, Rentsch KM, Gutteck U, Heverin M, Olin M, Andersson U, et al. Brain cholesterol synthesis in mice is affected by high dose of simvastatin but not of pravastatin. J Pharmacol Exp Ther. 2006 Mar;316(3):1146–52.
132. Campos-Martorell M, Cano-Sarabia M, Simats A, Hernández-Guillamon M, Rosell A, Maspoch D, et al. Charge effect of a liposomal delivery system encapsulating simvastatin to treat experimental ischemic stroke in rats. Int J Nanomedicine. 2016;11:3035–48.
133. Yin W, Al-Wabli RI, Attwa MW, Rahman AFMM, Kadi AA. Detection and characterization of simvastatin and its metabolites in rat tissues and biological fluids using MALDI high resolution mass spectrometry approach. Sci Rep. 2022;12(1):4757.
134. Fracassi A, Marangoni M, Rosso P, Pallottini V, Fioramonti M, Siteni S, et al. Statins and the Brain: More than Lipid Lowering Agents? Curr Neuropharmacol. 2019;17(1):59–83.
135. Chen C, Lin J, Smolarek T, Tremaine L. P-glycoprotein has differential effects on the disposition of statin acid and lactone forms in mdr1a/b knockout and wild-

type mice. Drug Metab Dispos. 2007 Oct;35(10):1725–9.
136. Pirzad Jahromi G, P Shabanzadeh A, Mokhtari Hashtjini M, Sadr SS, Rasouli Vani J, Raouf Sarshoori J, et al. Bone marrow-derived mesenchymal stem cell and simvastatin treatment leads to improved functional recovery and modified c-Fos expression levels in the brain following ischemic stroke. Iran J Basic Med Sci. 2018 Oct;21(10):1004–12.
137. Shehadah A, Chen J, Cui X, Roberts C, Lu M, Chopp M. Combination treatment of experimental stroke with Niaspan and Simvastatin, reduces axonal damage and improves functional outcome. J Neurol Sci. 2010;294(1):107–11.
138. Pirzad Jahromi G, Seidi S, Sadr SS, Shabanzadeh AP, Keshavarz M, Kaka GR, et al. Therapeutic effects of a combinatorial treatment of simvastatin and bone marrow stromal cells on experimental embolic stroke. Basic Clin Pharmacol Toxicol. 2012 Jun;110(6):487–93.
139. Zhu M, Lu C, Xia C, Qiao Z, Zhu D. Simvastatin pretreatment protects cerebrum from neuronal injury by decreasing the expressions of phosphor-CaMK II and AQP4 in ischemic stroke rats. J Mol Neurosci. 2014 Dec;54(4):591–601.
140. Zhang J-Y, Bai Q-K, Zhang Y-D. Pretreatment with simvastatin upregulates expression of BK-2R and CD11b in the ischemic penumbra of rats. J Biomed Res. 2018 Sep;32(5):354–60.
141. Balduini W, De Angelis V, Mazzoni E, Cimino M. Simvastatin protects against long-lasting behavioral and morphological consequences of neonatal hypoxic/ischemic brain injury. Stroke. 2001 Sep;32(9):2185–91.
142. Li A, Lv S, Yu Z, Zhang Y, Ma H, Zhao H, et al. Simvastatin attenuates hypomyelination induced by hypoxia-ischemia in neonatal rats. Neurol Res. 2010 Nov;32(9):945–52.
143. Chen Z, Xiang Y, Bao B, Wu X, Xia Z, You J, et al. Simvastatin improves cerebrovascular injury caused by ischemia‑reperfusion through NF‑κB‑mediated apoptosis via MyD88/TRIF signaling. Mol Med Rep. 2018 Sep;18(3):3177–84.
144. Guluma KZ, Lapchak PA. Comparison of the post-embolization effects of tissue-plasminogen activator and simvastatin on neurological outcome in a clinically relevant rat model of acute ischemic stroke. Brain Res. 2010 Oct;1354:206–16.
145. Laufs U, Gertz K, Dirnagl U, Böhm M, Nickenig G, Endres M. Rosuvastatin, a new HMG-CoA reductase inhibitor, upregulates endothelial nitric oxide synthase and protects from ischemic stroke in mice. Brain Res. 2002;942(1):23–30.
146. Laufs U, Endres M, Stagliano N, Amin-Hanjani S, Chui DS, Yang SX, et al. Neuroprotection mediated by changes in the endothelial actin cytoskeleton. J

Clin Invest. 2000 Jul;106(1):15–24.
147. Lapchak PA, Han MK. Simvastatin improves clinical scores in a rabbit multiple infarct ischemic stroke model: synergism with a ROCK inhibitor but not the thrombolytic tissue plasminogen activator. Brain Res. 2010 Jul;1344:217–25.
148. Dobrovolskaia MA, McNeil SE. Understanding the correlation between in vitro and in vivo immunotoxicity tests for nanomedicines. J Control release Off J Control Release Soc. 2013 Dec;172(2):456–66.
149. Cyprotex. In vitro Hemolysis Background Information [Internet]. 2015 [cited 2022 Jun 27]. p. 20–1. Available from: http://www.cyprotex.com/toxicology/mechanistic-toxicity/hemolysis
150. Silva TD, Oliveira MA, de Oliveira RB, Vianna-Soares CD. Development and Validation of a Simple and Fast HPLC Method for Determination of Lovastatin, Pravastatin and Simvastatin. J Chromatogr Sci. 2012;50(9):831–8.

Supplementary Data

S.1. Estimation of theoretical plasma concentration of simvastatin and sample dilution for hemolysis test

An equation for estimating theoretical plasma concentration based on the most common dose used in animals was used to determine the concentrations in the test sample. Due to the lack of intranasal delivery studies using simvastatin in ischemic stroke, data regarding other routes of administration reported in the literature were used to determine the appropriate dose (Table S1). A dose of 20 mg/Kg was selected since it was the most commonly used throughout different administration strategies (oral, subcutaneous, and intraperitoneal) and in different animal species (mice, rats, and rabbits).

Table S1. Different *in vivo* approaches of simvastatin in ischemic stroke in the literature regarding animal model, dose, administration route, drug form, and ischemic stroke model used.

Animal Model	Dose (mg/Kg)	Administration	Form	Model	Reference
Wistar Rats	40	Intraperitoneal	Prodrug	MCAo	(136)
	1	Oral	Prodrug	MCAo	(137)
	40	Intraperitoneal	Activated	MCAo	(138)
Sprague Dawley Rats	20	Oral	Prodrug	MCAo	(139)
	2 10 50	Oral	Prodrug	MCAo	(140)
	20	Subcutaneous	Activated	Unilateral Carotid Artery Ligation + Hypoxia	(141)
	20	Subcutaneous	Activated	Unilateral Carotid Artery Ligation + Hypoxia	(142)
	20	Subcutaneous	Activated	MCAo	(29)
	10	Intravenous	Activated	Unilateral Carotid Artery Ligation	(143)
Fisher 344 Rats	20	Intraperitoneal	Prodrug	Embolic	(144)
129/SV Mice	20	Subcutaneous	Activated	MCAo	(145)
Mice	20	Subcutaneous	Activated	MCAo	(146)
Rabbits	20	Subcutaneous	Prodrug	Embolic	(147)

Assuming the dose of 20 mg/Kg, according to the equation S1 proposed by Dobrovolskaia *et. al.* (148), the human equivalent would be:

$$human\ dose = \frac{animal\ dose}{12.3} = \frac{20}{12.3} = 1.63\ mg/Kg \text{ (eq. S1)}$$

Since blood volume is approximately 8% of the body weight and an average human weighs about 70 Kg, the approximately blood volume is 5.6 L. Assuming a bioavailability of 100% in the bloodstream, the maximum theoretical concentration in blood can be calculated according to equation S2:

$$maximum\ theoretical\ concentration = \frac{human\ dose * human\ mass}{blood\ volume} = 6\ L \approx 0.02\ mg/mL \text{ (eq. S2)}$$

To prepare the stock solutions of the test samples used in the assay, accordingly to the initial strength of simvastatin, micro and nanoemulsions were first diluted to stock solutions at 0.9 mg/mL of simvastatin or to a solution with an equivalent concentration of excipients in the case of vehicles controls:

1. Nanoemulsions vehicle (without simvastatin): 150 mg of formulation diluted in 10 mL of PBS.

2. Nanoemulsions with 5.66% simvastatin: 159 mg of formulation diluted in 10 mL of PBS.

3. Microemulsion vehicle (without simvastatin): 90 mg of formulation diluted in 10 mL of PBS.

4. Microemulsion with 9.09% simvastatin: 99 mg of formulation diluted in 10 mL of PBS.

To obtain the different concentrations used in the assay, the stocks were then diluted using PBS to a final volume of 2 mL and prepared in concentrations 2 times higher than the final concentration desired. For nanoemulsions, the concentrations used were 0.04 mg/mL (theoretical concentration after the 2-fold dilution when incubating with the blood), 0.08 mg/mL and 0.16 mg/mL. For microemulsions, the concentrations used were 0.04 mg/mL 0.16 mg/mL, and 0.9 mg/mL.

S.2. Incomplete Hemolysis

There was an apparent incomplete hemolysis of the positive control group in the initial protocol of the hemolysis assay. The apparent incomplete hemolysis (lower than expected absorbance) in the positive controls was possibly caused by an interference of erythrocytes stroma released after hemolysis. The stroma content acts as an inhibitor of Drabkin's solution, explaining why in groups with expected high hemolysis, such as the

positive control, the hemolysis values were much lower (≈30%) than the predicted values. Therefore, the procedure needed some optimization. Another hemolysis assay protocol gave important information about the expected percentage of lysis using different reagents at different concentrations. Instead of the 3 hours described in the initial protocol, a far shorter incubation period of 45 minutes was used, and the predicted hemolysis for Triton X-100 at a stock concentration of 1% was 70%, almost two times the amount obtained (149).

Different approaches were used to solve this problem, and despite the lack of success of the majority of the attempts, some conclusions were very important for the development and optimization of a new protocol.

One of the first hypotheses was that the concentration or the incubation time was not appropriate in order to reach almost full hemolysis of the blood. The incubation time was higher than the majority of other hemolysis assays and this could have been creating destabilization in the hemoglobin. To assess this, three different solutions were used as positive controls: Triton X-100 1%, Triton X-100 0.1%, and ultrapure water, which can be used as a positive control due to its hypotonicity. Hemolysis was measured at shorter incubation times (30, 45, 60, 75, and 90 minutes) to see if the incubation time had any influence. The results are plotted in Figure S1.

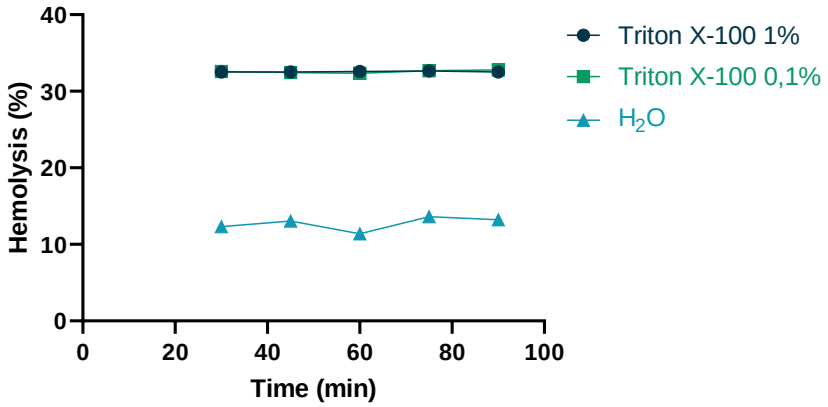

Figure S1. Hemolysis percentage over time using Triton X-100 at different concentrations (1% and 0.1%) and ultrapure water (H2O).

The hemolysis threshold of 30% was not surpassed by any of the solutions tested at any incubation period. Despite not being successful, this test showed no difference between the two concentrations of Triton X-100 (1% and 0.1%). For that, it was questioned if the problem could be the reagent used. It was also shown that the hemolysis process occurs almost instantaneously and did not change with higher incubation periods.

Different alternatives to the Triton X-100 solution were tested, such as SDS at 1%. Once again, the threshold was not exceeded and SDS at 1% managed a hemolysis percentage of 29.89%, indicating the problem was not related to the reagent used either.

A different hypothesis was that centrifuging after incubation could be interfering with the measurement. That assumption was mainly made since in the standard curve preparation described by the protocol Drabkin's solution was added to blood at different concentrations, and measurements were carried out directly without the samples being centrifuged. To test this, Triton X-100 0.1%, SDS 1%, and ultrapure water were incubated for 30 minutes with blood, and hemolysis was measured before and after centrifuging. Regarding Triton X-100 and SDS, the premise was once again wrong since hemolysis percentages were almost the same before and after centrifuging (Figure S2). In opposition, in the ultrapure water group, hemolysis before and after centrifuging was a lot different. Visual inspection of the samples before and after centrifuging also gives quite good information. In fact, the samples with Triton X-100 and SDS demonstrated no difference between before and after centrifuging and no pellet formation. That means that there are no intact red blood cells and that they are all lysed in the supernatant. the same cannot be said for the samples with ultrapure water that, after centrifuging, present a pellet with the supernatant having a much lighter red color, which can mean that some red blood cells were lysed but others were not. This helped to understand that Triton X-100 and SDS had more hemolytic power than ultrapure water and that in fact hemolysis detection was being covered for groups with high hemolysis but not for groups with moderate to low hemolysis.

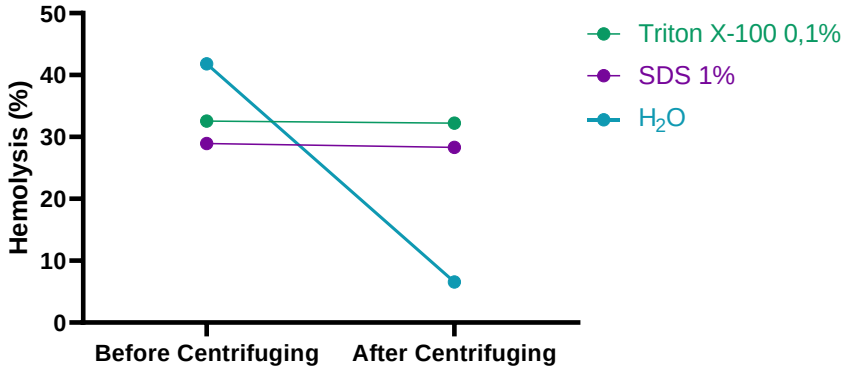

Figure S2. Hemolysis percentage using different hemolytic solutions before and after centrifuging. The hemolytic solutions used were Triton X-100 at 0.1%, SDS at 1%, and ultrapure water (H2O).

Despite meeting all the quality criteria and expiring date, Drabkin's solution was the next element questioned for reasons such as the possible loss of properties due to storage conditions. The test that followed tried to determine if the proportion between blood and

Drabkin's solution affected hemolysis quantification. The initial protocol and initial validation were made by preparing a series of diluted blood samples to a known concentration using PBS and adding 100 µl of the prepared diluted blood to 100 µl of Drabkin's solution. To test this proportion, diluted blood at 5 mg/mL was diluted to 2.5 mg/mL using PBS. Then, from this new diluted blood, different proportions of blood were combined with Drabkin's solution to a final volume of 200 µl.

A similar parallel test was done using Triton X-100 0.2% instead of PBS to perform the first dilution from 5 mg/mL to 2.5 mg/mL. This mixture (Blood + Triton) was then added in a different proportion to Drabkin's Solution to a final volume of 200 µl. Mean absorbances of the dilution are present in Table S2.

Table S2. Absorbance difference of different dilutions using Drabkin's Solution and blood or hemolyzed blood with Triton X-100.

	Proportion of sample to Drabkin's Solution				
Groups	1:1	1:3	1:9	1:19	1:39
Blood	1.247	0.319	0.146	0.084	0.065
Blood + Triton X-100	0.496	0.273	0.132	0.080	0.066
Difference	0.751	0.047	0.014	0.004	-0.001

Despite having the same final blood concentration, the absorbances of both groups only start to be the same after the 20-fold dilution, showing that, at the dilution used in the initial protocol, the positive control could only reach approximately one-third of the absorbance. This indicates a difference between the interaction between Drabkin's solution and previously hemolyzed blood and Drabkin's solution and non-hemolyzed blood. In fact, Drabkin's solution acts as a hemolytic agent itself, releasing the hemoglobin from red blood cells and, only after, as a quantification agent converting hemoglobin into methemoglobin to be detected at 540 nm. The results indicate that one of those features might be inhibited in the presence of high hemolyzed blood.

In order to evaluate if centrifuging could solve the problem, Drabkin's solution was mixed in different concentrations with diluted blood at 5 mg/mL. Then, measurements were taken after centrifuging, collecting 200 µl of supernatant, and directly placing it in a 96-well plate without adding Drabkin's solution:

1. 200 µl Blood + 200 µl PBS + 400 µl Drabkin's solution
2. 200 µl Blood + 600 µl Drabkin's solution

The first mixture had mean absorbance of 0.123 and formed a pellet after centrifuging unlike the second mixture which had an absorbance of 0.490, and no pellet. The proportion necessary to hemolyze all the blood was 1:3 and Drabkin's solution seemed, once again, to be the problem.

Lastly, two new groups of mixtures were made using blood at 2 concentrations (10 mg/mL and 7 mg/mL) and measurements were taken before and after centrifuging:

1. E1: 400 µl Blood + 400 µl Triton X-100 + 800 µl Drabkin's solution
2. E2: 400 µl Blood + 1200 µl Drabkin's solution

If both absorbances were the same before and after centrifuging, it meant that all the blood that was in the sample was already lysed. So, if the absorbances were equal between groups, the solution for measuring 100% hemolysis was simply replacing the PBS used to dilute the blood for Triton X-100.

Table S3. Mixture and centrifuging test.

Groups	Centrifuging	Blood Concentration		
		10 mg/mL	7 mg/mL	
E1	No	0.925	0.675	
	Yes	0.922	0.661	
		0.003	0.014	Difference
E2	No	0.927	0.659	
	Yes	0.896	0.64	
		0.031	0.019	Difference

E2 was not the same before and after centrifuging meaning the blood was not fully lysed and confirming that Drabkin's solution was not producing full hemolysis in high concentration blood samples. On the other hand, E1 had almost the same absorbances, meaning hemolysis percentages calibrated in the standard curve would match the percentages obtained after incubation and centrifuging the assay samples and the positive control. By replacing PBS for Triton X-100, samples would first be fully hemolysed and only then a correct correspondence between hemoglobin concentration and absorbance could be established.

S.3. Hemolysis Positive, Intermediate and Interference Controls

Positive and intermediate controls, performed in each of the experiments in parallel with the referred formulations, are plotted in Figure S3. It was confirmed that, despite a slight variability, both complete and intermediate hemolysis could be achieved in all the tests performed.

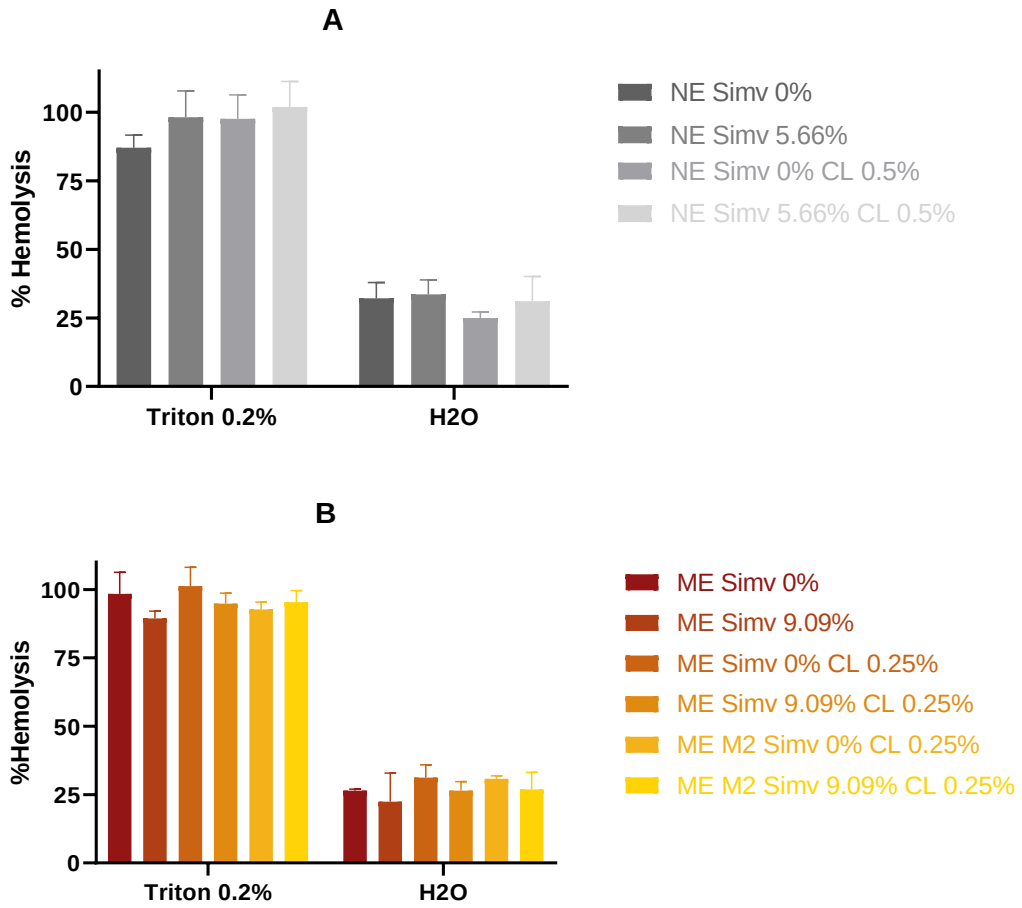

Figure S3. Nanoemulsion (A) and microemulsion (B) positive and intermediate controls for all the groups tested during the hemolysis assays.

Interference controls, evaluating if the formulations could be interfering with the hemolysis quantification, are plotted in Figure S4. It was confirmed that the formulations were not interfering with hemolysis quantification.

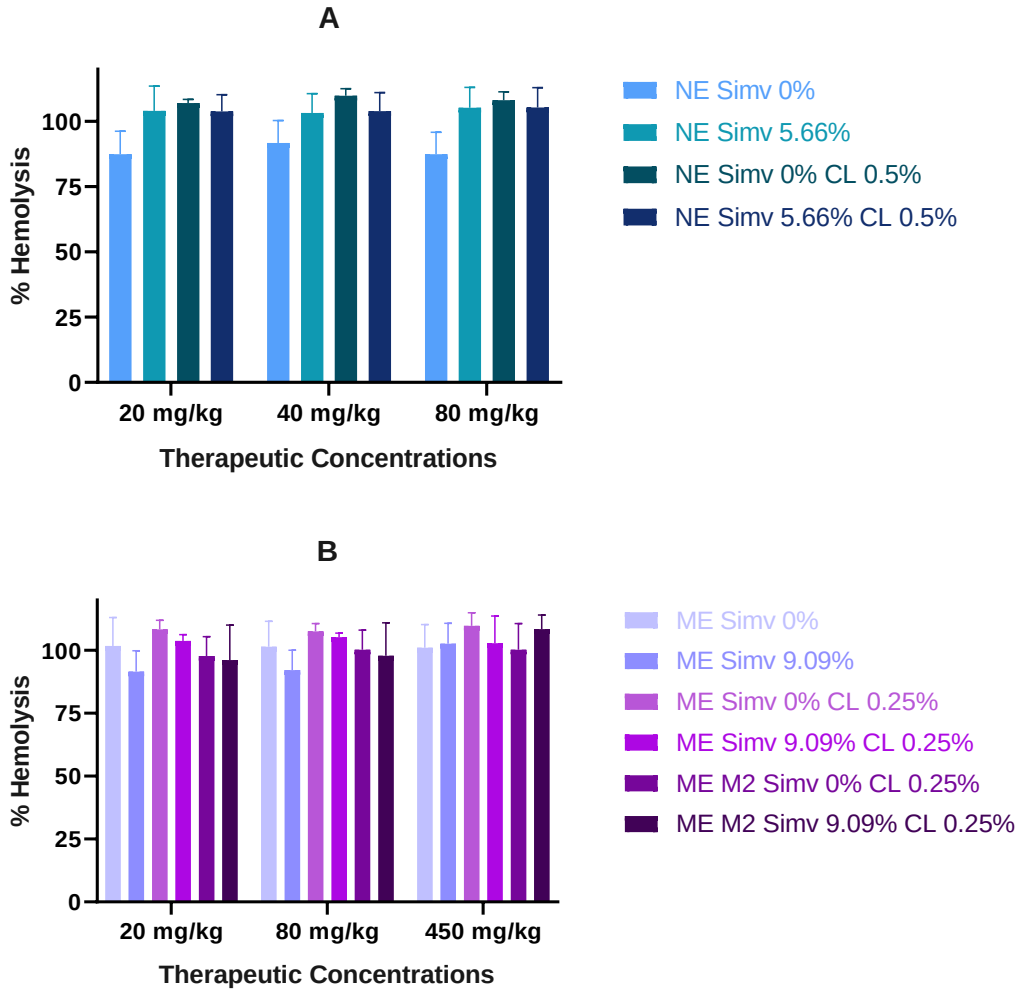

Figure S4. Nanoemulsion (A) and microemulsion (B) interference control for all the groups tested during the hemolysis assays.

S.4. Simvastatin Degradation

Another piece of evidence confirming drug degradation besides the reduction in simvastatin concentration was the detection of new peaks in the HPLC chromatogram throughout the chemical stability assay. Regarding the nature of the peak, it is difficult to compare our data with the already provided in the literature to determine the correspondence between simvastatin's degradation product and peak's RT. This is mainly due to the different experimental conditions used and the quantification method. In our method, the only correspondence possible was with tenivastatin, with an RT of 2.2 minutes.

The new peaks were similar between the nanoemulsions tested (A, B, and D) but in the microemulsion (C) additional or distinct peak profiles were detected. To determine if the

peaks detected were a consequence of simvastatin degradation or excipient degradation, two formulations without simvastatin ('ME M2 Simv 0% CL 0.25%' and NE Simv 0% CL 0.5%') were placed at 40 °C and evaluated after 2 months. The temperature was chosen to speed the degradation since this test only started when the chemical and physical stability assay was already at 2 months. At 40 °C simvastatin also had higher degradation (see section 4.8) and thus higher degradation peak areas.

When comparing the same formulations with and without simvastatin it is possible to see that formulation excipients also play a role in new peak formation. After 2 months a peak eluted before the simvastatin peak with an RT of 3.6 min (Excipient Degradation 1) was present both in the formulations with and without simvastatin at 40 °C (Figure 40). Both the microemulsion and nanoemulsions had a peak composed of the fusion of multiple peaks with an RT of 1.3 min (Simvastatin Degradation 1) and the microemulsion also had a peak eluting after simvastatin with an RT of 5.9 min (Simvastatin Degradation 2) (Figure 40). During the assay, no tenivastatin peak was found in the samples which can possibly be related to another degradation process affecting tenivastatin. In fact, Silva *et. al.* (150) developed and validated an HPLC method to detect simvastatin under acid and alkaline hydrolysis, thermal stress (100 °C), and oxidative stress (H2O2). The chromatographic conditions were similar to the ones used in our method and the RT for both simvastatin and tenivastatin was 2 minutes longer (6.5 and 4.2, respectively) than those obtained in our method. In the study during the alkaline hydrolysis, which is expected to form tenivastatin, only a very small signal of tenivastatin was observed with the author reporting that tenivastatin might suffer further degradation into higher hydrophilic components that are not detected.

Identifying the degradation products might be important to understand simvastatin's main mechanism of chemical degradation and to find strategies to increase its stability. In the study by Silva *et. al.* (150) the main product obtained after oxidative stress (more hydrophilic than simvastatin) was a peak with an RT of 2.55 minutes. If the same 2-minute difference between peaks previously mentioned is considered, this would mean the oxidative degradation product would be eluted during the solvent front in our method and thus not detected. Since our method was only focused on simvastatin, the conditions and validation would need to be modified in order to have a higher resolution for hydrophilic degradation products.

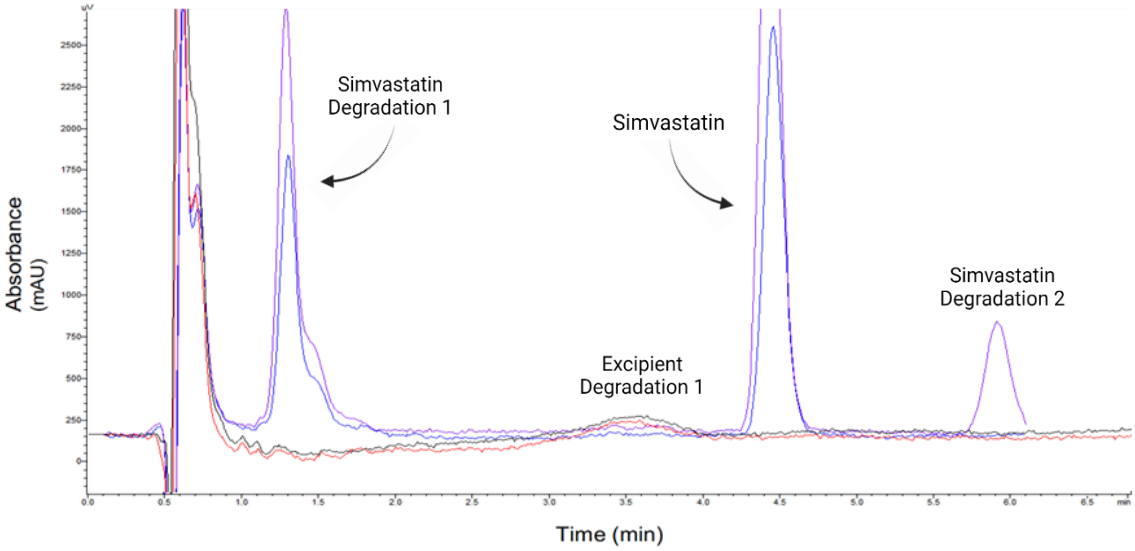

Figure S5. Simvastatin's and excipients' degradation peaks.
Chromatograms of a microemulsion M2 cationic lipid 0.25% with and without simvastatin (purple and black chromatogram, respectively) and nanoemulsion cationic lipid 0.5% with and without simvastatin (blue and red chromatogram, respectively) after 2 months at 40 °C.

Annex

A1. Course in animal experimentation conducted at *Centro de Cirugía de Mínima Invasión Jesús Usón* (Cáceres, Spain) and approval by the FCS-UBI animal welfare responsible entity (ORBEA).

FACULDADE CIÊNCIAS DA SAÚDE

Declaração

A equipa constituinte do ORBEA da FCS-UBI declara que o Investigador **Francisco Gama Sousa** realizou a formação "Curso para el desempeño de las funciones b, c y d en roedores, lagomorfos, carnívoros, cerdos y pequeños rumiantes" no Centro de Cirurgia de Mínima Invasión Jesús Usón, em Cáceres (Espanha), de 4 de novembro a 17 de dezembro de 2021, e realizou com sucesso a avaliação sobre Legislação Portuguesa relativa à proteção dos animais utilizados para fins científicos em 07 de fevereiro de 2022, no Centro de Investigação em Ciências da Saúde.

Covilhã, 10 de fevereiro de 2022

Graça Baltazar

Maria João Silva

Ana Clara Cristovão

Cláudio Maia

Universidade da Beira Interior | Faculdade de Ciências da Saúde
Avenida Infante D. Henrique
6200-506 Covilhã | PORTUGAL
Tel.: +351 275 319 700 | E-mail: pcabral@ubi.pt
www.ubi.pt

A2. Poster and oral presentation certificate at "*16º Congresso Português do AVC 2022*".

CICS-UBI
Centro de Investigação em Ciências da Saúde
Health Sciences Research Centre

16º CONGRESSO PORTUGUÊS DO AVC
3 a 5 fevereiro
VIRTUAL EDITION

FACULDADE CIÊNCIAS DA SAÚDE

Desenvolvimento de Micro e Nanoemulsões para Entrega Intranasal de Sinvastatina em AVC isquémico

Francisco Gama[1,2], Sara Meirinho[1,2], Patrícia Pires[2,3], Adriana O. Santos[1,2]

[1]Faculdade de Ciências da Saúde, Universidade da Beira Interior, Covilhã, Portugal; [2]Centro de Investigação em Ciências da Saúde (CICS-UBI), Universidade da Beira Interior; [3]Faculdade de Farmácia da Universidade de Coimbra (FFUC), Coimbra, Portugal

Introdução

- O acidente vascular cerebral (AVC) é das principais causas de morte e incapacidade no mundo, sendo o AVC isquémico o mais comum [1]. A atual terapia passa pela administração de uma agente fibrinolítico que apenas remove a obstrução responsável pelo evento isquémico [2].
- A sinvastatina apresenta propriedades neuroprotetoras, reduz os danos do AVC e melhora a recuperação pós AVC [3]. No entanto é lipofílica e apresenta baixa biodisponibilidade oral.
- A administração intranasal promove o transporte direto para o cérebro e evita o efeito de primeira passagem hepático [4].
- Formulações que são micro e nanoemulsões têm a capacidade de aumentar a dosagem de fármaco e potencialmente a sua absorção [5].

Objetivo: Desenvolver micro e nanoemulsões para administração intranasal, com elevada dosagem de sinvastatina, homogéneas, estáveis e seguras.

Metodologia

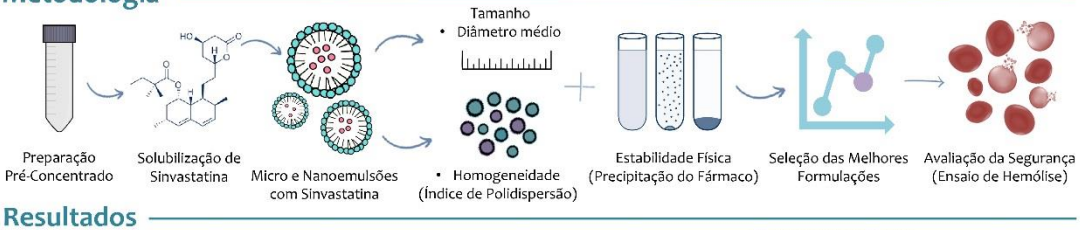

Resultados

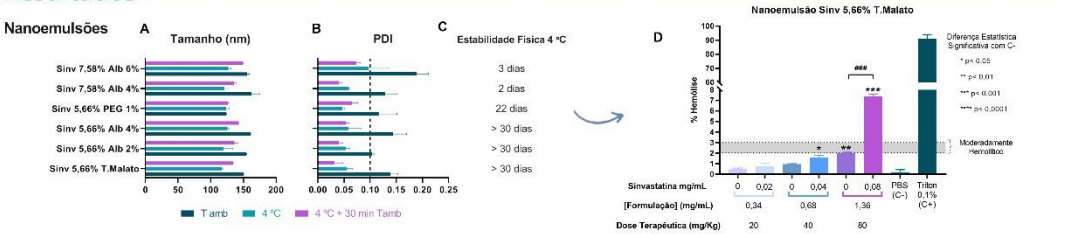

Figura 1. Caracterização das Nanoemulsões: Diâmetro médio **(A)** e índice de polidispersão (PDI) **(B)** a diferentes temperaturas; estabilidade física a 4 ºC **(C)** e ensaio de hemólise em sangue humano **(D)**. Análise estatística através *two-way* ANOVA seguida por teste de comparação múltipla de Sidak.

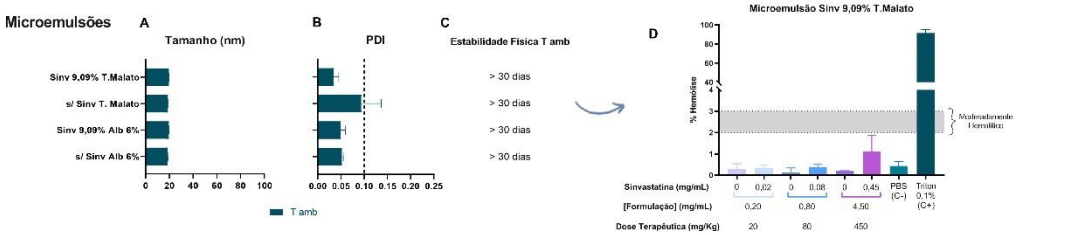

Figura 2. Caracterização das microemulsões: Diâmetro médio **(A)** e índice de polidispersão (PDI) **(B)** a diferentes temperaturas; estabilidade física à temperatura ambiente **(C)** e ensaio de hemólise em sangue humano **(D)**.

Conclusões

Obtiveram-se formulações nanométricas com elevada dosagem de sinvastatina, extremamente homogéneas (PDI < 0,1), com estabilidade física superior a 30 dias, e seguras quanto à indução de hemólise, promissoras para avançar no desenvolvimento.

Referências

[1] Katan M, Semin Neurol. 2018
[2] Barthels D, Biochim Biophys Acta Mol Basis Dis. 2020
[3] Squizzato A, Cochrane Database Syst Rev. 2011
[4] Hanson LR, BMC Neurosci. 2008
[5] Santosh Nemichand Kale, SRP. 2017

Agradecimentos: Drª Isabel Torrão, Centro Hospitalar Universitário Cova da Beira (CHUCB)

Compromissos: Francisco Gama beneficiou de uma Bolsa Iniciação à Investigação (FCT); Trabalho financiado por verbas do financiamento base (UIDB/00709/2020) e do financiamento programático (UIDP/00709/2020) do CICS-UBI, com fundos nacionais.

FCT COMPETE 2020 PORTUGAL 2020


APRESENTAÇÃO DE TRABALHO
CERTIFICADO
CERTIFICA-SE QUE
Francisco Gama
APRESENTOU O SEU TRABALHO, NO 16.º CONGRESSO PORTUGUÊS DO AVC, QUE DECORREU ENTRE OS DIAS 3 E 5 DE FEVEREIRO DE 2022, EM FORMATO VIRTUAL.
(CASTRO LOPES, PRESIDENTE DO CONGRESSO)
16º CONGRESSO PORTUGUÊS DO AVC
3 a 5 fevereiro 2022
VIRTUAL EDITION
POSTER
Desenvolvimento de Micro e Nanoemulsões para Entrega Intranasal de Sinvastatina em AVC.
Autores: Francisco Gama[1], Sara Meirinho[1], Patrícia Pires[1,2], Adriana Oliveira Santos[1]
Instituições: [1]Faculdade de Ciências da Saúde e Centro de Investigação em Ciências da Saúde (CICS-UBI), Universidade da Beira Interior, Covilhã, Portugal, [2]Faculdade de Farmácia da Universidade de Coimbra (FFUC), Coimbra, Portugal
Um "não " dito com convicção é mais importante que um "sim" dito meramente para agradar ou, pior ainda, para evitar complicações.
Mahatma Chandi
World Stroke Organization